The Identification of MTF2-specific Synthetic Lethal Interactions in Refractory Acute Myeloid Leukemia Using CRISPR

by

Christopher Cafariello

A thesis submitted to the University of Ottawa
in partial fulfillment of the requirements for the degree of
Master of Science, Cellular & Molecular Medicine

Faculty of Medicine
University of Ottawa

Supervisor: Dr. William L. Stanford

Abstract

Acute myeloid leukemia (AML) is a disease characterized by overproduction of abnormally differentiated, hyper-proliferative myeloid cells known as blasts in bone-marrow and blood. Our laboratory has previously demonstrated that loss of epigenetic repression by the polycomb repressive complex 2 (PRC2), which is mediated by complex member metal response element binding transcription factor 2 (MTF2), drives chemo-resistance resulting in refractory AML. In this study, to identify MTF2-specific synthetic lethal interactions, a genome-scale CRISPR Knock-out (GeCKO) synthetic lethal screen was performed in matched MTF2-deficient and rescued THP-1 cells both in the absence and presence of the induction chemotherapeutic cytarabine. Following careful analysis of screening data using specialized software, 104 highly significant MTF2-specific synthetic lethal interactions as well as 15 cytarabine-specific synthetic lethal interactions were identified. Reduced stringency upon analysis helped to identify an additional seven MTF2-specific synthetic lethal interactions that could be targeted with commercially available small-molecule inhibitors. Among eight small molecule inhibitors, two DNA Polymerase A/Ribonucleotide Reductase Catalytic Subunit M1 (POLA/RRM1) dual inhibitors (clofarabine and fludarabine) were shown to induce toxicity with specificity for MTF2-deficient THP-1 cells at low concentrations only in the absence of cytarabine.

In the future, further testing of the therapeutic potential of clofarabine and fludarabine in treating MTF2-deficient AML will be conducted in patient derived bone-marrow aspirates which better represent the true clonal and hierarchical nature of this life-threatening malignancy. Furthermore, lentiviral delivery of short-hairpin RNAs (shRNAs) targeting highly significant, non-enzymatic MTF2 and cytarabine-specific synthetic lethal interactions will be performed in both THP-1 cells as well as in patient derived bone-marrow aspirates. Eventually, *in vitro*

validated targets will be validated under *in vivo* conditions using a patient derived xenograft (PDX) preclinical animal model of AML using immunocompromised NOD *scid* gamma (NSG) mice.

Acknowledgements

I would like to take this opportunity to thank all of those who have played a role in mentoring me, assisting me as well as providing support, this project would have not been possible otherwise.

Firstly, I would like to thank my supervisors Drs. William Stanford and Caryn Ito for not only providing me with the opportunity to complete my Master's degree as part of the MTF2/AML group, but for their continuous support and training on all aspects of the scientific method including but not limited to experimental design, academic writing and research integrity. I would also like to thank all of the past and present members of the MTF2/AML group for both training me when I first entered the lab (Hari and Hani) as well as for the highly collaborative landscape that has resulted in the publication of two independent manuscripts as well as several other remarkable accomplishments (Sam, Charlotte, Caroline, Roberta, Hannah, Safwat, Eric, Joel, Michelle, Sierra and Anne-Marie). Moving forward, I expect this hard work and dedication to translate into improved therapeutics for treating acute myeloid leukemia especially since we have had and continue to have the pleasure of collaborating with Dr. Mitchell Sabloff, a hematologist at The Ottawa Hospital. Not only have members of the MTF2/AML group been invaluable to my success, all members of the Stanford-Ito lab have in some way contributed to my development as a scientist. Two noteworthy individuals include Julien Yockell-Lelièvre, who assisted me with designing several molecular cloning strategies and Sean Delaney who assisted with comprehension of the GeCKO screening platform and in particular, deep-sequencing and MAGeCK analysis. My success would also not have been possible without the support of Ottawa Hospital Research Institute staff including bioinformatician Chris Porter

who provided me with a crash course on PYTHON and Fernando Ortiz, a flow cytometrist, for his willingness to sort cells at all hours of the day.

I would also like to thank the Canadian Cancer Institute for funding this project as well as the Ontario Student Assistant Program for assisting with tuition costs. Furthermore, I would like to thank the University of Ottawa for all of their services as well as my jury for all of their feedback. I would like to especially thank my Thesis Advisory Committee; Dr. Kin Chan and Dr. Ryan Russell for their sincere and highly valuable mentorship throughout this experience as well as their continued support moving forward into the job market.

It would be short-sighted of me to not acknowledge the impact that my family and friends have had in the completion of this project. I would of course like to thank my parents for all that they do and to keep this short, I won't list it all. I would also like to thank my best Cornwallite friends (Heath, Ben, Justin, Kelsey and Yuxuan) for forcing me to take some breaks from the lab to refresh my perspective. Finally, I would like to thank my Girlfriend Isabelle, an avid Philip K. Dick reader, for all of her support and I would also like to mention that without her silence, this thesis would have never been completed.

Table of Contents

List of Abbreviations

aa: amino acids
AEBP2: Adipocyte Enhancer Binding Protein 2
AML: Acute Myeloid Leukemia
AraC: Cytarabine
ASO: Anti-sense Oligonucleotide
BGA: Bovine Growth Serum
bp: base pair
BSA: Bovine Serum Albumin
Cas9: CRISPR-associated 9
CBX: Chromobox
CDK4/6: Cyclin Dependant Kinase 4/6
cDNA: complementary Deoxyribonucleic Acid
CEBPA: CCAAT/Enhancer-Binding Protein Alpha
CLP: Common Lymphoid Progenitor
CMP: Common Myeloid Progenitor
CpG: Cytosine-Guanosine dinucleotide
CRISPR: Clustered Regularly Interspaced Short Palindromic Repeats
crRNA: CRISPR RNA
DMEM: Dulbecco's Modified Eagle Medium
DMSO: Dimethylsulphoxide
DNA: Deoxyribonucleic Acid
DNMT3A: DNA Methyltransferase 3A
EDTA: Ethylenediaminetetraacetic Acid
EED: Embryonic Ectoderm Development
EFS: EF1a Short
ELN: European Leukemia Net
ESC: Embryonic Stem Cell
EZH1/2: Enhancer of Zeste 1/2
FACS: Fluorescent Activated Cell Sorting
FDR: False Discovery rate
FBS: Fetal Bovine Serum
GAPDH: Glyceraldehyde Phosphate Dehydrogenase
GART: Phosphoribosylglycinamide Formyltransferase
G-CSF: Granulocyte-Colony Stimulating Factor
gDNA: genomic Deoxyribonucleic Acid
GeCKO: Genome-scale CRISPR Knock-out
GeCKOv2: GeCKO version 2
GFP: Green Fluorescent Protein
GMP: Granulocyte Monocyte Progenitor
H2Ak119ub1: Histone H2A Lysine 119 mono-ubiquitination
H3K27me3: Histone H3 Lysine 27 tri-methylation
H3K36me3: Histone H3 Lysine 36 tri-methylation
HEK293T: Human Embryonic Kidney 293T
HEPES: 4-(2-hydroxyethyl)-1-piperazineethanesulphonic acid

HMT: Histone Methyl-Transferase
HSC: Hematopoietic Stem Cell
IDH1/2: Isocitrate Dehydrogenase 1/2
IgG: Immunoglobin G
IL-3: Interleukin-3
JMML: Juvenile Myelomonocytic Leukemia
LDL: Low-density Lipoprotein
lncRNA: long non-coding RNA
LSC: Leukemic Stem Cell
IMDM: Iscove's Modified Dulbecco's Medium
IQR: Inter-quartile Range
KEGG: Kyoto Encyclopedia of Genes and Genomes
mAb: monoclonal antibody
MAGeCK: Model-based Analysis of Genome-wide CRISPR/Cas9 Knock-out
MDM2: Mouse Double Minute 2
MDS: Myelodysplastic Syndrome
MEP: Megakaryocyte Erythrocyte Progenitor
MFI: Mean Fluorescent Intensity
miRNA: micro RNA
MLE: Maximum Likelihood Estimation
MLL: Mixed Lineage Leukemia
MPL: Myeloproliferative Leukemia
MPP: Multipotent Progenitor
MTF2: Metal response element binding Transcription Factor 2
NSG: Non-obese diabetic (NOD) Severe-combined immunodeficient (SCID) Gamma
pAb: polyclonal antibody
PBS: Phosphate Buffered Saline
PCR: Polymerase Chain Reaction
Pc: Polycomb
PCL: Polycomblike
PcG: Polycomb Group
PDX: Patient Derived Xenograft
PEI: Polyethyleneimine
PHD: Plant Homeodomain
POLA/B: DNA Polymerase A/B
PRC1/2: Polycomb Repressive Complex 1/2
RBBP: Retinoblastoma Binding Protein
RFP: Red Fluorescent Protein
RHEB: Ras Homolog Enriched in Brain
RIGER: RNAi Gene Enrichment Ranking
RING: Ring Finger Protein
RNA: Ribonucleic Acid
RNAi: RNA interference
RNAseq: RNA sequencing
RPMI 1640: Roswell Park Memorial Institute 1640
RRA: Robust Ranking Algorithm

RRM1/2: Ribonucleotide Reductase Catalytic Subunit M1/2
RSA: Redundant siRNA Activity
RT: Room Temperature
RT-qPCR: Real Time-quantitative PCR
SAMHD1: Sterile alpha motif and HD domain-containing protein 1
SCF: Stem Cell Factor
sgRNA: single guide RNA
shRNA: short hairpin RNA
SNP: Single Nucleotide Polymorphism
STYX: Serine/Threonine/Tyrosine interacting protein
SUZ12: Suppressor of Zeste 12
TAE: Tris Acetate EDTA
TET2: Ten Eleven Translocase 2
TKI: Tyrosine Kinase Inhibitor
trxG: trithorax Group
TYMS: Thymidylate Synthetase
UBC: Umbilical Cord Blood Cells

List of Figures

List of Tables

Chapter 1: Introduction

1.1 Mammalian Hematopoiesis

Mammalian Hematopoiesis is a hierarchical process that evolves clonally across ontogeny to produce and maintain a sufficient quantity of blood cells throughout life.[1,2] At the top of the hierarchy is a heterogenous population of long-term and short-term multipotent hematopoietic stem cells (HSCs) that can both self-renew and differentiate into evermore lineage restricted oligopotent progenitors and eventually into the mature cells of the blood lineage which undertake roles in oxygen transport, adaptive and innate immunity as well as anti-cancer immuno-surveillance ***(Figure 1)***.[3,4,5] Although much remains to be discovered concerning the exact mechanisms governing how HSCs achieve a balance between self-renewal and differentiation, both internal cues including tight regulation of transcription as well as external autocrine and paracrine niche effects are known to contribute to this dynamic process.[6,7] Despite efforts, further elucidation of these mechanisms is required to better understand not only how HSCs function, but how and why hematopoiesis goes awry to result in life-threatening malignant states including anemias, leukemias and lymphomas and how more targeted, less toxic therapies can be harnessed to increase patient survival.

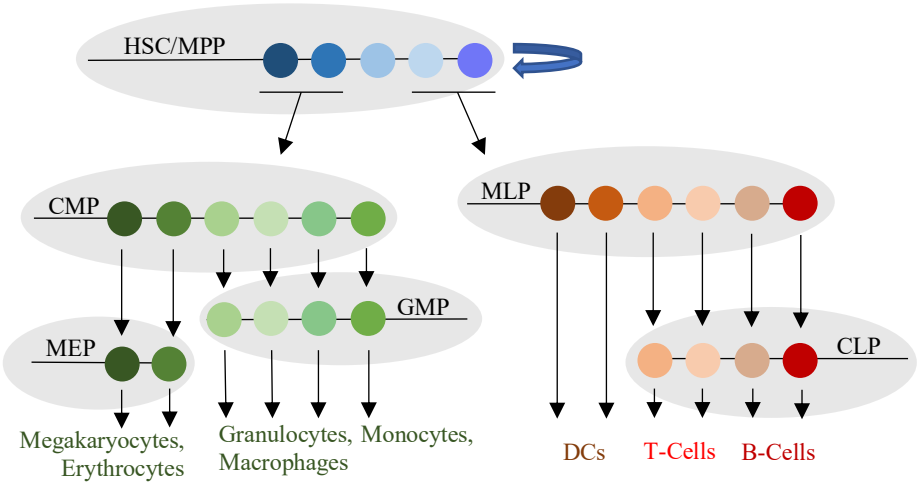

Figure 1. Schematic of hematopoietic hierarchy. Heterogenous HSCs and MPPs self-renew and differentiate into more restricted progenitors and eventually into the mature cells of the blood lineage.

1.2 Acute Myeloid Leukemia

Acute myeloid leukemia (AML) is a disease characterized by expansion into the bone marrow and blood by abnormally differentiated, and often poorly differentiated, hyper-proliferative myeloid cells called blasts. AML is the most common form of adult leukemia in Canada with a disappointing 5-year overall survival rate below 40%, ranking it among the most life-threatening hematological malignancies.[8] The current frontline therapy regimen for AML patients under the age of 65 is induction chemotherapy, which includes treatment with the cytotoxic agent cytarabine along with an anthracycline such as daunorubicin or idarubicin. Unfortunately, as many as 20% of patients fail to respond and are thus classified as refractory, while an additional 40% initially respond yet relapse shortly thereafter. For patients over 65, intensive induction is usually not an option with alternative maintenance therapies only achieving a 5-year overall survival in approximately 5% of cases. Dismal outlook among patients is the result of vast heterogeneity in the molecular etiology of AML; including abnormal cytogenetics, gain and loss of function mutations, and altered epigenetic landscapes rendering a single treatment regimen unlikely to suit all those affected.

While frontline therapy has remained relatively unchanged for almost 40 years, recent advances in DNA sequencing technologies have resulted in dramatic progress in the study of AML genetics. This enhanced understanding has resulted in the establishment of the ELN risk stratification of AML that was last updated in 2017 and divides patients into favourable, intermediate and adverse risk categories based on commonly observed mutations and cytogenetic abnormalities.[9] Although this advancement has been useful for risk management, a major shortcoming includes the inability to prospectively identify refractory or relapse patients which reside among all three risk categories prompting an urgent need for robust biomarkers of

cytarabine resistance as well as the development of alternative and more precision medicine therapeutic strategies. Interestingly, genetic studies have also shown that among the most commonly observed mutations in AML are epigenetic modifiers including but not limited to DNMT3A, IDH1/2 and TET2 which are highly indicative of poor prognosis.[10,11]

1.3 Epigenetics in Acute Myeloid Leukemia

Epigenetics refers to any changes in gene expression that are heritable by cell division, yet not caused by changes to the DNA sequence itself.[12] This can be achieved through covalent modifications to either DNA or histone proteins as well as through RNA mediated gene-silencing in many cases affecting the 3-dimensional chromatin structure as well as transcription factor access to DNA.[13] Stem cells including HSCs are defined by their unique ability to both self-renew and differentiate into specialized cell types. Terminal differentiation involves substantial changes to cell function and morphology which is accomplished in great part through modification of gene expression by epigenetic mechanisms; specifically, genes involved in self-renewal are repressed while genes involved in cell-specific functions are activated.[14]

As previously mentioned, altered expression programs, particularly caused by recurrent somatic mutations in epigenetic modifiers, are common among AML patients with poor prognosis.[15,16,17] Epigenetic dysregulation has also been reported for AML in the form of perturbed genome-wide DNA methylation signatures which hold useful prognostic value.[18] Furthermore, clinical and experimental observations report that epigenetic dysregulation is not only present in pre-leukemic HSCs, but also accumulates with age in healthy individuals.[19] Taken together along with the consideration that unlike genetic changes, epigenetic changes are frequently reversible, treatment strategies either targeting aberrantly expressed epigenetic regulators or reversing disrupted epigenetic landscapes could be used to target more

ontologically antecedent clones. Ultimately, this could result in complete eradication of blasts while simultaneously preventing future relapse caused by underlying quiescent populations of leukemic stem cells (LSCs).

1.4 Polycomb Group Proteins

One notable class of critical epigenetic regulators are the polycomb group (PcG) proteins which are responsible for dynamically establishing and maintaining transcriptional programs governing cell fate decisions in both embryonic and adult stem cells. Originally discovered in *D. melanogaster*, the Polycomb (Pc) gene was identified as an important negative regulator of homeotic gene expression.[20] Subsequent discoveries cataloguing a variety of other genes with similar knock-out phenotypes led to the classification of the PcG while antagonistic positive regulators were grouped together under the trithorax group (trxG).[21,22] The highly coordinated temporal and spatial expression patterns of both PcG and trxG complex members during development ensures appropriate limb growth and axial development, while their ability to maintain altered genome-wide expression landscapes facilitates epigenetic memory across ontogeny.[23]

Mammalian PcG proteins are divided into 2 major polycomb repressive complexes; PRC1 and PRC2. PRC2 includes core members SUZ12, EED and the mutually exclusive EZH1 and EZH2 which both contain catalytic histone methyl transferase (HMTase) activity and play complementary roles throughout development.[24] This complex controls gene expression by establishing and maintaining the repressive epigenetic mark, histone H3 lysine 27 trimethylation (H3K27me3) that is recognized by CBX, a core component of PRC1. CBX is then recruited along with the catalytic RING subunit to establish histone H2A lysine 119 monoubiquitination (H2AK119ub1), which in combination with H3K27me3 further compacts chromatin to inhibit

transcription ***(Figure 2)***.[25,26,27,28] Even though the PRC2 complex is generally thought to precede PRC1 mediated gene silencing, in the presence of the PRC1 accessory proteins Rybp/Yap2 and absence of CBX, PRC1 can catalyze H2AK119ub1 outside of H3K27me3 recognition which subsequently recruits PRC2 to establish H3K27me3 deposition.[29, 30] Interestingly, sub-stoichiometric accessory proteins, such as the polycomblike (PCL) proteins, are also very important for the function of the PRC2 complex since neither EED, SUZ12 nor EZH1/2 are capable of binding chromatin.[31]

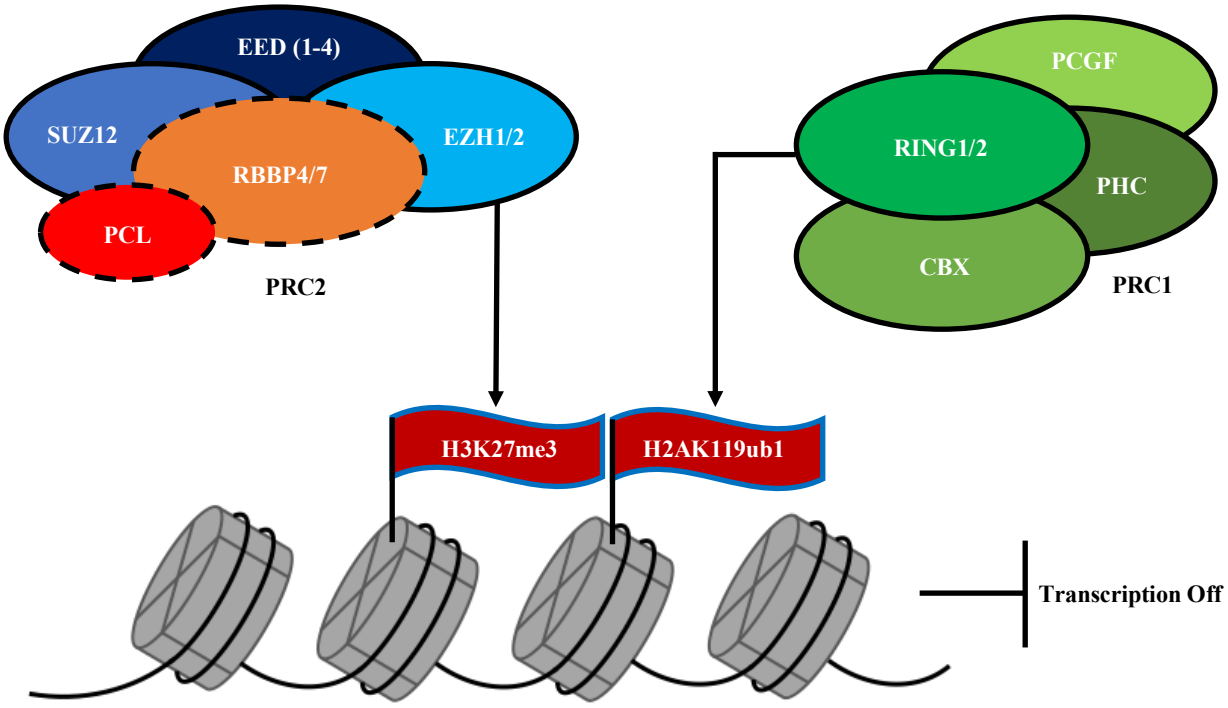

Figure 2: Schematic of PRC1 and PRC2 mediated histone modification. PRC2, including core members; SUZ12, EED and EZH1/2 along with sub-stoichiometric accessory members; RBBP4/7 and PCL group initially establish and maintain H3K27me3. PRC1 subsequently catalyzes H2AK119ub1 further compacting chromatin.

1.5 PRC2 Accessory Proteins

The HMTase activity of the PRC2 complex requires the activity of the three core complex members; SUZ12, EZH1/2 and EED while deletion of any of these factors leads to embryonic lethality in mice at early gastrulation.[32, 33, 34] In contrast, deletion of sub-stoichiometric accessory proteins including AEBP2, RBBP4/7, JARID2 and PCL only leads to varying levels and distribution of H3K27me3 deposition. It is thought that modulation of PRC2 activity by differential expression of accessory proteins can finetune complex activity across different species and cell types.

1.5.1 AEBP2

Adipocyte Enhancer binding protein 2 (AEBP2) is an accessory protein of the PRC2 complex that was originally identified by mass-spectrometry in purified HMTase activity. Although not much about this factor is understood, it is known to contain a zinc-finger domain that could facilitate DNA binding while its presence significantly increases the HMTase activity of the PRC2 complex.[35]

1.5.2 RBBP Subunits

Human Retinoblastoma Binding Proteins (RBBP) are accessory proteins of the PRC2 complex that were originally identified as factors binding to retinoblastoma protein suggesting an effect on cell proliferation. Since then, many more potential binding partners to RBBP class proteins have been identified including AEBP2.[36] Although the function of RBBP proteins in the PRC2 complex thus far remains elusive, loss of this factor has been associated with age-related diseases including Alzheimer's.[37]

1.5.3 JARID2

Jumonji And AT-Rich Interaction Domain Containing 2 (JARID2) is a well-studied accessory protein of the PRC2 complex that was originally discovered as a component required for both neural and cardiac development in mice.[38] Subsequent discoveries not only found JARID2 to be required for Embryonic Stem Cell (ESC) differentiation, but also necessary for epidermal cell differentiation.[39, 40, 41] Although JARID2 is a member of the jumonji class of histone demethylases, it is not enzymatically active while containing a DNA binding domain suggesting a role in PRC2 recruitment to a subset of genomic loci.[42, 43] Interestingly, JARID2 has yet to be found bound to a complex also containing PCL proteins. This mutual exclusivity further suggests the possibility of alternate modulation of the PRC2 complex by accessory proteins.[44]

1.5.4 Polycomblike

Polycomblike (PCL) was originally identified during a screen for polycomb mutations in *Drosophila melanogaster* as a separate mutant with a similar phenotype to Pc.[45] Although this factor was initially only classified as a transcriptional repressor, it was eventually determined to be essential for the recruitment of Enhancer of zeste to target loci for enhanced H3K27me3 deposition.[46, 47] In mammals, there are three homologs of PCL; PCL1/PHF1, PCL2/MTF2 and PCL3/PHF19 all containing both a TUDOR domain for chromatin recognition as well as multiple PHD-fingers for DNA binding suggesting a role in PRC2 recruitment to target loci which has been demonstrated for PCL2/MTF2.[48]

Unlike PCL2/MTF2 and PCL3/PHF19 which generally confer a proliferative advantage, PCL1/PHF1 evolved a divergent role as a p53 stabilizing protein promoting cellular quiescence in murine embryonic fibroblasts.[49] Aside from this PRC2-independent role, PCL1/PHF1 also acts as a PRC2 accessory protein modulating HMTase activity at hox gene loci.[50] PCL3/PHF19

is an accessory protein to the PRC2 complex that is both mutually exclusive with JARID2 and a known oncogene.[51, 52] Not only is PCL3/PHF19 involved in modulation of PRC2 HMTase activity, it is also involved in recruitment of this complex to sites of trxG mediated H3K36me3.[53, 54] Another mammalian homologue of PCL is PCL2/MTF2, henceforth referred to as MTF2, which is expressed as 3 alternatively spliced isoforms; MTF2A, MTF2B, and MTF2C all containing C-terminal PHD fingers involved in the recruitment and binding of the PRC2 complex to target loci while only MTF2A and MTF2B contain an N-terminal tudor domain involved in chromatin recognition and binding (***Figure 3)***.[55, 56, 57] MTF2 has not only been implicated in the regulation of chick left-right asymmetry through repression of sonic hedgehog, loss of this factor has been shown to increase self-renewal at the expense of differentiation capacity in murine ESCs while loss of MTF2 in murine hematopoietic progenitors impairs erythropoiesis.[58, 59, 60] Considering the highly tissue and species specific roles of MTF2, more experimentation is required to better understand how aberrant expression of this increasingly investigated tumour suppressor can lead to malignancies including breast cancer and AML, particularly through its recurring role as an indirect regulator of p53 stability.[61, 62]

1.6 PRC2 members in Acute Myeloid Leukemia

Although increased EZH2 expression has been observed in many adult cancers, it in contrast remains among the most commonly mutated tumour suppressor genes in AML and Myelodysplastic Syndromes (MDS) affecting approximately 2% of patients.[63, 64] It has been proposed that loss of this methyltransferase drives resistance to both standard chemotherapy as well as TKI treatment in AML as a result of HOXA9 and HOXB7 derepression while sensitivity can be restored through proteasomal inhibition.[65] Strikingly, small molecule inhibitors of EZH1/2 have also been shown to be highly efficacious in cases where MLL rearrangements have

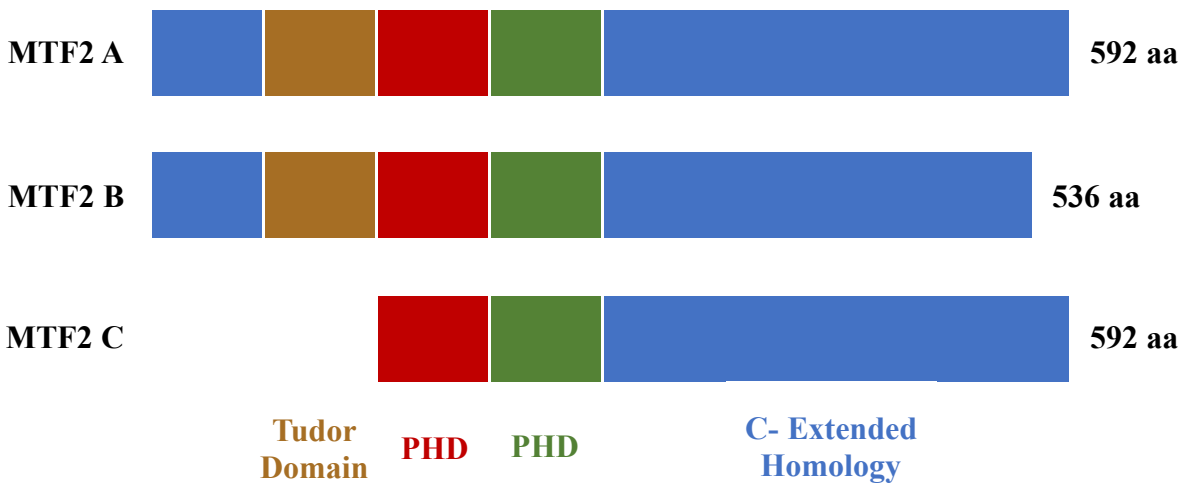

Figure 3: Schematic of MTF2 protein isoforms. MTF2 is produced as three separate isoforms with MTF2A containing all 15 exons, MTF2B lacking exon 11 and MTF2C lacking exons 1-3 which contain the tudor domain. N to C termini are displayed from left to right.

occurred further highlighting the importance of personalizing therapeutics when treating AML.[66] Not only is H3K27me3 deposition associated with CpG island hypermethylation at sites of transcriptional repression in adult cancers, both hypo and hyper-methylation have also been observed in AML particularly at sites that are transcriptionally regulated by the PRC2 complex across ontogeny.[67] One such target for promoter region hypermethylation is the PRC2 accessory protein, MTF2. MTF2-deficiency has been shown to serve as a robust biomarker and driver of resistance to standard chemotherapy in AML through loss of PRC2-mediated repression of MDM2.[62] Although, chemosensitivity can be restored both *in vitro* as well as *in vivo* through MDM2 inhibition, this strategy likely will not work for AML patients harboring bi-allelic TP53 mutations which make up approximately 10% of the affected population at diagnosis. In addition, loss of p53 as a result of treatment with cytotoxic drugs is a common cause of therapy acquired resistance indicating an immediate need to identify both MTF2-specific synthetic lethal

interactions that do not rely on p53 restoration as well as modalities of sensitizing p53-null leukemic blasts to standard and novel therapeutics.[68] Moreover, since the predictive potential of MTF2-deficiency resides within the $CD34^+$, $CD38^-$ compartment of patient-derived bone-marrow blasts, strategies focussing on MTF2-deficiency could better target rare disease maintaining LSCs, further limiting the potential for future relapse.

1.7 Synthetic Lethality

As a result of recent advances in DNA sequencing technology, numerous driver mutations have been identified among several human cancer types which fall into two main categories; gain of function mutations in oncogenes and loss of function mutations in tumour suppressors. Although the former can be directly targeted using small molecule inhibitors or antibodies, the latter requires either genetic correction or vector-mediated rescue which still remains therapeutically challenging.[69] Synthetic lethality can be described as an interaction between two non-essential genes where simultaneous inhibition of both results in cell death.[70] The first published example of this phenomenon appeared in 1922 when two sex-linked mutations in *Drosophila* were found to result in the premature death of larvae.[71] Targeting the synthetic lethal interactions corresponding to loss of tumour suppressor function represents a useful solution and since it exploits a genotype-specific cancer liability, it is unlikely to affect healthy cells. While this has already been achieved in breast cancer, non-small cell lung cancer and AML among many others, robust identification of synthetic lethal interactions remains exceedingly difficult.[72, 73, 74] This difficulty is not only due to the rareness of such genetic interactions, they are also highly conditional and result in loss of cell viability rendering mutant recovery and cataloguing extremely challenging. Initial attempts at high throughput screening therefore took advantage of model organisms including *Saccharomyces cerevisiae, Drosophila*

melanogaster and *Caenorhabditis elegans.* While numerous useful synthetic lethal interactions were identified using this strategy, not only was whole-genome interrogation not achieved, but relevance to human disease remained limited.[75, 76, 77, 78, 79] Fortunately, recent advances in both RNAi and CRISPR editing technology have made it possible to carry out genome-scale, unbiased and multi-conditional lethality screening in human cell-lines.

1.8 CRISPR

Clustered Regularly Interspaced Short Palindromic Repeats (CRISPR) and CRISPR associated (Cas) effector proteins facilitate adaptive immune response against exogenic infection in most archaea and some eubacteria.[80, 81]

CRISPR loci contain 21-72bp spacer sequences flanked by 23-55bp repeats that can span over 500 iterations in multiple locations across prokaryotic genomes. Even though CRISPR loci were initially discovered as far back as 1987, Cas effector proteins were only first identified in 2002.[82, 83] In 2005, the foreign origin of spacer sequences was formally proven using both molecular and bioinformatic approaches.[84, 85, 86] Subsequently, experiments involving the strategic addition and removal of spacer sequences in *S. thermophilus* provided the first evidence of CRISPR/Cas-mediated adaptive immunity against bacteriophage insult.[87] Specifically, Cas effector proteins which both contain endonuclease activity and can interact with DNA and RNA, cleave foreign genetic material into small pieces that are subsequently inserted into CRISPR loci as spacer sequences. Afterwards, different Cas effector proteins process both spacer sequences along with palindromic and thus hairpin prone repeats to form a crRNA. Following repeat infection from the same pathogen, crRNAs can recruit Cas effector proteins to the familiar foreign genetic material for sequence specific cleavage of double stranded DNA achieving attenuation and thus immunity.[88] Evidently, a hallmark feature of CRISPR/Cas systems is a

diverse set of Cas effector proteins that execute diverse yet highly coordinated functions to achieve immunization. Cataloguing studies based on the presence or absence of different Cas effector proteins have identified 3 major CRISPR/Cas systems; type 1, 2 and 3.[89] While Cas1 and Cas2 are ubiquitous among all three types and carry out spacer sequence acquisition, certain Cas proteins such as Cas3, Cas9 and Cas10 are specific to type 1, type 2 and type 3 systems respectively. Furthermore, phylogenetic studies have also shown that while type 2 CRISPR/Cas systems are exclusive to eubacteria, type 1 and 3 systems are biased towards archaea and hyperthermophiles.[90]

The discovery and systematic interrogation of CRISPR/Cas function and mechanisms led to an eruption of industrial and agricultural applications including the enhancement of biofuel production pathways in industrially relevant organisms as well as the improved engineering of infection resistant crops.[91] In 2012, it was also demonstrated that the type 2 effector protein Cas9 could be programmed to achieve sequence-specific double-stranded DNA lesions in the presence of a newly designed and easily modifiable sgRNA which combined the spacer and repeat sequences from naturally occurring crRNAs.[92] Shortly thereafter, this discovery was leveraged to perform efficient genome editing in mammalian cells eventually leading to unprecedented frontiers in experimental medicine and drug discovery.[93] The ability to insert, delete or modify DNA with a high degree of precision in complex genomes not only permitted the efficient production of genetic knock-outs, knock-ins and SNPs for disease modelling, these strategies could also be used to correct rare somatic mutations from patient autologous cell sources reducing the incidence of graft rejection.[94, 95, 96, 97] Finally, the resulting generation of whole-genome knock-out libraries based on the CRISPR/Cas9 gene editing system rather than RNAi has helped in the struggle to identify genome-wide synthetic lethal interactions corresponding to

loss of tumour suppressor activity in cancer since both a lower incidence of off-target effects is observed reducing false positive detection while complete knock-out compared to partial knock-down reduces false-negative detection.[98, 99]

1.9 Genome-scale CRISPR Knock-out

Genome-scale CRISPR Knock-out (GeCKO) is the process of using CRISPR technology to perform genetic knock-out of every gene in the genome concurrently. To achieve this, cells of interest are initially engineered to express codon optimized *Streptococcus pyogenes* Cas9 endonuclease followed by transduction with a pooled lentiviral library of sgRNA sequences targeting every known protein coding and miRNA gene in the genome. Transduction conditions are optimized to ensure that each sgRNA sequence in the library is delivered to hundreds of individual cells to achieve adequate coverage while also avoiding dual transduction. Since vector delivery is facilitated by lentivirus, sgRNA sequences are integrated into the genome of both dividing and non-dividing cells and can therefore serve as a barcode for which specific gene was targeted in any given cell. Deep sequencing of PCR amplified sgRNA genomic integrations can be used to determine the representation of individual sgRNA sequences in the library at different timepoints, such as directly following transduction as well as at an endpoint. Comparison of individual sgRNA representation between timepoints can be used to determine which sgRNA genomic integrations affect cell fitness. sgRNA sequences that are depleted at the endpoint compared to the baseline implicate genes that when inhibited reduce cell fitness while the opposite is true for sgRNA sequences that are enriched. Performing GeCKO experiments in parallel using cells with differential expression of a key gene of interest or in both the presence and absence of a key drug of interest is therefore a powerful and unbiased method of probing the

entire genome for synthetic lethal interactions or pathways leading to drug resistance.[100,101,102,103,104,105]

The human dual vector GeCKOv2 library includes two component lentivectors; the LentiCas9-Blast which is used to generate stable Cas9-expressing clones following transduction and prolonged blasticidin selection, and the LentiGuide-Puro which comes as a pooled library of 123,411 different sgRNA sequences targeting 19,050 protein-coding genes with six unique sequences per gene, 1864 miRNA genes with four unique sequences per gene and 1000 non-targeting controls.[106] Although this library remains among the most comprehensive available, it along with its equivalents fail to probe the vast number of recently discovered non-coding elements including lncRNA molecules. In the future, genome-scale CRISPR knock-out strategies must be adapted to address this gap in understanding.

1.10 Model-based Analysis of Genome-wide CRISPR/Cas9 Knock-out

The vast quantity of data generated from GeCKO experiments pose several challenges for computational analysis. Firstly, due to the large time commitment and cost involved in assay optimization and deep sequencing, experiments are often carried out with few to no replicates necessitating an appropriate statistical model for estimating read count variance. Secondly, it is often challenging to account for the variable differences in knock-out efficiency among redundant sgRNA sequences targeting the same gene creating the need for a robust method for aggregation of data from multiple sgRNA sequences. Thirdly, robust read count normalization is required when comparing samples from different conditions since baseline library representation can vary greatly even among technical replicates.[107] Although, algorithms designed for the analysis of differential gene expression from RNAseq microarray data such as EdgeR, DESeq and BaySeq have been used in the past, analysis was limited to the level of the individual sgRNA

sequence while gene level data was difficult to generate often requiring advanced knowledge of computational strategies.[108, 109. 110] More recently, software commonly used to analyze data from RNAi based genome-scale knock-down experiments such as RSA and RIGER have been successfully used to generate weighted ranks at the level of the gene while also providing a detailed pathway analysis which is essential for translating genetic knock-out data into tangible therapeutic options.[111, 112] Unfortunately, these options were designed for siRNA based assays while there still remained a need for tools better tailored to sgRNA identification. Model-based Analysis of Genome-wide CRISPR/Cas9 knock-out (MAGeCK) is specialized software designed for the analysis of sequencing data from GeCKO experiments. The first software package is called Robust Ranking Algorithm (RRA) and solves the aforementioned dilemmas through a 4-step workflow:

1. *Median normalization of read counts:* The read count median for each sample is normalized and scaled to the median of the sample with the lowest total read count.
2. *Mean-variance modelling of read counts:* Since few to no replicates are performed, MAGeCK-RRA assumes that the read count variance is a smooth function of the read count mean while also borrowing information about the read count variance from individual sgRNA sequences from sequencing data.
3. *Identification of negatively and positively selected sgRNA sequences:* MAGeCK-RRA assumes the sgRNA sequences follow a negative binomial distribution and uses this model to assign both negative and positive selection p-values to each individual sgRNA sequence in the library.
4. *Identification of negatively and positively selected genes:* MAGeCK-RRA aggregates the statistical information from redundant sgRNA sequences targeting the same gene and

produces a negative and positive selection RRA score for each gene that can then be used for gene ranking.

As previously mentioned, MAGeCK-RRA produces separate depletion and enrichment RRA scores for every gene targeted by the GeCKOv2 library making it difficult to compare data between conditions to isolate treatment related synthetic lethal interactions. As a solution, a more advanced software package has been developed called Maximum Likelihood Estimation (MLE) which combines both enrichment and depletion RRA scores into single Beta scores for each gene. A negative beta score indicates depletion of associated redundant sgRNA sequences compared to respective baselines while a positive score indicates enrichment. Eventually, the development of MAGeCK-VISPR helped to further overcome computational challenges by employing the MLE framework to not only define a set of quality control measurements but to also extend analysis to a web-based data visualization framework.[113] Finally, MAGeCK-Flute packages have enabled the comparisons of beta-scores between treatments for the easy separation of treatment related changes in sgRNA sequence abundance effectively producing a list of synthetic lethal gene targets. Furthermore, Fisher exact p-values are applied to genes from the resulting list to identify highly significant synthetic lethal pathways.

1.11 Rational

AML is a disease characterized by a vastly heterogenous etiology severely limiting the efficacy of a single treatment modality. Recently, our lab has discovered that deficiency in MTF2 destabilizes the PRC2 complex and drives resistance to standard induction therapy in AML while sensitization can only be achieved through p53 rescue as a result of MDM2 inhibition. Unfortunately, MDM2 inhibition would likely fail in the absence of wildtype p53, which is the case for approximately 8% of *de novo* AML cases while the frequency is even greater in MTF2-

deficient patients who have previously undergone standard chemotherapy and failed to achieve complete remission. Therefore, identifying both MTF2 as well as cytarabine-specific synthetic lethal interactions that do not rely on p53 activity will greatly benefit such poor-prognosis patients.

The THP-1 acute myelomonocytic leukemia cell line is not only MTF2-deficient compared to bone-marrow mononuclear cells derived from healthy individuals, it also contains biallelic 26 bp p53 frameshift mutations rendering the protein completely inactive.[114, 115] As a result, THP-1 cells are highly resistant to treatment with standard therapeutics such as cytarabine. Additionally, since THP-1 cells are sufficiently durable to sustain serial lentiviral transduction and antibiotic selection, they are an ideal model for performing matched MTF2-deficient and rescued genome-scale CRISPR knock-out in both the absence and presence of cytarabine ***(Figure 4)***. Such a screen would not only identify MTF2-specific synthetic lethal interactions that are potentially efficacious both alone or in combination with cytarabine, it would also identify cytarabine-specific synthetic lethal interactions tailored to both MTF2-deficient and MTF2-basal, p53 mutant genetic backgrounds. Following synthetic lethal screening, highly significant targets and pathways can be isolated through the use of MAGeCK software while further validation could be performed in both matched MTF2-deficient and rescued THP-1 cells as well as in MTF2-deficient patient derived bone-marrow aspirates. Subsequently, *in vitro* validated targets will be validated under *in vivo* conditions using a patient derived xenograft (PDX) preclinical animal model of AML using immunocompromised NOD *scid* gamma (NSG) mice.

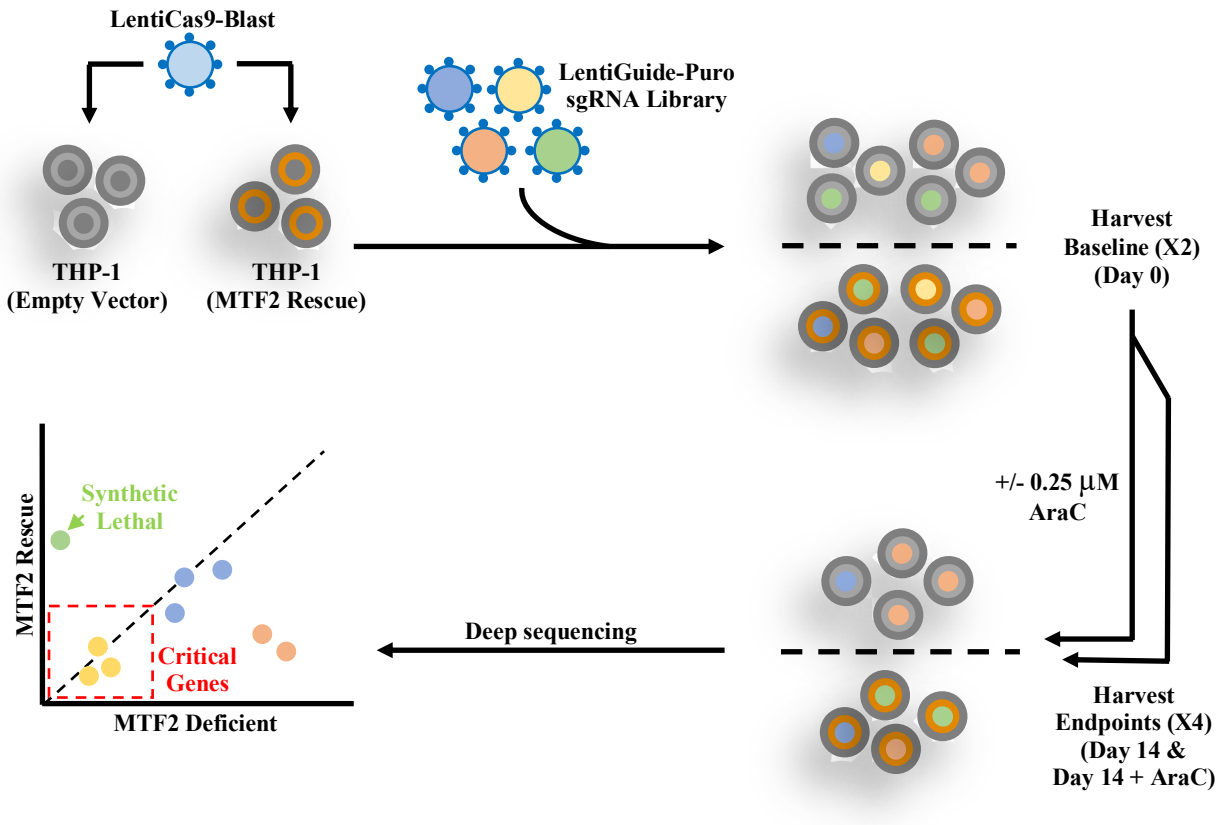

Figure 4: Schematic for GeCKO in matched MTF2-deficient and rescued THP-1 cells.

Overarching Hypothesis

A GeCKO screen in matched MTF2-deficient and rescued THP-1 cells in both the absence and presence of cytarabine will identify MTF2 and cytarabine-specific synthetic lethal interactions that can be harnessed to target p53-mutant, chemoresistant AML cells.

Research Aims

1. Optimize and carry out a GeCKO screen in matched MTF2-deficient and rescued THP-1 cells both in the absence and presence of the standard induction chemotherapeutic cytarabine.
2. Optimize a flow cytometric apoptosis assay to validate druggable targets identified from GeCKO screening to identify new candidate therapeutics for *in vivo* testing.

Chapter 2: Materials and Methods

2.1 Reagents

Blasticidin, puromycin and zeocin antibiotics were used to select transduced cells. (Invivogen, ant-bl-05, ant-pr-1 and ant-zn-05 respectively). All PCR and RT-qPCR primers were purchased from Integrated DNA Technologies. Annexin V – BUV395 flow cytometry stain was purchased from BD Biosciences (569871). SYTOX Green and 7-AAD DNA dyes were both purchased from ThermoFisher Scientific (S7020 and 00-6993-50 respectively). The α-Cas9 monoclonal antibody was purchased from ThermoFisher Scientific (7A9 3A3) while the α-MTF2 polyclonal antibody was purchased from Genway (GWB-FA7207). Alexafluor647 goat α-rabbit IgG and Alexafluor488 goat α-mouse IgG secondary antibodies were also purchased from ThermoFisher Scientific (A21244 and A11001 respectively). Both formalin and methanol for fixing cells was purchased from Fisher Chemical (BP531-500 and A412-4 respectively). Triton X-100 for cell permeabilization was purchased from Bioshop (TRX506). Bovine serum albumin was purchased from Multicell (800-095-EG) while fetal bovine serum was purchased from ThermoFisher Scientific (Gibco –10082147). Lentiviral packaging plasmids psPAX2 and pMD2.G were purchased from Addgene (#12259 and #12260 respectively). MTF2 rescue and matching empty vector control lentiviral vectors, pLenti-GIII-CMV-RFP-2A-Puro were purchased from Abmgood (LV229463). pXPR_011 Cas9-reporter lentiviral vector was purchased from Addgene (#59702). Human dual vector GeCKOv2 library was purchased from Addgene (#1000000049). PEI transfection reagent was purchased from Polysciences Inc. (24765) while polybrene and lentiblast transduction reagents were purchased from Sigma Aldrich (TR-1003-6) and OZBiosciences (9LB00500) respectively.

2.2 Cell lines

The HEK293T cell line used for lentivirus production was purchased from ATCC (CRL-11268) and cultured in DMEM (ThermoFisher Scientific – 11885-084) with 4.5 g/L D-Glucose, 1.5 g/L L-Glutamine and 110 mg/L Sodium Pyruvate supplemented with 10% v/v Bovine Growth Serum (Hyclone – SH30541.03). The KG-1 acute myelogenous leukemia cell-line was purchased from ATCC (CCL-246) and cultured in IMDM (ThermoFisher Scientific – 12440-053) with L-Glutamine and 25 mM HEPES Buffer supplemented with supplemented with 20% v/v Bovine Growth Serum, and 1% v/v PenStrep (Gibco – 14140-122). The THP-1 myelomonocytic leukemia cell-line used for screening was kindly provided by Dr. Marceline Côté at the University of Ottawa and cultured in RPMI Media 1640 (ThermoFisher Scientific – A10491-01) with 4.5 g/L D-Glucose, 2.383 g/L HEPES Buffer, L-Glutamine, 1.5 g/L Sodium Bicarbonate and 110 mg/L Sodium Pyruvate supplemented with 10% v/v Bovine Growth Serum, 1% v/v PenStrep and 0.1% v/v 2-mercaptoethanol (Gibco – 21985-023). The HL-60 acute promyelocytic leukemia cell-line was purchased from ATCC (CCL-240) and cultured in RPMI Media 1640 with 4.5 g/L D-Glucose, 2.383 g/L HEPES Buffer, L-Glutamine, 1.5 g/L Sodium Bicarbonate and 110 mg/L Sodium Pyruvate supplemented with 10% v/v Bovine Growth Serum, and 1% v/v PenStrep. Patient derived samples were cultured in IMDM with L-Glutamine and 25 mM HEPES Buffer supplemented with 15% v/v BIT9500 (Stem Cell Technologies – 09500), 1% v/v PenStrep, 0.1% v/v 2-mercaptoethanol, 100 ng/mL Recombinant Human SCF (PeproTech – 300-07), 50 ng/mL Recombinant Human FLT3-Ligand (PeproTech – 300-19), 20 ng/mL Recombinant Human IL-3 (PeproTech – 200-03) and 20 ng/mL Recombinant Human G-CSF (PeproTech – 300-23). Human umbilical cord-blood cells were cultured in IMDM with L-Glutamine and 25 mM HEPES Buffer supplemented with 20% v/v BIT9500, 1% v/v PenStrep,

100 ng/mL Recombinant Human SCF, 50 ng/mL Recombinant Human Flt3-Ligand, 20 ng/mL Recombinant Human TPO (PeproTech – 300-18) and 0.01% v/v LDL (Stem Cell Technologies – 02698). CD34 enrichment was achieved using the EasySep Human CD34 Positive Selection Kit (17856) and “The Big Easy" EasySep Magnet (18001) from Stem Cell Technologies according to manufacturer’s protocol.

2.3 Lentivirus production and transduction

2.5 million HEK293T cells were seeded in 15 mL of defined media in 150 mm tissue culture dishes (Falcon – 353025). Cells were left to expand at 37°C for 72 hours or until 70% confluent followed by media replacement 2 hours prior to transfection. For each dish, two separate transfection mixtures were generated; the first contained 19.83 µg psPAX2, 10.79 µg pMD2.G, equimolar transfer vector, 0.15 mL of 1.5 M NaCl and unsupplemented DMEM to 1.5 mL while the second contained 0.8 mL unsupplemented DMEM, 0.55 mL PEI and 0.15 mL 1.5 M NaCl. The second mixture was then added to the first mixture drop wise and left to incubate at RT for 30 minutes followed by dropwise addition of the combined 3 mL to the pre-incubated HEK293T cells. 18 hours following addition of the transfection mixture, transfection efficiency was estimated by fluorescence microscopy using the Zeiss Axio Observer.A1 and media was replaced if transfection efficiency was satisfactory (>50%). 24 hours following transfection assessment, dilute viral supernatant was stored at -80°C (Lentiguide-Puro) or concentrated by ultracentrifugation at approxametely 112,000 x g for 90 minutes at 4°C (all other transfer vectors). Upon lentiviral transduction, 1.0 million cells were seeded in 2 mL of defined media and kept in 6 well tissue culture plate wells (Falcon – 353846) with 8 µg/mL polybrene. Lentivirus was added in pre-titrated quantities and the mixture was centrifugated at 1000 x g for

60 minutes at 37°C. Lentiviral transduced cells were then left to incubate for 18 hours followed by media replacement. Cells were then subjected to either antibiotic selection or FACS 48 hours later.

2.4 Antibiotic selection curves

To determine the threshold Blasticidin, Zeocin and Puromycin antibiotic concentrations required for enrichment of successfully transduced THP-1 cells, THP-1 cells were incubated with increasing concentrations of each compound for 96 hours. Every 24 hours, cells were collected by centrifugation at 400 x g for 5 minutes at RT, washed with PBS with 2% FBS and 100 µM EDTA and 1µL of 7-AAD viability dye was added. Cells were then filtered through a 70 µm filter into a polypropylene tube (Falcon – 352063) and left to incubate at RT for 15 minutes in the dark prior to analysis using the BD LSR Fortessa flow cytometer. Antibiotic concentrations that resulted in over 95% positive 7-AAD signal after 72 hours of incubation were used for all subsequent enrichments following lentiviral transduction.

2.5 Cell sorting

Lentiviral transduced THP-1 cells were collected by centrifugation at 400 x g for 5 minutes at RT followed by resuspension in PBS with 2% FBS and 100 µM EDTA at a density of less than 10^7 cells/mL. Cells were then filtered through a 70 µm filter into a polypropylene tube before the addition of 5 µL of 7-AAD viability dye or 1 µl of 30 µM SYTOX Green. Prepped cells were left to incubate at RT for 15 minutes in the dark prior to cell sorting with the MoFlo XDP Cell Sorter into defined media.

2.6 Generation of Cas9 expressing THP-1 cells

THP-1 cells were transduced with ultracentrifuge concentrated LentiCas9-Blast lentivirus as described above followed by blasticidin selection at 20 μg/mL for 2 weeks beginning 48 hours after media replacement.

2.7 Cas9 reporter assay

Untransduced and LentiCas9-Blast transduced THP-1 cells were both transduced with lentivirus delivering pXPR-011. 72 hours following transduction, all pXPR_011 transduced cells were left to incubate for 72 hours in the presence of 2 μg/mL puromycin. Directly following antibiotic selection as well as 6 days after antibiotic selection, cells were collected by centrifugation at 400 x g for 5 minutes at RT followed by resuspension in PBS with 2% FBS and 100 μM EDTA, filtered through a 70 μm filter into a polypropylene tube and percent GFP expression was quantified in all samples using the BD LSR Fortessa flow cytometer.

2.8 Generating matched MTF2-deficient and rescued THP-1 cells

MTF2 Rescue and corresponding Empty Vector control lentivectors (pLenti-GIII-CMV-RFP-2A-Puro^R) were modified to replace the SV40-RFP-2A-Puro^R moiety with an EF1a-GFP-E2A-Zeo^R for compatibility with the Human Dual-vector GecKOv2 library which requires puromycin selection for enrichment of successfully transduced cells. Cas9 expressing THP-1 cells were transduced with ultracentrifuge concentrated pLenti-GIII-CMV-GFP-2A-Zeo (both MTF2 Rescue and Empty Vector separately) lentivirus as previously described. Cells were left to incubate for 48 hours after media replacement before FACS was used to isolate the GFP (+) and 7-AAD (-) compartment of cells. Sorted cells were then left to incubate for an additional 72

hours and expanded to numbers suitable for screening in the presence of 300 µg/mL zeocin. MTF2 expression was measured at both the transcript and protein levels upon transduction with the dual vector GeCKOv2 library. For all validation experiments using THP-1 cells, this same protocol was followed except the original pLenti-GIII-CMV-RFP-2A-Puro matched lentivectors were used while sorting isolated the RFP (+) SYTOX Green (-) compartment of cells. 2 µg/mL puromycin was used to enrich for successfully transduced cells upon expansion.

2.9 MTF2 transcript quantification

RNA was extracted from 2.5 x 10^4 untransduced, Empty Vector transduced and MTF2 Rescue transduced cells using the PicoPure RNA Isolation Kit (ThermoFisher Scientific – KIT0204) according to the manufacturer's protocol. RNA was then converted to cDNA using SuperScript II Reverse Transcriptase (ThermoFisher Scientific – 18064014) according to the manufacturer's protocol. For all RT-qPCR reactions, Lightcycler 480 SYBR Green I Master Mix (Roche - 4887352001) was used along with between 2-10 ng of converted cDNA/well in a 10 µL total volume and run in the Roche Lightcycler 480. A pre-incubation step at 95°C for 300 seconds was followed by 45 cycles of denaturation, annealing and elongation at 95°C for 10 seconds, 60°C for 10 seconds and 72°C for 10 seconds respectively. The reaction was completed following continuous melting at 95°C. Relative MTF2 transcript levels were determined by normalization to GAPDH transcript levels using the following formula where ΔC_t is the difference in C_t values between treatments for a given primer.

$$Fold\ change = 2^{-(\Delta Ct(MTF2) - \Delta Ct(GAPDH))}$$

2.10 Protein quantification by flow cytometry

In each case, 1 million THP-1 cells were washed in ice cold unsupplemented PBS and fixed by resuspension in 500 µL of 10% formalin and incubation at RT for 15 minutes. Fixed cells were again washed in ice cold unsupplemented PBS and permeabilized by resuspension in ice cold 100% methanol to a final concentration of 90% methanol in unsupplemented PBS (450 µL methanol to 50 µL PBS). After 30 minutes incubation on ice, permeabilized cells were washed in ice cold unsupplemented PBS, resuspended in 100 µL of PBS with 5% BSA and 2 µl (1/50) primary antibody and left to incubate on ice for 1 hour. Cells were then washed in ice cold PBS with 5% BSA, resuspended in 100 µL of PBS with 5% BSA and 0.1 µL 1/1000 secondary antibody before being left to incubate on ice for 1 hour in the dark. Antibody labelled cells were then washed with PBS with 5% BSA, resuspended in unsupplemented PBS and run on the BD LSR Fortessa flow cytometer where the ratio of geometric mean fluorescent intensity between samples was used to determine relative protein levels as normalized to an isotype or secondary control.

2.11 Immunofluorescence Imaging of Cas9

1 million untransduced or LentiCas9-Blast transduced THP-1 cells were washed in ice cold unsupplemented PBS and fixed by resuspension in 500 µL of 10% formalin and incubation at RT for 15 minutes. Fixed cells were again washed in ice cold unsupplemented PBS and permeabilized by resuspension in ice cold 100% methanol to a final concentration of 90% methanol in unsupplemented PBS (450 µL methanol to 50 µL PBS). After 30 minutes incubation on ice, permeabilized cells were washed in ice cold unsupplemented PBS, resuspended in 100 µL of PBS with 5% BSA and 2 µL (1/50) of mouse α-Cas9 monoclonal antibody and left to

incubate on ice for 1 hour. Cells were then washed in ice cold PBS with 5% BSA, resuspended in 100 µL of PBS with 5% BSA and 0.1 µL (1/1000) of Alexafluor488 goat α-mouse IgG secondary antibody before being left to incubate on ice for 1 hour in the dark. Antibody labelled cells were then washed with PBS with 5% BSA and resuspended in unsupplemented PBS before 1.0 x 10^5 cells were fixed to a glass slide and imaged using the Zeiss – Axio Obsrver.A1.

2.12 Genome-scale CRISPR knock-out

From each cohort – Empty Vector and MTF2 Rescue Cas9 expressing THP-1 cells – 2.05 x 10^8 cells were separately transduced with thawed LentiGuide-Puro supernatant pre-titrated to 30% transduction efficiency to achieve 500-fold coverage of the GeCKOv2 library as described in section 2.3.

$$500X\ cells/sgRNA\ \times \frac{123411\ sgRNA}{library} \times \frac{100\%}{30\%} = 205\ 685\ 000\ cells$$

In each case, lentiviral transduced cells were left to incubate at 37°C for 18 hours followed by media replacement and further incubation for an additional 48 hours. To enrich for successfully transduced cells, incubation with 2 µg/mL puromycin was then carried out for 72 hours at 37°C. Directly following puromycin selection, 6.0 x 10^7 (500X average coverage) cells from each cohort were flash frozen and stored at -80 °C to serve as a baseline for library representation. All remaining cells from each cohort were then split and left to incubate in two competing maintenance conditions; 0.1% DMSO vehicle and 0.25µM Cytarabine for 14 days with media replacement every 72 hours and 1.0 x 10^8 cells (>800X coverage) carried forward each time. Upon the end point, 1.2 x 10^8 cells (2 x 500X coverage) from each of the 4 conditions were flash frozen and stored at -80 °C.

2.13 Library preparation and deep sequencing

For each of the 6 samples, 6.0 x 10^7 cells (500X coverage) were thawed and genomic DNA (gDNA) was extracted. An initial PCR step was performed on each gDNA sample using primers designed to amplify LentiGuide-Puro genomic integrations out of the gDNA. For this reaction, a pre-incubation step at 98°C for 30 seconds was followed by 12 cycles of denaturation and annealing/elongation at 98°C for 10 seconds and 65°C for 75 seconds respectively. The reaction was completed following a final elongation at 65°C for 300 seconds. For each sample, 82 reactions were performed using 5 µg of gDNA in a 50 µL final volume to maintain 500X library coverage.

$$\left[500X\ cells/sgRNA \times \frac{123411\ sgRNA}{library} \times \frac{6.6\ \mu g\ gDNA}{10^6\ cells}\right] \div \frac{5\ \mu g\ gDNA}{reaction} = 81.45\ reactions$$

After pooling the product from the first PCR step, 5 µL was carried forward to a second PCR step that used a single forward primer and 6 unique reverse primers designed to attach 8 bp demultiplexing barcodes to the initial amplicon as well as Illumina sequencing adapters for use with the Illumina HiSeq 2500 platform. A pre-incubation step at 98°C for 30 seconds was followed by 12 cycles of denaturation, annealing and elongation at 98°C for 1 seconds, 70°C for 5 seconds and 72°C for 35 seconds respectively. The reaction was completed following a final elongation at 72°C for 60 seconds. This PCR step was performed in 13 replicates to maintain library diversity while both PCR step 1 and PCR step 2 were performed using Phusion High-Fidelity DNA Polymerase in GC Buffer (ThermoFisher Scientific – F530L). PCR step 2 products were then pooled and run on 13 lanes of a 1% agarose gel in TAE buffer at a constant 125 V for 30 minutes at 2 amperes. The 375 bp expected products were isolated from the gel using the

Purelink Quick Gel Extraction Kit (Invitrogen – K210012) and shipped for sequencing at Donnelly Sequencing Centre at the University of Toronto.

2.14 MAGeCK

MAGeCK analysis software was downloaded from sourceforge.net and installed using the following commands:

tar xvzf mageck-0.5.4.tar.gz
cd mageck-0.5.4
python setup.py install --prefix=$HOME

Read counting was carried out using the following commands:

mageck count -l library_name -n escneg --sample-label sample_label --fastq fastq_filenames

MAGeCK mle for all comparisons was carried out using the following command:

mageck mle -k escneg.count.txt -d designmatrix_filename -n EmptyVector_vs_MTF2OE

MAGeCK-VISPR and MAGeCK-Flute software were used for all subsequent data visualizations where a loess normalization was included.

2.15 Bone-marrow processing

Bone marrow aspirate samples from AML patients were acquired from a clinical collaborator at the Ottawa Hospital according to protocols approved by The Ottawa Hospital Research Ethics Board. Samples were diluted in an equal volume of unsupplemented PBS, added to 15 mL conical centrifuge tubes containing 2 mL of ficoll-Paque Premium (GE Life Sciences – 17544202) and centrifuged at 400 x g for 20 minutes with rotor brakes deactivated. The leukemic blast layer was then isolated, diluted in PBS with 2% FBS and 100 μM EDTA and re-centrifuged at 400 x g for 10 minutes. The resulting cell pellet was resuspended in 1 mL of red blood cell lysis buffer (9.98 mM Potassium bicarbonate, 160 mM Ammonium chloride, 0.4 mM EDTA)

and incubated under gentile agitation for 5 minutes at RT. Cells were then diluted in 2 mL of PBS with 2% FBS and 100 µM EDTA, centrifuged at 400 x g for 10 minutes and resuspended in PBS with 2% FBS and 100 µM EDTA. For long term culture, cells were resuspended in defined media at 2.0 x 10^6 cells/mL. Patient derived leukemic blasts were expanded by tail-vein injection of 1.0 x 10^6 cells into sublethally irradiated 8-12-week-old female NSG mice. Engrafted leukemia cells were collected from the injected mice by flushing the bone marrow from each rear femur and tibia upon loss of approximately 20% total body mass or signs of severely declining health.

2.16 Human Umbilical Cord Blood Processing

Human umbilical cord blood samples were acquired from Canadian Blood Services. Samples were diluted 4:1 in Hespan (Cardinal Health Canada – BBL6511), in 50 mL conical centrifuge tubes and centrifuged at 50 x g for 10 minutes at RT with rotor brakes deactivated. The upper mononuclear cells were then isolated, and again centrifuged at 400 x g for 10 minutes at RT. The resulting cell pellet was resuspended in 40 mL of red blood cell lysis buffer and incubated under gentile agitation for 5 minutes at RT. Cells were then centrifuged at 400 x g for 10 minutes at RT before moving onto counting and CD34 enrichment.

2.17 Apoptosis assay

Inhibitor treated THP-1 cells or PDX expanded patient derived samples were washed with unsupplemented PBS, centrifuged at 400 x g for 10 minutes at RT, resuspended in 100 µL Annexin V binding buffer and filtered through a 70 µm filter into a polypropylene tube. 1 µL of Annexin V - BUV395 and 1 µL of either SYTOX green dead cell stain (THP-1 cells) or 7-AAD dead cell stain (PDX expanded patient derived samples) was added to cells before being left to

incubate in the dark for 15 minutes at RT. Stained cells were then diluted with an additional 100 µL Annexin V binding buffer and analyzed using the BD LSR Fortessa flow cytometer.

Chapter 3: Results

3.1 Preparation of matched cell-lines for GeCKO

3.1.1 Selection of model cell-line

To identify a functional cell line for matched GeCKO screening and to determine suitable conditions for lentiviral transduction, three p53-mutant and chemorefractory AML cell-lines with low MTF2 protein expression compared to healthy bone-marrow and $CD34^+$ umbilical cord blood controls were transduced with dilute pXPR_011 lentiviral supernatant both in the presence and absence of two small-molecule transduction enhancers: polybrene and lentiblast. Relative to the mean of 2 bone-marrow samples from healthy individuals (1.00 ± 0.33), $CD34^+$ UBC cells express 1.25 ± 0.21-fold more MTF2 protein while KG-1, THP-1 and HL-60 cell-lines express 0.42 ± 0.01, 0.43 ± 0.01 and 0.59 ± 0.04-fold as much, respectively ***(Figure 5A)***. Flow cytometric analysis of percent GFP expression in the pXPR_011 transduced cells compared to untransduced controls were used to determine transduction efficiency. Unlike the KG-1 and HL-60 cell-lines, a significant percentage of THP-1 cells expressed GFP 72 hours following lentiviral transduction from the dilute source of lentivirus with an efficiency of 9.5%, 63.4% and 56.6% in the virus alone, polybrene and lentiblast conditions respectively; for all other cell lines in every condition, transduction efficiency was below 4% ***(Figure 5B)***. Since polybrene out-performed lentiblast, THP-1 cells transduced with pXPR_011 both alone and with polybrene were selected for further optimization and for use in GeCKO experiments.

3.1.2 Optimization of lentiviral transduction of THP-1 cells

To avoid dual transduction of targeted sgRNA sequences during GeCKO experiments, a transduction efficiency of between 20% and 50% is recommended. To achieve a transduction

efficiency within the recommended range, THP-1 cells were transduced with dilute pXPR_011 lentiviral supernatant that had either been ultracentrifuge concentrated 20-fold, 2-fold or diluted 5-fold both in the presence and absence of polybrene. For the virus alone condition, an average transduction efficiency of 73.93% ± 19.17%, 21.33% ± 6.09% and 2.58% ± 1.40% was observed for the 20-fold concentrate, the 2-fold concentrate and the 5-fold dilution respectively. Furthermore, over 95% viability (negative signal for 7-AAD DNA dye) was observed in all cases excepted for when the 20-fold concentrated supernatant was used where an average viability of 52.57% ± 11.55% was observed ***(Figure 5C-D)***. For the replicates where polybrene was used to enhance transduction efficiency, an average efficiency of 83.40% ± 14.55%, 68.80% ± 9.04% and 29.57% ± 28.11% was achieved for the 20-fold concentrate, the 2-fold concentrate and the 5-fold dilution respectively while viability dropped below 95% in all cases except the untransduced control at an average of 2.65% ± 1.14%, 53.03% ± 20.15% and 84.03% ± 16.68% respectively. One representative replicate of the flow cytometric data summarized in figure 5C is shown in ***Figure 5E***.

3.1.3 Antibiotic selection curves

To determine optimal antibiotic concentrations for enrichment of clones successfully transduced with the LentiCas9-Blast, LentiGuide-Puro, pXPR_011, pLenti-GIII-CMV-RFP-2A-Puro and pLenti-GIII-CMV-GFP-2A-Zeo lentivectors, THP-1 cells were incubated in the presence of increasing amounts of blasticidin, puromycin and zeocin. Following addition of antibiotics to cells, cell death by percent of cells positive for 7-AAD DNA dye compared to untreated and unstained controls was measured by flow cytometry at 0, 24, 48, 72 and 96 hours while an antibiotic concentration that resulted in approximately 90% cell death by 72 hours was chosen for all subsequent selections with corresponding lentivectors. After 72 hours,

concentrations of 20 µg/mL blasticidin, 2 µg/mL puromycin and 300 µg/mL zeocin resulted in 88.9%, 94.7% and 96.0% positive signal for 7-AAD respectively and were used for all subsequent long-term antibiotic selections ***(Figure 6)***.

3.1.4 Generation of stable Cas9 expressing THP-1 cells

THP-1 cells were transduced with 2-fold concentrated LentiCas9-Blast lentiviral supernatant in the presence of polybrene followed by 2 weeks of blasticidin selection at 20 µg/mL beginning 48 hours after initial transduction. Both LentiCas9-Blast transduced and untransduced THP-1 cells were stained with a mouse anti-Cas9 mAb and corresponding IgG isotype control. Compared to isotype controls, 0.1% of untransduced cells produced a positive signal for Cas9 while LentiCas9-Blast transduced cells were 36.3% positive 48 hours following transduction and 77.0% positive following 2 weeks of blasticidin selection as measured by flow cytometry ***(Figure 7A)***. Relative to untransduced controls, the average ratio of geometric mean fluorescent intensity (MFI) of cells stained with the antiCas9 mAB compared to cells stained with the IgG isotype was 1.41 ± 0.082 directly following lentiviral transduction and 5.58 ± 0.24 following 2 weeks of blasticidin selection ***(Figure 7B)***. Since the observed signal for Cas9 protein expression from both flow cytometric as well as immunofluorescence imaging analysis (shown in ***Figure 7C***) was dim, Cas9 activity was tested by transduction of both untransduced and blasticidin selected LentiCas9-Blast transduced cells with lentivirus delivering pXPR_011 which delivers both GFP as well as a sgRNA sequence targeting GFP. 6 days following puromycin selection at 2 µg/mL for 72 hours, over 95% of blasticidin selected LentiCas9-Blast transduced cells had lost GFP expression while untransduced controls remained over 99% positive for GFP demonstrating that although Cas9 expression levels were low, Cas9 activity was

sufficient for achieving the efficient genetic knock-out required for GeCKO experiments ***(Figure 7D)***.

3.1.5 Generation of matched MTF2-deficient and rescued Cas9 expressing THP-1 cells

Cas9 expressing THP-1 cells were expanded in the presence of 20 µg/mL blasticidin and transduced with the pLenti-GIII-CMV-GFP-2A-Zeo lentivector rescuing MTF2 or corresponding empty vector control, followed by FACS and expansion in the presence of 300 µg/mL zeocin ***(Figure 8A)***. By qRT-PCR, untransduced cells expressed 0.98 times as much MTF2 transcript as empty vector transduced cells while MTF2-rescued cells expressed 2.18-fold more when normalized to GAPDH expression. ***(Figure 8B)***. MTF2 protein levels were measured by flow cytometric analysis that detected increased MTF2 intracellular staining in MTF2-rescued cells compared to both untransduced and empty vector transduced cells ***(Figure 8C)***. The geometric MFI of untransduced and MTF2-rescue transduced cells relative to empty vector transduced cells was 0.948 and 1.865 respectively ***(Figure 8D)***. As expected, both empty vector and MTF2-rescue transduced cells initially expanded slowly when compared to untransduced controls. Consistent with the tumour suppressive role of MTF2, empty vector transduced cells eventually achieved an average growth rate of 2.25-fold expansion per day similar to that of untransduced cells (2.23-fold) whereas MTF2-rescue transduced cells only achieved an average growth rate of 1.52-fold expansion per day ***(Figure 8E)***. Following prolonged expansion of dual transduced THP-1 cells in the presence of both blasticidin and zeocin, Cas9 protein expression was remeasured by flow cytometry. In both empty vector and MTF2-rescued cohorts, over 95% of cells were positive for Cas9 protein expression compared to IgG isotype controls ***(Figure 8F)***.

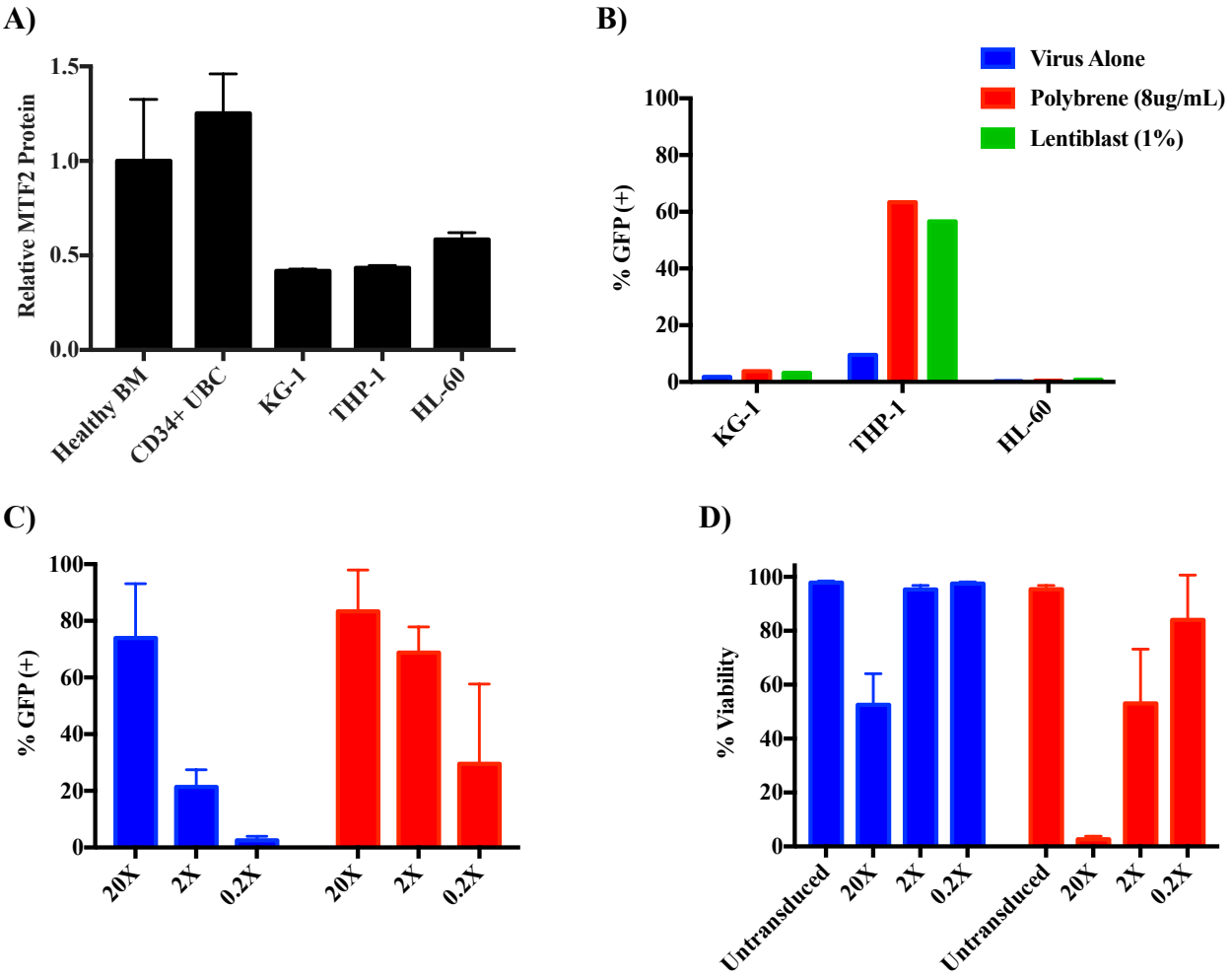
A)
Relative MTF2 Protein
1.5
1.0
0.5
0.0
Healthy BM
CD34+ UBC
KG-1
THP-1
HL-60
B)
Virus Alone
Polybrene (8ug/mL)
Lentiblast (1%)
% GFP (+)
100
80
60
40
20
0
KG-1
THP-1
HL-60
C)
% GFP (+)
100
80
60
40
20
0
20X
2X
0.2X
20X
2X
0.2X
D)
% Viability
100
80
60
40
20
0
Untransduced
20X
2X
0.2X
Untransduced
20X
2X
0.2X

E)

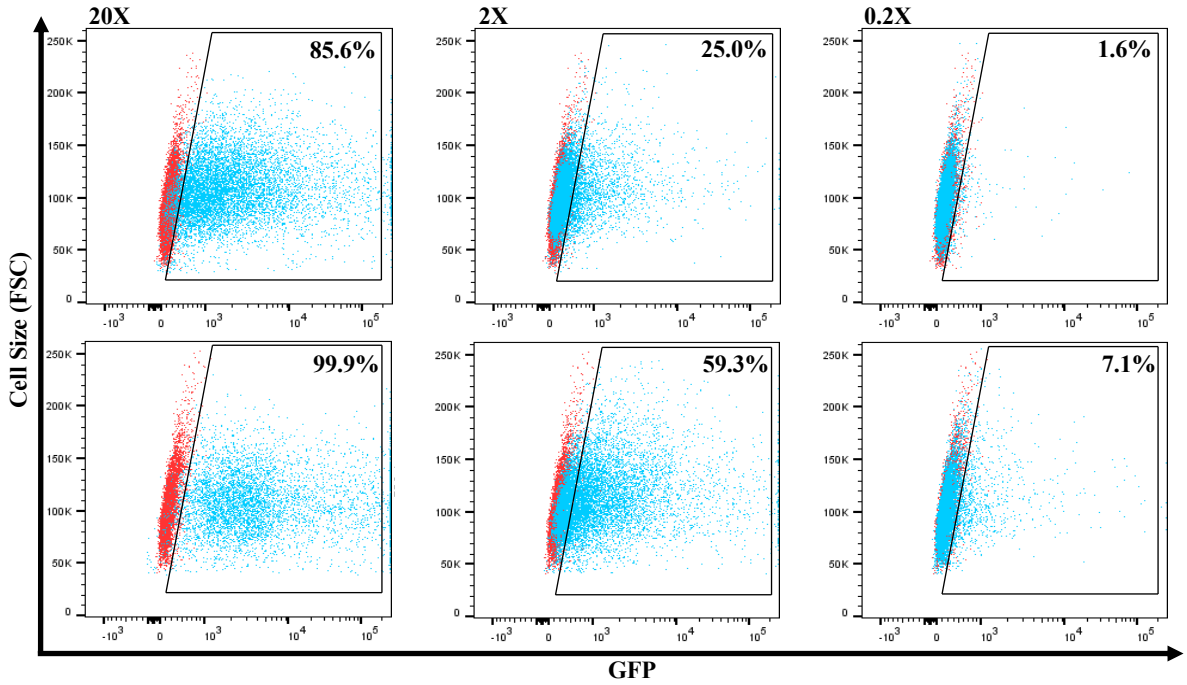
20X
85.6%
2X
25.0%
0.2X
1.6%
99.9%
59.3%
7.1%
Cell Size (FSC)
GFP

Figure 5: Selection of model cell-line and optimization of lentiviral transduction. ***A)*** Relative total geometric MFI of MTF2 protein expression relative to healthy bone-marrow aspirates normalized to secondary controls. Error bars represent standard deviation about the mean of n=2 replicates. ***B)*** Percent GFP expression in AML model cell-lines following transduction with dilute pXPR_011 lentiviral supernatant incubated in either the presence or absence of the transduction enhancers polybrene (8 µg/mL) or lentiblast (1%). Gates are set to untransduced controls at 0.1% GFP positive. ***C)*** Percent GFP expression in THP-1 cells following transduction with either concentrated or diluted pXPR_011 lentiviral supernatant in either the presence or absence of polybrene (8 µg/mL). Gates are set to untransduced controls at 0.1% GFP positive. Error bars represent standard deviation about the mean of n=3 replicates. ***D)*** Cell viability as percent positive for 7-AAD DNA dye following transduction with either concentrated or diluted pXPR_011 lentiviral supernatant in either the presence or absence of polybrene (8 µg/mL). Gates are set to untransduced and unstained controls at 0.1% 7-AAD positive. Error bars represent standard deviation about the mean of n=3 replicates. ***E)*** One representative replicate of the flow cytometric data summarized in ***Figure 5C*** is shown. Cells transduced without polybrene are on top with cells transduced with 8 µg/mL polybrene below. Untransduced controls are in pink while test transductions are in blue. All data was collected on the BD LSR Fortessa flow cytometer and analyzed using FlowJo software.

A) Blasticidin

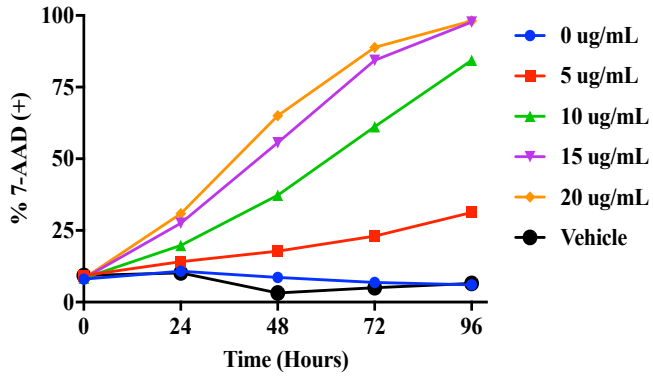

B) Puromycin

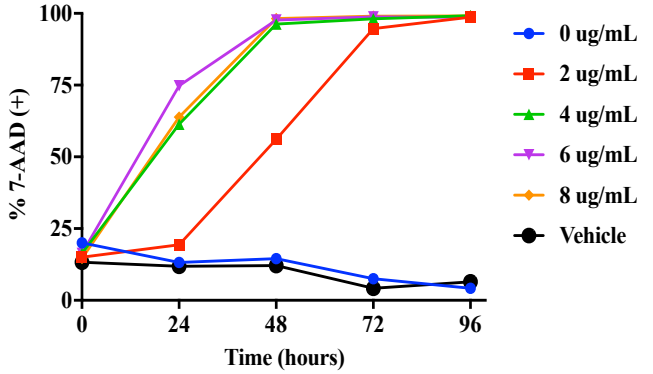

C) Zeocin

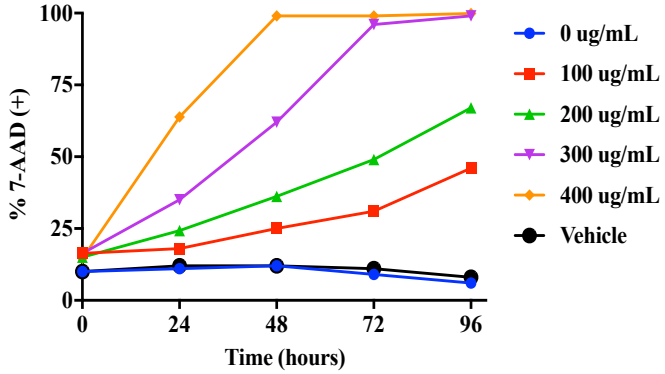

Figure 6: Titration of selection antibiotics in THP-1 cells. ***A)*** Blasticidin titration in THP-1 cells. ***B)*** Puromycin titration in THP-1 cells. ***C)*** Zeocin titration in THP-1 cells. All gates are set to untreated and unstained controls at 0.1% 7-AAD positive using DMSO as a vehicle control. Data was collected on the BD LSR Fortessa flow cytometer and analyzed using FlowJo software.

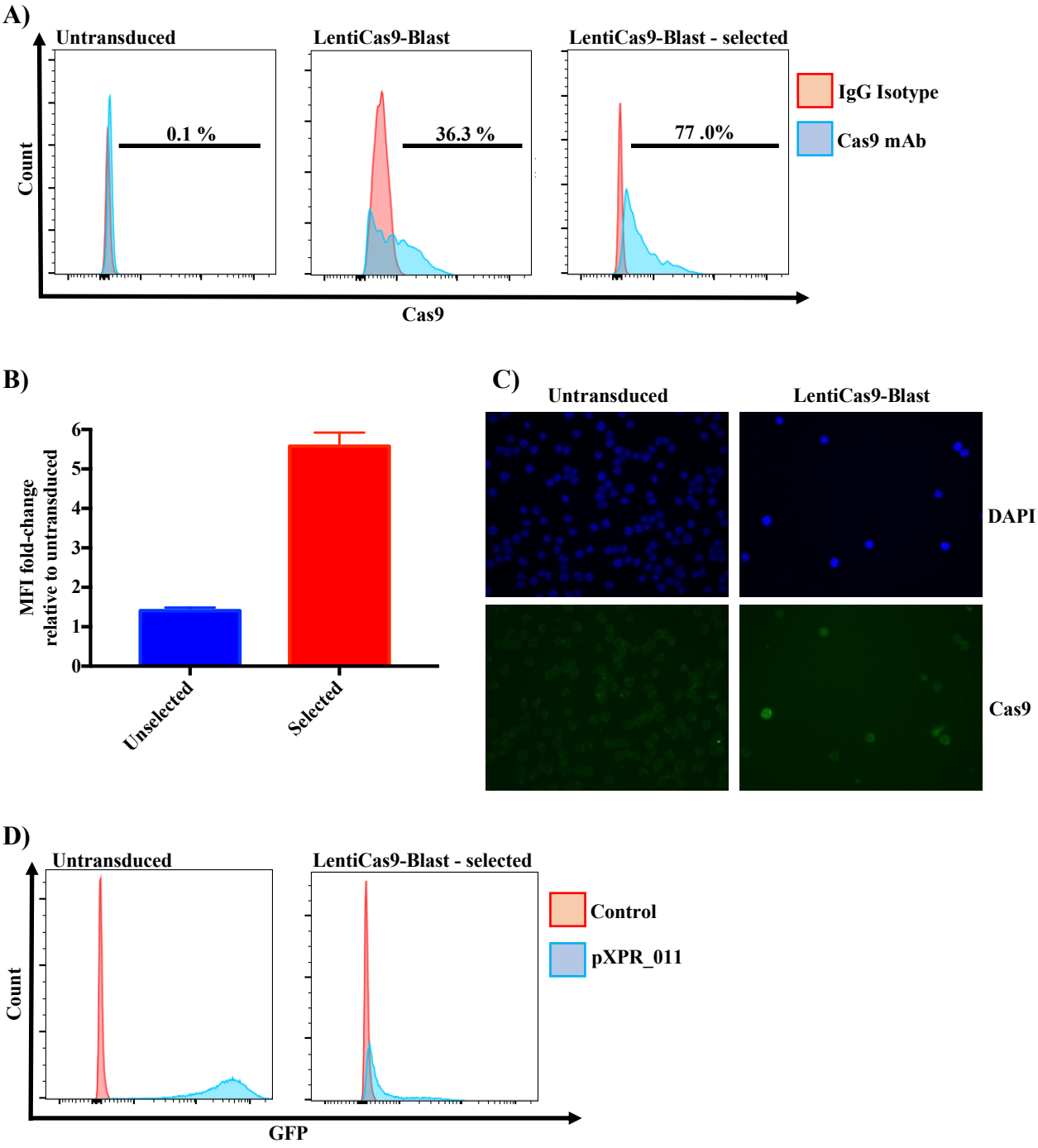
A)
Untransduced
LentiCas9-Blast
LentiCas9-Blast - selected
0.1 %
36.3 %
77 .0%
IgG Isotype
Cas9 mAb
Count
Cas9
B)
MFI fold-change relative to untransduced
0
1
2
3
4
5
6
Unselected
Selected
C)
Untransduced
LentiCas9-Blast
DAPI
Cas9
D)
Untransduced
LentiCas9-Blast - selected
Control
pXPR_011
Count
GFP

Figure 7: Generation and validation of Cas9 expressing THP-1 cells. ***A)*** Reactivity to an anti-Cas9 mouse monoclonal antibody (blue) and mouse IgG isotype (pink) in untransduced THP-1 cells, LentiCas9-Blast transduced THP-1 cells, and LentiCas9-Blast transduced THP-1 cells following 2 weeks of blasticidin selection at 20 μg/mL. Gates are set to isotype controls at 0.1% positive for Alexafluor647 secondary antibody. ***B)*** MFI fold change for reactivity to an anti-Cas9 mouse monoclonal antibody relative to untransduced THP-1 cells in each case normalized to the mouse IgG isotype. Error bars represent standard deviation about the mean of n=2 replicates. ***C)*** Immunofluorescence imaging of untransduced and LentiCas9-Blast transduced THP-1 cells stained with an anti-Cas9 mouse monoclonal primary antibody and alexafluor488 secondary antibody. Images were taken using the Zeiss Axio Observer.A1. ***D)*** GFP expression in untransduced and blasticidin selected LentiCas9-Blast transduced THP-1 cells following transduction with pXPR_011 (untransduced: pink, pXPR_011 transduced: blue), puromycin selection for 72 hours at 2 μg/mL and incubation for 6 days. All flow cytometric data was collected on the BD LSR Fortessa flow cytometer and analyzed using FlowJo software.

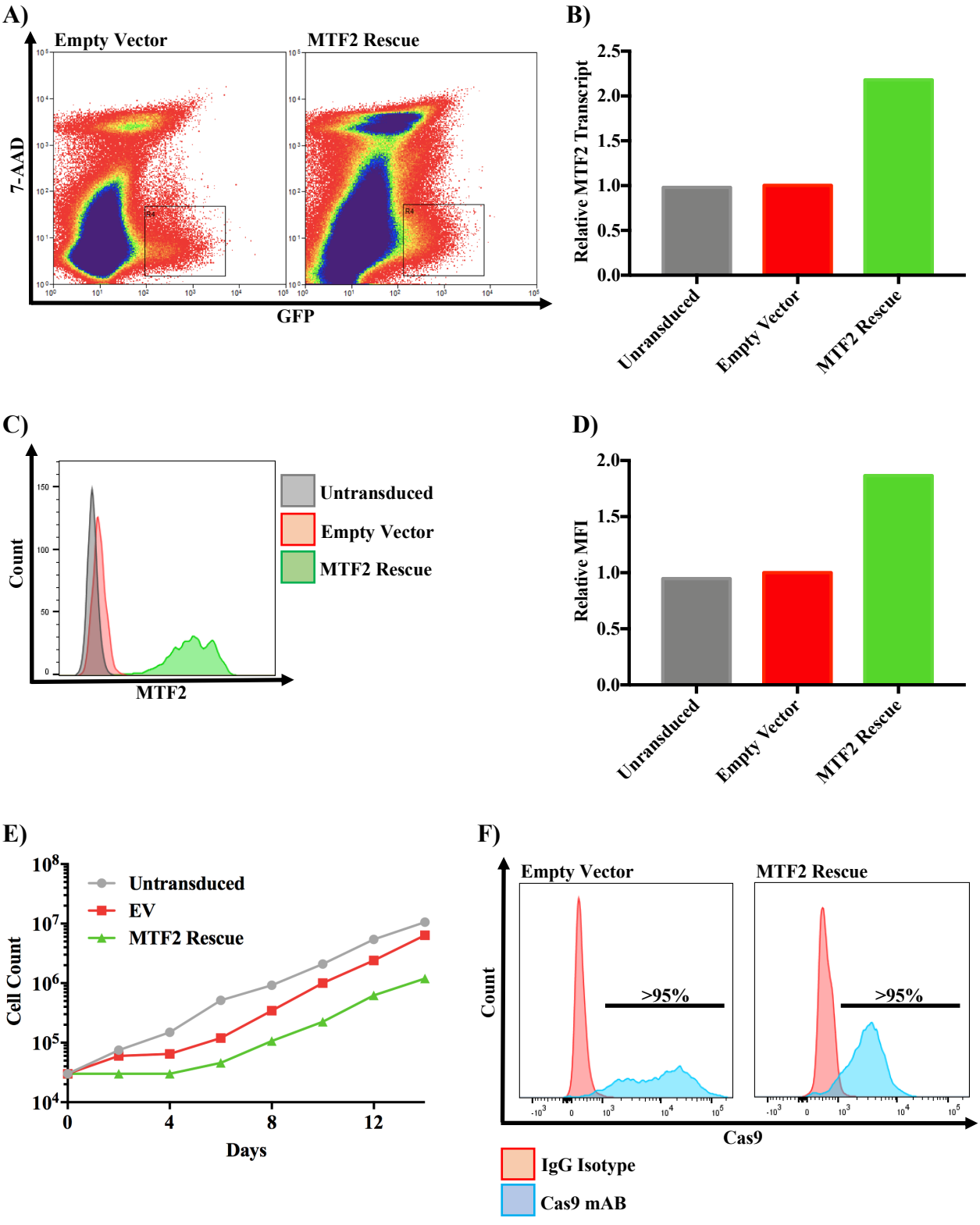
A)
Empty Vector
MTF2 Rescue
7-AAD
GFP
B)
Relative MTF2 Transcript
Unransduced
Empty Vector
MTF2 Rescue
C)
Count
MTF2
Untransduced
Empty Vector
MTF2 Rescue
D)
Relative MFI
Unransduced
Empty Vector
MTF2 Rescue
E)
Cell Count
Days
Untransduced
EV
MTF2 Rescue
F)
Empty Vector
MTF2 Rescue
Count
>95%
>95%
Cas9
IgG Isotype
Cas9 mAB

Figure 8: Generation of matched MTF2-deficient and rescued Cas9 expressing THP-1 cells. ***A)*** FACS plots for THP-1 cells following transduction with pLenti-GIII-CMV-GFP-2A-Zeo and corresponding empty vector lentivirus. 7-AAD DNA dye was added to isolate exclusively viable cells. ***B)*** Relative quantification of MTF2 transcript in either untransduced or sorted THP-1 cells following transduction with pLenti-GIII-CMV-GFP-2A-Zeo or corresponding empty vector lentivirus. Transcript quantities are normalized to GAPDH expression and presented as fold changes relative to empty vector transduced THP-1 cells. ***C)*** Reactivity to an anti-MTF2 rabbit polyclonal antibody in either untransduced or sorted THP-1 cells following transduction with pLenti-GIII-CMV-GFP-2A-Zeo and corresponding empty vector lentivirus. ***D)*** Relative total geometric MFI of MTF2 protein expression in either untransduced or sorted THP-1 cells following transduction with pLenti-GIII-CMV-GFP-2A-Zeo or corresponding empty vector lentivirus. Protein expression is normalized to a secondary control and presented as fold changes relative to empty vector transduced THP-1 cells. ***E)*** Comparative growth curve for both untransduced THP-1 cells and THP-1 cells following transduction with pLenti-GIII-CMV-GFP-2A-Zeo and corresponding empty vector lentivirus. Cells were originally seeded at 3.0×10^4 cells in 100 µL defined media. ***F)*** Reactivity to an anti-Cas9 mouse monoclonal antibody (blue) and mouse IgG isotype (pink) in THP-1 cells following transduction with pLenti-GIII-CMV-GFP-2A-Zeo and corresponding empty vector lentivirus. Gates are set to isotype controls at 0.1% Alexafluor647 positive. All flow cytometric data was collected on the BD LSR Fortessa flow cytometer and analyzed using FlowJo software.

3.2 Genome-scale CRISPR knock-out

3.2.1 Pilot GeCKO quality control

To test out the GeCKO platform, 2.05 x 10^8 stable Cas9 expressing THP-1 cells were transduced with sufficient pooled GeCKOv2 library to achieve 30% transduction efficiency. Following 72 hours of puromycin selection at 2 µg/mL, the resulting LentiGuide-Puro genomic integrations from 6.0 x 10^7 cells (487X) were PCR amplified and sequenced to establish the baseline representation of sgRNA sequences. Amplification and sequencing of remaining LentiGuide-Puro genomic integrations was repeated after 14 days of incubation in maintenance conditions to identify both depleted and enriched sgRNA sequences compared to the baseline (***Figure 9A)***. From MAGeCK-RRA analysis of sequencing data, the median representation for each sgRNA sequence in the library was approxametely 500 for both the baseline and endpoint. The inter-quartile range (IQR), which is a robust measurement of the dispersion of the middle 50% of the read counts, increased at the endpoint compared to the baseline which is also evident from the change in total read count distribution ***(Figure 9B-C)***. MAGeCK-RRA software was then used to generate RRA scores based on a weighted rank of the depletion data for all redundant sgRNA sequences targeting a given gene for the entire GeCKOv2 library to identify the most highly depleted and enriched sets of sgRNA sequences (***Figure 9D)***. PFN1, a member of the profilin family of small actin binding proteins, was among the top ten genes with the most depleted sets of sgRNA sequences with each individual sgRNA sequence decreasing at least 2-fold at the endpoint compared to the baseline ***(Figure 9E)***. The set of guide sequences targeting the mTORC1 regulator, TSC2 were among the most enriched sets with 5 out of 6 sgRNA sequences being highly enriched between baseline and endpoint.

3.2.2 Matched MTF2-deficient and rescued GeCKO quality control

The GeCKO platform was repeated in matched MTF2-deficient and rescued Cas9 expressing THP-1 cells in both the absence and presence of 0.25 μM cytarabine. Following deep sequencing of PCR amplified LentiGuide-Puro genomic integrations, library coverage for the baseline, endpoint and endpoint with cytarabine (AraC) for both the empty vector and MTF2 rescue cohorts was 81.7, 70.6, 62.2, 50.4, 74.0 and 68.7 million reads respectively while the mean quality score was approxametely 34.4 for every timepoint and condition ***(Figure 10A-B)***. MAGeCK-VISPR analysis determined the normalized median sgRNA representation to be approxametely 408 ($10^{2.61}$) for all samples while IQR increased for both endpoints compared to baselines whether or not cytarabine was added to maintenance conditions ***(Figure 10C)***. Furthermore, total missed sgRNA sequences as well as Gini coefficients which are a measure of divergent read count distribution increased for all endpoints compared to baseline samples. ***(Figure 10D-E)***.

3.2.3 MTF2-specific synthetic lethal interactions

MAGeCK-Flute software was used to generate and plot normalized beta scores for every gene targeted by the GeCKOv2 library for both empty vector and MTF2-rescue THP-1 cells under both maintenance conditions. Group 1 genes represent potential MTF2-specific synthetic lethal interactions since beta scores of less than -0.1 are observed for the empty vector cohort while beta scores of between -0.1 and 0.1 are observed for the MTF2-rescue cohort suggesting that cells transduced with sgRNA sequences targeting those genes were depleted in empty vector transduced cells while being relatively unchanged upon MTF2 rescue. When maintenance conditions contained a DMSO vehicle control, 1358 genes had a synthetic lethal interaction with MTF2 belonging mainly to the KEGG pathways; Spliceosome, Ribosome, transcriptional

misregulation in cancer and RNA transport while the trial that included 0.25 μM cytarabine in maintenance conditions resulted in 1484 MTF2-specific synthetic lethal interactions mainly belonging to similar pathways such as Spliceosome, RNA transport, Ribosome, Proteosome, Ribosome biogenesis in eukaryotes and thermogenesis ***(Figure 11A-B)***. To identify the most significant MTF2-specific synthetic lethal interactions, a strict FDR cut-off of 0.05 was applied, narrowing down the list of potential validation targets to 100 when a DMSO vehicle control was added to maintenance conditions and 168 when 0.25 μM cytarabine was added to maintenance conditions. To further isolate targets that had reduced toxicity to tissues outside of the hematopoietic system, all 1580 pan-essential fitness genes identified by the Hart *et al*. 2015 daisy model were removed to produce final lists of 48 and 74 respectively, 18 of which were conserved among both maintenance conditions, while a small subset of 4 were previously identified by RNAseq to be upregulated upon MTF2 knock-down by shRNA in lineage depleted UBCs ***(Figure 11C)***.[62] To isolate MTF2-specific synthetic lethal interactions that could be targeted by commercially available small molecule inhibitors, a less-stringent FDR cut-off of 0.2 was applied isolating 7 targets, 2 of which are conserved among the two maintenance conditions and 4 that have been previously identified by RNAseq to be upregulated upon MTF2 knock-down by shRNA in lineage depleted UBCs. ***(Figure 11D)***.[62]

3.2.4 Cytarabine-specific synthetic lethal interactions

It is also possible to use MAGeCK-Flute to compare beta scores between cells that were either treated with 0.25 μM cytarabine or the DMSO vehicle control to identify cytarabine-specific synthetic lethal interactions for both the empty vector and MTF2-rescue THP-1 cells ***(Figure 12A)***. For empty vector transduced THP-1 cells, 773 genes were represented by sets of sgRNA sequences that were depleted only when cytarabine was included in maintenance

conditions while 1251 genes were identified as synthetic lethal with cytarabine when MTF2 was rescued. An FDR cut-off of 0.2 was applied to identify the most significant targets isolating 10 hits for empty vector transduced cells and 6 upon MTF2 rescue; only SAMHD1 was conserved among the two while only STYX had been previously identified by RNAseq to have been upregulated upon MTF2 knock-down by shRNA in lineage depleted UBCs ***(Figure 12B)***.[62]

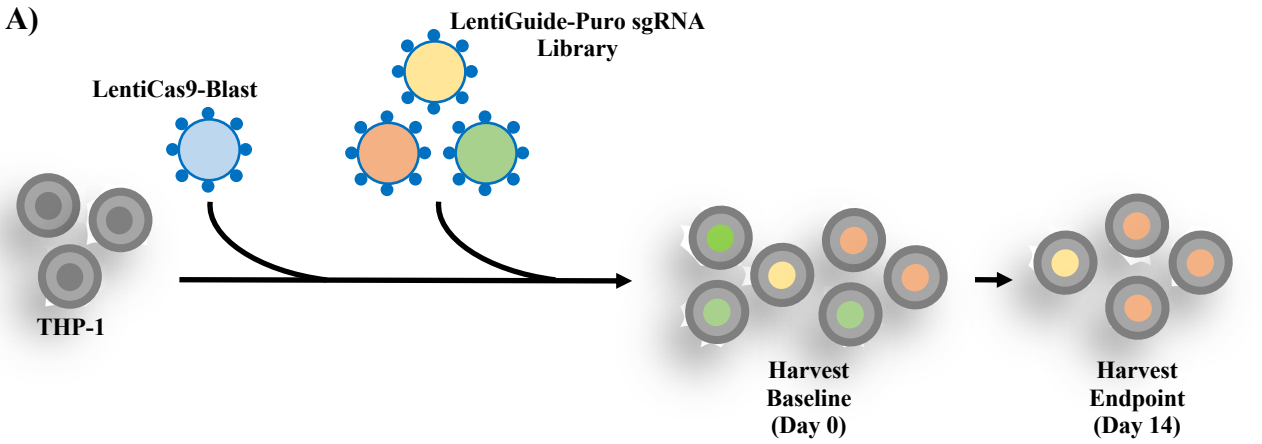
A)
LentiGuide-Puro sgRNA Library
LentiCas9-Blast
THP-1
Harvest Baseline (Day 0)
Harvest Endpoint (Day 14)

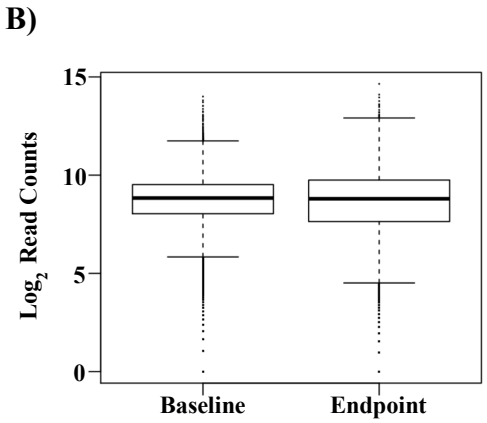
B)
Log2 Read Counts
15
10
5
0
Baseline
Endpoint

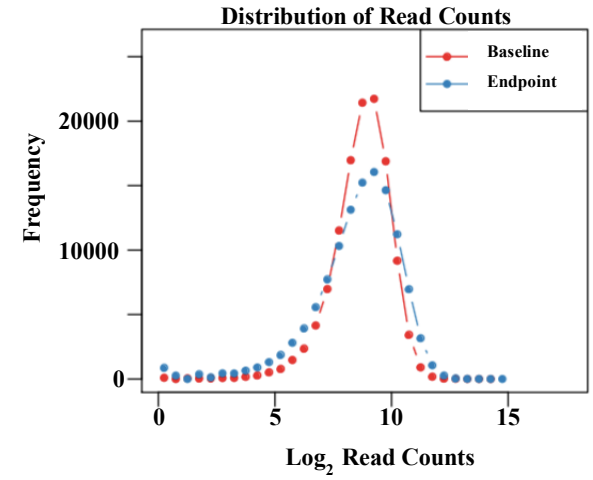
C)
Distribution of Read Counts
Baseline
Endpoint
Frequency
20000
10000
0
0
5
10
15
Log2 Read Counts

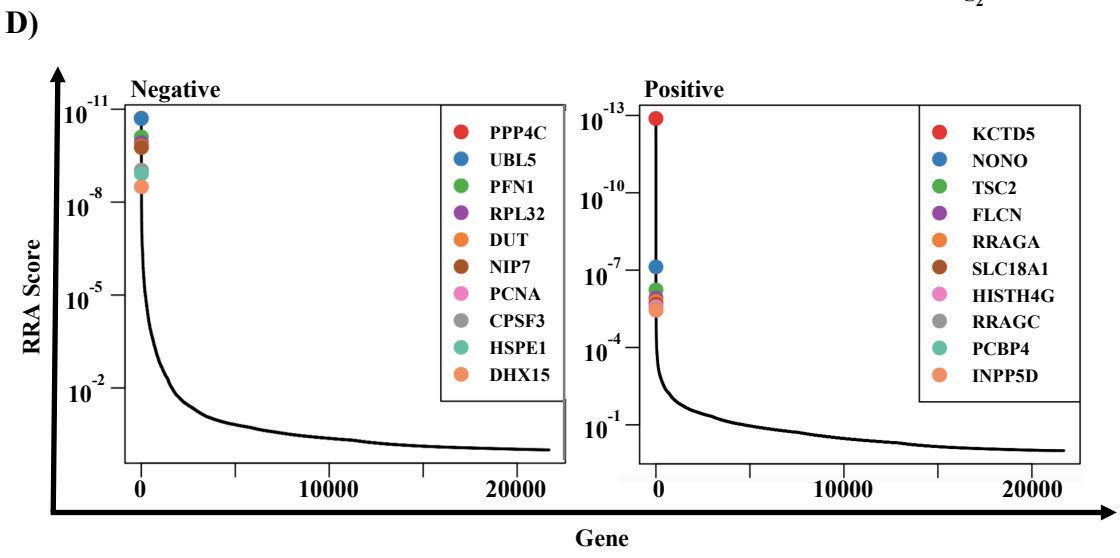
D)
Negative
Positive
RRA Score
PPP4C
UBL5
PFN1
RPL32
DUT
NIP7
PCNA
CPSF3
HSPE1
DHX15
KCTD5
NONO
TSC2
FLCN
RRAGA
SLC18A1
HISTH4G
RRAGC
PCBP4
INPP5D
0
10000
20000
Gene

E)

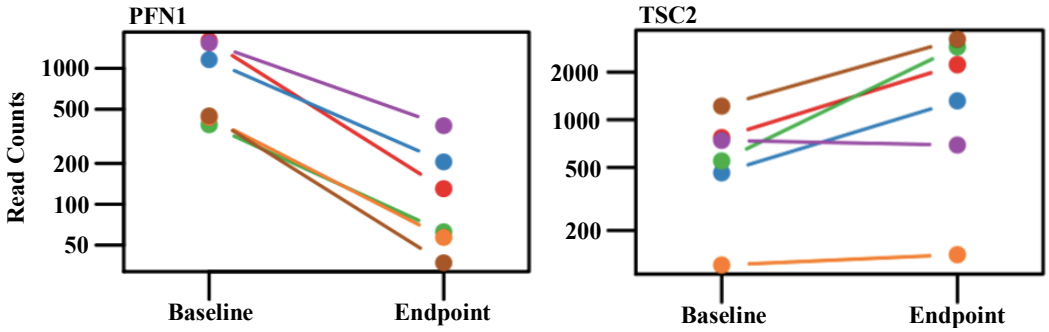
PFN1
Read Counts
1000
500
200
100
50
Baseline
Endpoint
TSC2
2000
1000
500
200
Baseline
Endpoint

Figure 9: Pilot GeCKO quality control. ***A)*** Schematic for pilot GeCKO in Cas9 expressing THP-1 cells. ***B)*** MAGeCK-RRA generated box plot for log_2 read counts for both baseline and endpoint sgRNA sequences. Horizontal bars represent 1.5 IQR. ***C)*** MAGeCK-RRA generated distribution of log_2 read counts across sgRNA frequency for both baseline and endpoint sgRNA sequences. ***D)*** MAGeCK-RRA generated distribution of normalized RRA scores and list of top ten most depleted (left) and enriched (right) sets of sgRNA sequences. **E)** MAGeCK-RRA generated normalized read count for representative top 10 depleted (PFN1) and enriched (TSC2) sets of sgRNA sequences.

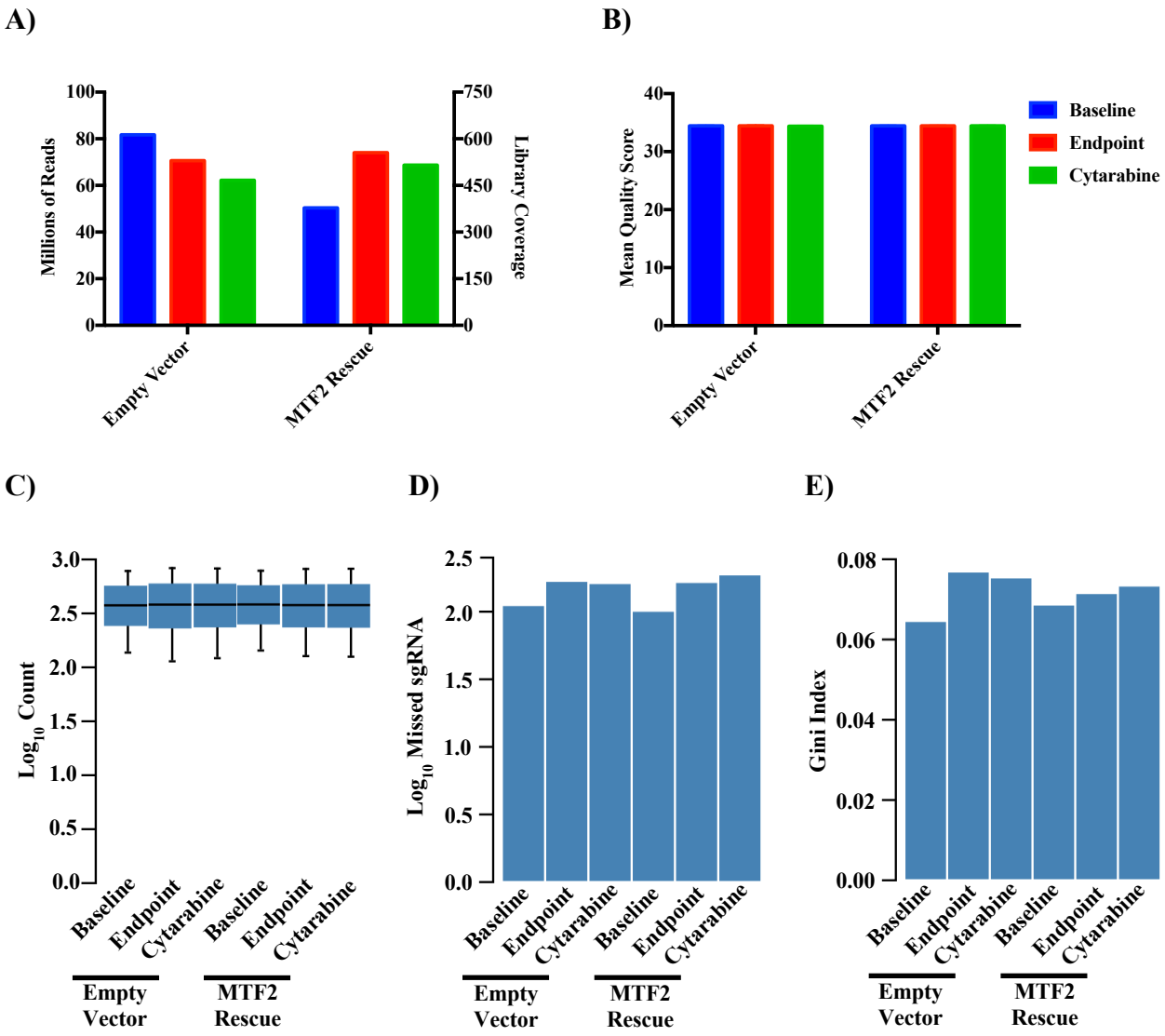
A)
Millions of Reads
Library Coverage
Empty Vector
MTF2 Rescue
B)
Mean Quality Score
Baseline
Endpoint
Cytarabine
Empty Vector
MTF2 Rescue
C)
Log10 Count
Baseline
Endpoint
Cytarabine
Empty Vector
MTF2 Rescue
D)
Log10 Missed sgRNA
E)
Gini Index

Figure 10: Matched MTF2-deficient and rescued GeCKO quality control. ***A)*** Total read count and GeCKOv2 library coverage for PCR amplified LentiGuide-Puro genomic integrations following deep sequencing for each timepoint (baseline, endpoint and cytarabine endpoint) and condition (empty vector and MTF2 rescue). ***B)*** Mean quality score for PCR amplified LentiGuide-Puro genomic integrations following deep sequencing for each timepoint and condition. ***C)*** MAGeCK-VISPR generated box plot for $\log_{10}$ read counts for each timepoint and condition. Horizontal bars represent 1.5 IQR. ***D)*** MAGeCK-VISPR generated $\log_{10}$ missed sgRNA sequences from sequencing data for each timepoint and condition. ***E)*** MAGECK-VISPR generated gini index from sequencing data for each timepoint and condition.

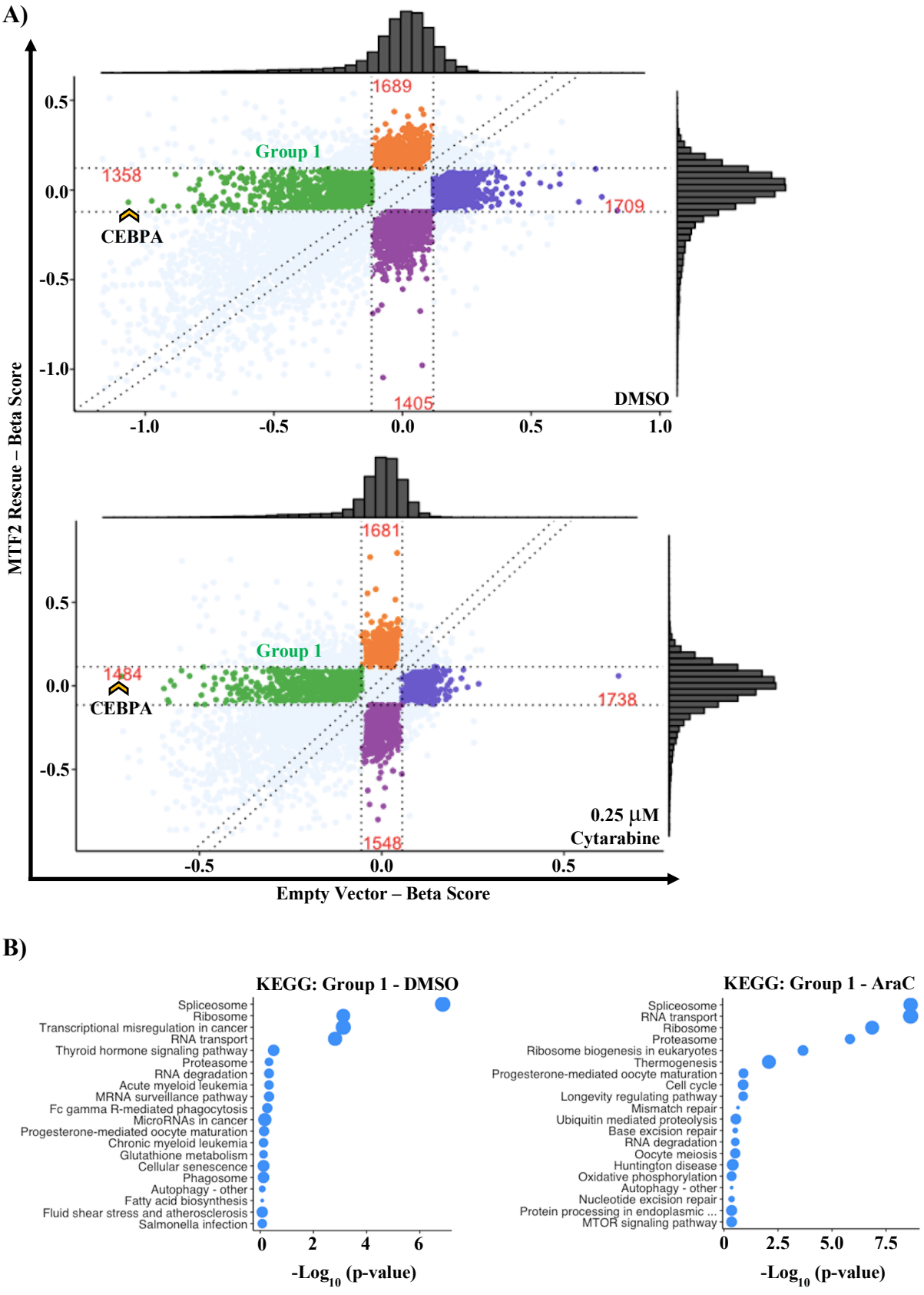
A)
MTF2 Rescue – Beta Score
Empty Vector – Beta Score
Group 1
1689
1358
1709
1405
CEBPA
DMSO
1681
1484
1738
1548
0.25 µM
Cytarabine
B)
KEGG: Group 1 - DMSO
Spliceosome
Ribosome
Transcriptional misregulation in cancer
RNA transport
Thyroid hormone signaling pathway
Proteasome
RNA degradation
Acute myeloid leukemia
MRNA surveillance pathway
Fc gamma R-mediated phagocytosis
MicroRNAs in cancer
Progesterone-mediated oocyte maturation
Chronic myeloid leukemia
Glutathione metabolism
Cellular senescence
Phagosome
Autophagy - other
Fatty acid biosynthesis
Fluid shear stress and atherosclerosis
Salmonella infection
-Log10 (p-value)
KEGG: Group 1 - AraC
Spliceosome
RNA transport
Ribosome
Proteasome
Ribosome biogenesis in eukaryotes
Thermogenesis
Progesterone-mediated oocyte maturation
Cell cycle
Longevity regulating pathway
Mismatch repair
Ubiquitin mediated proteolysis
Base excision repair
RNA degradation
Oocyte meiosis
Huntington disease
Oxidative phosphorylation
Autophagy - other
Nucleotide excision repair
Protein processing in endoplasmic ...
MTOR signaling pathway
-Log10 (p-value)

C)

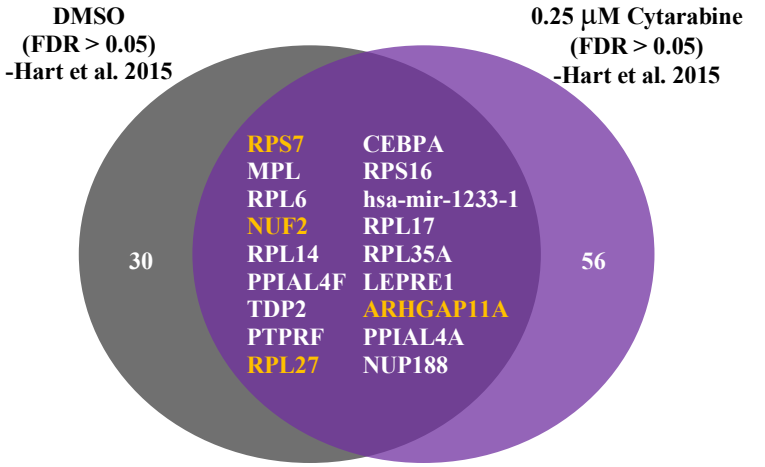
DMSO
(FDR > 0.05)
-Hart et al. 2015
0.25 μM Cytarabine
(FDR > 0.05)
-Hart et al. 2015
30
RPS7
MPL
RPL6
NUF2
RPL14
PPIAL4F
TDP2
PTPRF
RPL27
CEBPA
RPS16
hsa-mir-1233-1
RPL17
RPL35A
LEPRE1
ARHGAP11A
PPIAL4A
NUP188
56

D)

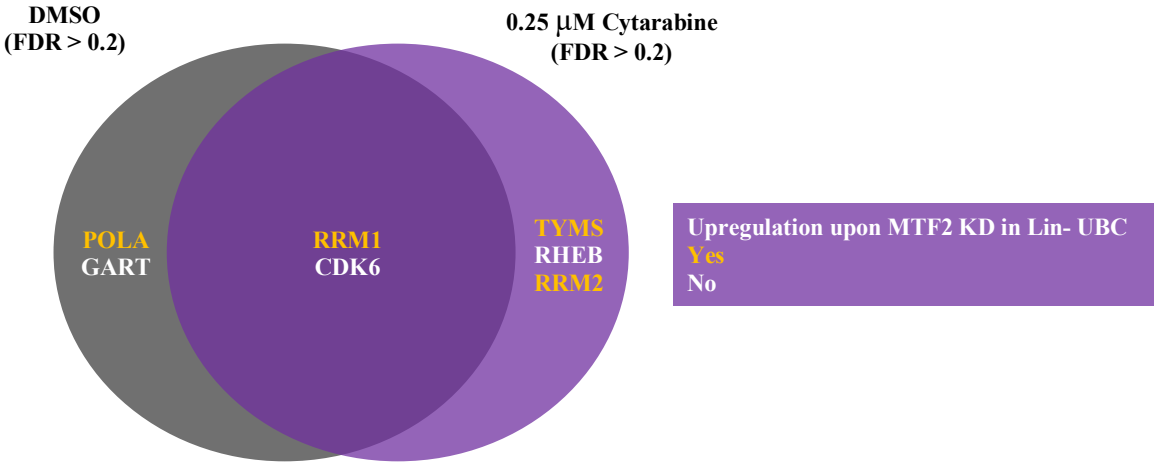
DMSO
(FDR > 0.2)
0.25 μM Cytarabine
(FDR > 0.2)
POLA
GART
RRM1
CDK6
TYMS
RHEB
RRM2
Upregulation upon MTF2 KD in Lin- UBC
Yes
No

Figure 11: MTF2-specific synthetic lethal interactions. ***A)*** 4-square scatter plots of beta-scores in MTF2-deficient (x-axis) and rescued (y-axis) THP-1 cells treated with either DMSO (top) or 0.25 μM cytarabine (bottom). MAGeCK-Flute software was used to generate analysis using a 4-square boundary cut-off of beta scores between -0.1 and 0.1. ***B)*** KEGG pathway analysis of group 1 hits in THP-1 cells under both the absence (left) and presence (right) of 0.25 μM cytarabine. A Fisher Exact p-value is applied to test for significance. ***C)*** Venn diagram of 4-square scatter plot group 1 hits that fall below an FDR cut-off of 0.05 and are not included in the Hart *et al*. 2015 daisy model of core fitness genes. Only genes conserved despite addition of 0.25 μM cytarabine to maintenance conditions are listed. ***D)*** Venn diagram of 4-square scatter plot group 1 hits that fall below an FDR cut-off of 0.2 that can be targeted by commercially available small molecule inhibitors. Genes in yellow have been previously validated by RNAseq analysis in lineage depleted UBCs to be upregulated upon MTF2 knock-down.

A)

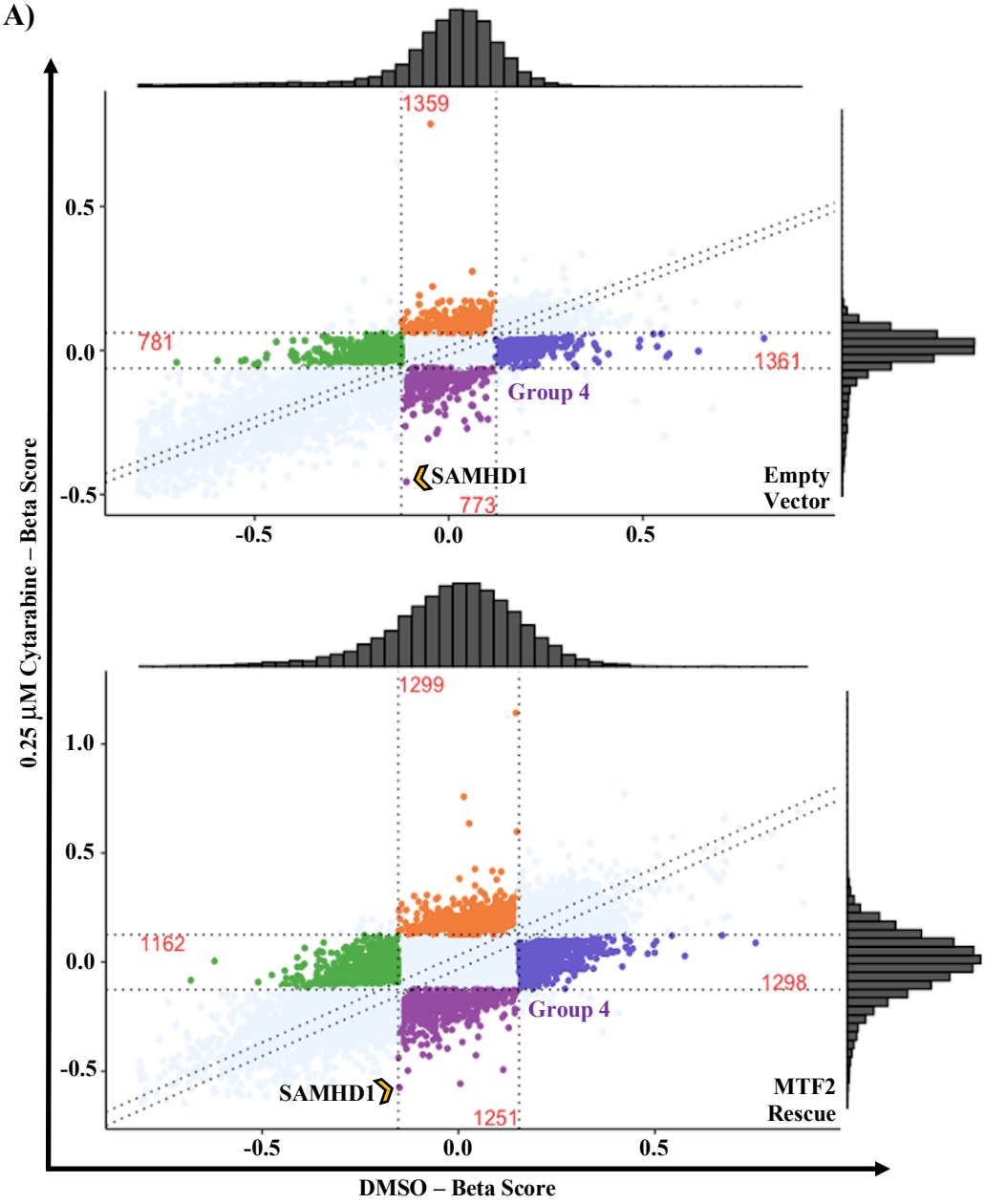
1359
0.5
0.0
-0.5
781
1361
Group 4
SAMHD1
773
Empty
Vector
-0.5
0.0
0.5
1299
1.0
0.5
0.0
-0.5
1162
1298
Group 4
SAMHD1
1251
MTF2
Rescue
-0.5
0.0
0.5
0.25 µM Cytarabine – Beta Score
DMSO – Beta Score

B)

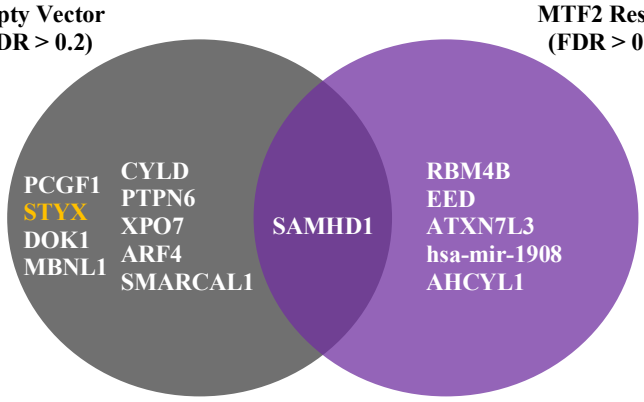
Empty Vector
(FDR > 0.2)
MTF2 Rescue
(FDR > 0.2)
PCGF1
STYX
DOK1
MBNL1
CYLD
PTPN6
XPO7
ARF4
SMARCAL1
SAMHD1
RBM4B
EED
ATXN7L3
hsa-mir-1908
AHCYL1

Figure 12: Cytarabine-specific synthetic lethal interactions. ***A)*** 4-square scatter plots of beta-scores in DMSO treated (x-axis) and 0.25 μM cytarabine treated (y-axis) THP-1 cells transduced with either the empty vector control (top) or the MTF2-rescue (bottom) lentivirus. MAGeCK-Flute software was used to generate analysis using a 4-square boundary cut-off of beta scores between -0.1 and 0.1. ***B)*** Venn diagram of 4-square scatter plot group 4 hits that fall below an FDR cut-off of 0.02. Genes in yellow have been previously validated by RNAseq analysis in lineage depleted UBCs to be upregulated upon MTF2 knock-down.

3.3 Validation of druggable targets

To validate the MTF2-specific synthetic lethal interactions identified from GeCKO screening that have commercially available small molecule inhibitors, matched MTF2-deficient and rescued THP-1 cells were generated by lentiviral transduction with the pLenti-GIII-CMV-RFP-2A-Puro and corresponding empty vector followed by FACS purification and expansion in the presence of 2 μg/mL puromycin ***(Figure 13A)***. Following expansion, RT-qPCR was used to validate an approximate 2-fold average increase in MTF2 mRNA expression in the MTF2-rescue cells compared to the untransduced and empty vector transduced cells (1.86x and 2.05x, respectively), normalized to GAPDH expression ***(Figure 13B)***. The resulting matched MTF2-deficient and rescued THP-1 cells were then incubated for 48 hours in the presence of either 2 μM cytarabine or a DMSO vehicle control followed by flow cytometric analysis of Annexin V/SYTOX Green penetration. When DMSO was included in maintenance conditions, the average cell viability (negative signal for both dyes) was 95.8% ± 1.93% for the empty vector transduced cohort and 96.6% ± 1.95% for the MTF2-rescue cohort suggesting little to no toxicity associated with the culturing method or vehicle control used. Upon addition of 2 μM cytarabine to maintenance conditions, viability in the empty vector cohort dropped to an average of 91.6% ± 7.1% while viability in the MTF2-rescue cohort dropped to an average of 39.5% ± 29.7% (p=0.0010***, 0.0021**) ***(Figure 13C)***. One representative replicate of the flow cytometric data from ***figure 13C*** is shown in ***Figure 13D***. Identical assays were repeated in matched THP-1 cells along with the addition of small molecule inhibitors targeting genes listed in ***figure 11D*** at concentrations pre-titrated to induce 90% cell death in untransduced THP-1 cells ***(Figure 14)***. Only in the case of dual POLA1/RRM1 inhibition in the absence of 2 μM cytarabine was a selective advantage observed for MTF2-rescue THP-1 cells. For clofarabine, which was included

at 1 μg/mL, the average viability following 48 hours of incubation in the absence of 2 μM cytarabine, was 9.5% ± 6.7% for the empty vector transduced cohort and 56.5% ± 25.2% for the MTF2-rescue cohort (p=0.0148*). For fludarabine, which was included at 3 μg/mL, the average viability following 48 hours of incubation in the absence of 2 μM cytarabine, was 9.9% ± 12.2% for the empty vector transduced cohort and 58.4% ± 13.5% for the MTF2-rescue cohort (p=0.0321*).

A)

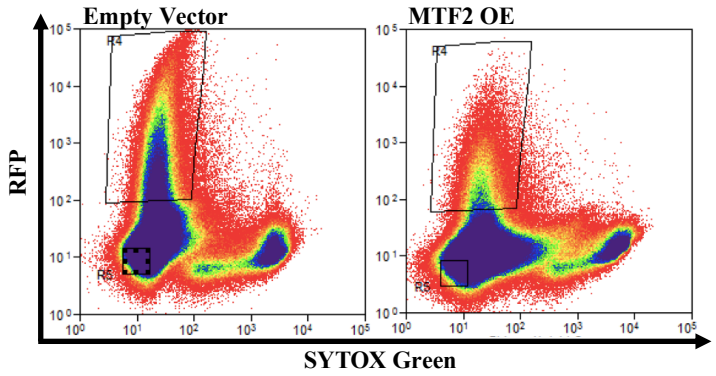
Empty Vector
MTF2 OE
RFP
SYTOX Green

B)

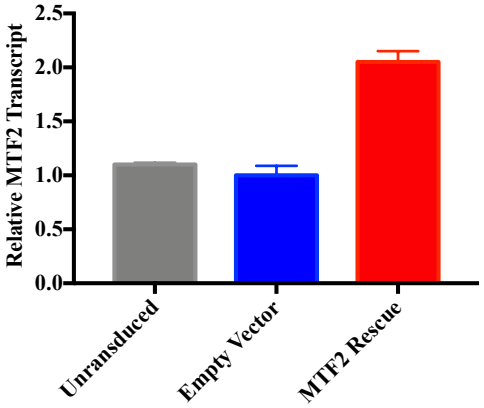
Relative MTF2 Transcript
Unransduced
Empty Vector
MTF2 Rescue

C)

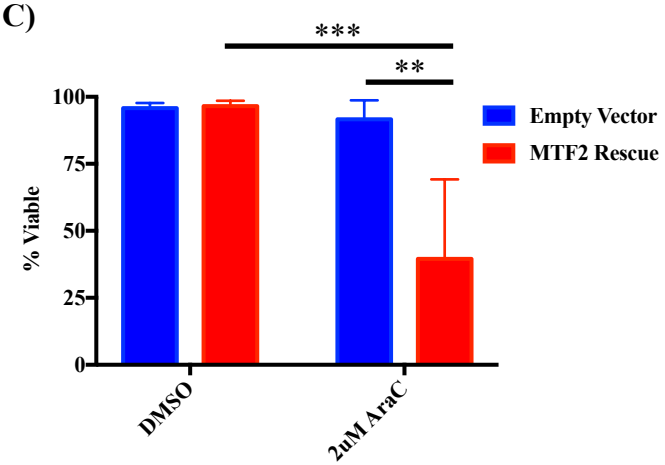
***
**
% Viable
Empty Vector
MTF2 Rescue
DMSO
2uM AraC

D)

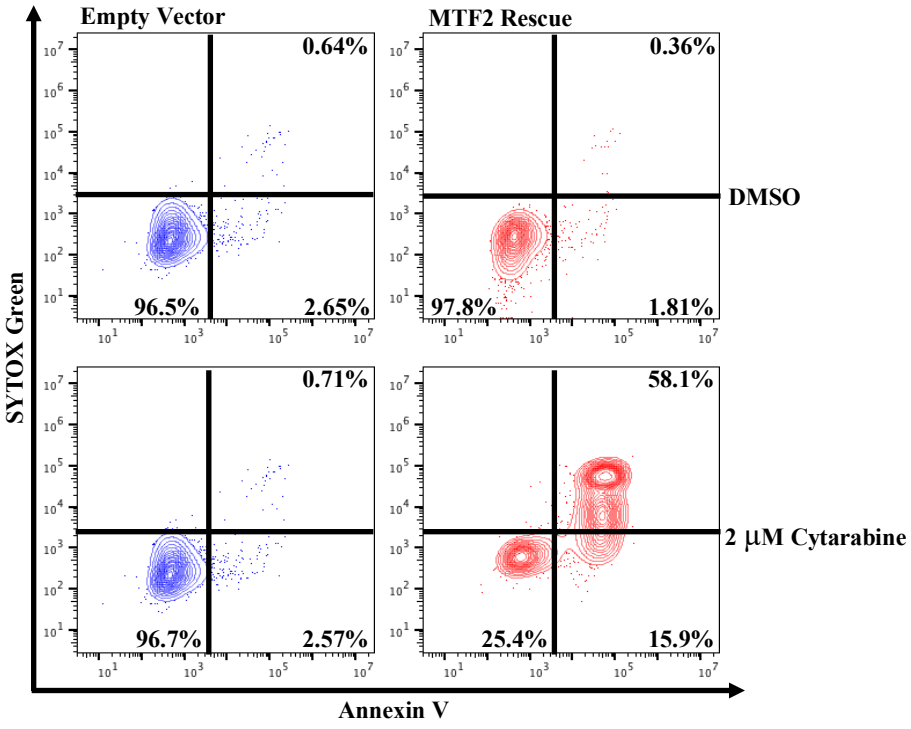
Empty Vector
MTF2 Rescue
0.64%
0.36%
96.5%
2.65%
97.8%
1.81%
DMSO
0.71%
58.1%
96.7%
2.57%
25.4%
15.9%
2 µM Cytarabine
SYTOX Green
Annexin V

Figure 13: Generation of matched MTF2-deficient and rescued THP-1 cells for target validation. ***A)*** FACS plots for THP-1 cells following transduction with pLenti-GIII-CMV-RFP-2A-Puro and corresponding empty vector lentivirus. SYTOX Green DNA dye was added to isolate exclusively viable cells. ***B)*** Relative quantification of MTF2 transcript in either untransduced or sorted THP-1 cells following transduction with pLenti-GIII-CMV-RFP-2A-Puro or corresponding empty vector lentivirus. Transcript quantities are normalized to GAPDH expression and presented as fold changes relative to empty vector transduced THP-1 cells. Error bars represent standard deviation about the mean of n=3 replicates. ***C)*** Cell viability by percent Annexin V(-)/SYTOX Green(-) following treatment of sorted empty vector or MTF2-rescue transduced THP-1 cells with either DMSO or 2 μM cytarabine. Gates are set to untreated and unstained empty vector transduced controls. Data was collected on the BD LSR Fortessa flow cytometer and analyzed using FlowJo software. Error bars represent standard deviation about the mean of n=3 replicates while a two-way ANOVA with multiple comparisons was used to test the significance of results. ***D)*** One representative replicate of the flow cytometric data summarized in ***Figure 13C*** is shown.

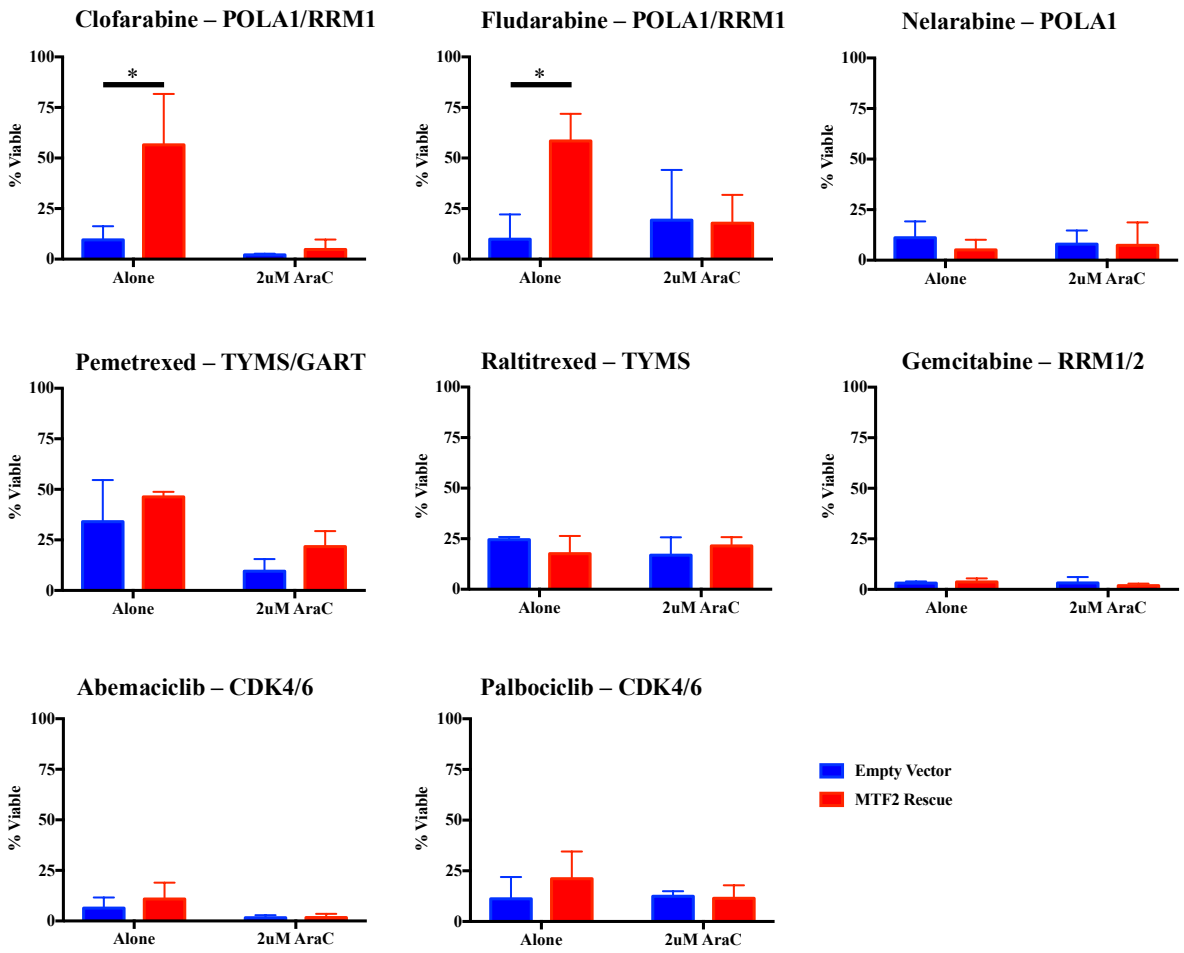
Clofarabine – POLA1/RRM1
Fludarabine – POLA1/RRM1
Nelarabine – POLA1
Pemetrexed – TYMS/GART
Raltitrexed – TYMS
Gemcitabine – RRM1/2
Abemaciclib – CDK4/6
Palbociclib – CDK4/6
% Viable
100
75
50
25
0
*
Alone
2uM AraC
Empty Vector
MTF2 Rescue

Figure 14: Validation of druggable targets. Cell viability by percent Annexin V(-)/SYTOX Green(-) following treatment of sorted empty vector or MTF2-rescue transduced THP-1 cells with small molecule inhibitors corresponding to targets specified in ***Figure 11D*** in either the absence or presence 2 μM cytarabine (AraC). Concentrations for clofarabine, fludarabine, nelarabine, pemetrexed, raltitrexed, gemcitabine, abemaciclib and palbociclib are 1μg/mL, 3 μg/mL, 500 μg/mL, 15 μg/mL, 15 μg/mL, 1 μg/mL, 100 μg/mL and 100 μg/mL respectively. Gates are set to untreated and unstained empty vector transduced controls. Cells were incubated with the inhibitors for 48 hours before data was collected on the BD LSR Fortessa flow cytometer and analyzed using FlowJo software. Error bars represent standard deviation about the mean of n=3 replicates while a two-way ANOVA with multiple comparisons was used to test the significance of results.

Chapter 4: Discussion

4.1 Preparation of matched cell-lines for GeCKO

4.1.1 Selection of model cell-line

The goal of this project was to perform a CRISPR/Cas9 synthetic lethal screen in matched MTF2-deficient and rescued, p53-mutant AML cells. A model cell line should therefore be representative of this patient cohort; p53-mutant and MTF2-deficient. In Maganti *et al.* 2018, the cut-off for MTF2 mRNA expression that correlates with p53-mediated chemoresistance in AML patient-derived bone-marrow aspirates was a Log_2 fold change of -1 or less when normalized to the average MTF2 mRNA expression in bone-marrow samples from seven healthy individuals.[62] Similarly, values between -1 and +1 where termed MTF2-basal. In contrast, this study quantified relative MTF2 protein expression normalized to the average of 2 bone marrow aspirates from health individuals ***(Figure 5A)***. $CD34^+$ UBCs which rely on MTF2 expression to achieve balanced self-renewal and differentiation expressed 1.25 ± 0.21-fold more MTF2 protein while all three p53-mutant AML cell-lines expressed decreased amounts. Since HL-60 cells expressed 0.59 ± 0.04-fold as much MTF2 protein as bone marrow aspirates from healthy individuals, they are considered MTF2-basal. This along with their status as an M3 acute promyelocytic leukemia cell line renders them the least representative among the three.[116] THP-1 M4 acute myelomonocytic leukemia cell line would be considered MTF2-deficient (0.43 ± 0.01); however, since it was originally derived from a 1-year-old male, it is representative of both rare and highly aggressive pediatric AML which may not be representative of the majority of AML patients who are adults. Finally, KG-1 M2 acute myelogenous leukemia cell line which is also MTF2-deficient (0.42 +/- 0.01), derives from a 59-year-old male suggesting that it is the most

representative among the three.[117] However, as discussed in more detail below, THP-1 cells are also highly durable and conducive to serial lentiviral transduction and are therefore better suited for assays that include multiple rounds of lentiviral transduction and antibiotic selection.

4.1.2 Optimization of lentiviral transduction of THP-1 cells

Robustness is exceptionally important since the selected cell line will be subject to 3 stages of lentiviral transduction and antibiotic selection to initially establish stable Cas9 expressing clones (LentiCas9-Blast and blasticidin selection), to then generate matched MTF2-deficient and rescued Cas9 expressing clones (MTF2-rescue/empty vector and zeocin selection) and to finally achieve transduction with the GeCKOv2 library (LentiGuide-Puro and puromycin selection). To identify which cell line among the three was most conducive to lentiviral transduction and therefore most functional, cells were transduced with dilute pXPR_011 lentiviral supernatant in both the presence and absence of the transduction enhancers; polybrene and lentiblast. THP-1 cells were the most conducive to lentiviral transduction regardless of the presence of a transduction enhancer which could be the effect of high LDL receptor expression on the surface of THP-1 cells which is used by the VSV-g envelope to achieve efficient transduction ***(Figure 5B)***. This finding prompted further lentiviral titration to determine specific transduction conditions sufficient for achieving between 20%-50% transduction efficiency to avoid dual transduction of sgRNA sequences upon screening while also maintaining high cell viability. Dilute pXPR_011 lentiviral supernatant was concentrated 2-fold, 20-fold and diluted 5-fold by ultracentrifugation before transducing THP-1 cells in both the presence and absence of polybrene. In the case of the 2-fold concentrated supernatant without polybrene, an average transduction efficiency of 21.33% ± 6.09% with over 95% viability was observed ***(Figure 5C-D)***. Although this strategy is appropriate for GeCKO experiments, further titration is required

before using the high titre LentiGuide-Puro as transduction dynamics will likely change. Upon addition of polybrene, an average transduction efficiency of 68.80% ± 9.04% was observed while cell viability was only 53.03% ± 20.15%. Although this strategy results in greater cell death, it remains an appropriate strategy for generation of stable cell lines since a higher transgene delivery rate will better facilitate successful antibiotic selection.

Although THP-1 cells are not as seemingly representative of cytogenetically normal AML patient blasts as KG-1 cells are, they not only harbour biallelic p53 loss of function mutations, they are both MTF2-deficient and highly conducive to serial lentiviral transduction and antibiotic selection. Moreover, their suitability for GeCKO is further solidified after considering their previous use in Genome-scale RNAi knock-down experiments where synthetic lethal interactions corresponding to gain of function mutations in IDH1/2 were identified and validated.[118]

4.1.3 Generation of stable Cas9 expressing THP-1 cells

To produce stable Cas9 expressing THP-1 cells, lentiviral transduction with 2-fold concentrated LentiCas9-Blast supernatant in the presence of polybrene was followed by 2 weeks of blasticidin selection at 20 μg/mL. Prior to antibiotic selection, 36.3% of transduced cells were reactive to an anti-Cas9 mAB while this value increased to 77.0% afterwards ***(Figure 7A)***. Even though the ratio of geometric MFI of the anti-Cas9 mAB compared to the isotype control was over 5 times greater in the blasticidin selected cells compared to the untransduced cells, low population separation from flow cytometric analysis along with dimness upon immuno-fluorescence imaging made it unclear whether a subpopulation (~23.0%) of cells was expressing low levels of Cas9, or whether they were negative for Cas9 yet still resistant to blasticidin ***(Figure 7B-C)***. To address this, LentiCas9-Blast transduced THP-1 cells that had undergone

blasticidin selection along with untransduced controls were again transduced with the pXPR_011 previously used for optimization of lentiviral transduction. While GFP expression was attenuated early for the former cohort reaching below 5% by day 6, the latter cohort remained over 99% GFP positive. This suggested that although Cas9 protein expression may have been low, endonuclease activity was high in at least 95% of the population ***(Figure 7D)***. The Cas9 reporter assay not only validated Cas9 activity, it was also informative of the time required for CRISPR/Cas9 mediated knock-out in THP-1 cells. Since almost complete attenuation was observed following just 6 days of incubation, a GeCKO platform that includes a 14-day incubation period is therefore sufficient. However, in contrast to a Cas9 reporter assay in which a single genomic integration is targeted, individual sgRNAs from the GeCKOv2 library will need to achieve monoploid, diploid and at times even triploid knock-out in THP-1 cells. Fortunately, it has been shown that the CRISPR/Cas9 gene editing system can achieve efficient knock-out for loci that appear up to 8 times across a genome but unfortunately heterozygosity has also been reported to dramatically reduce efficiency.[119, 120]

4.1.4 Generation of matched MTF2-deficient and rescued Cas9 expressing THP-1 cells

Following the generation of stable Cas9 expressing THP-1 cells, matched MTF2-deficient and rescued cohorts were generated by lentiviral transduction with the pLenti-GIII-CMV-GFP-2A-Zeo and corresponding empty vector followed by FACS and zeocin selection at 300 µg/mL ***(Figure 8A)***. Following lentiviral transduction and zeocin selection, cells must be expanded to over 2 x 10^8 cells for GeCKO experiments which takes approximately 1-2 weeks. Although MTF2-rescued transduced cells expressed 2.18-fold more MTF2 mRNA than empty vector transduced cells, at the protein level, only a 1.865-fold rescue was observed categorizing them as MTF2-basal, however; they likely remain below the average of bone-marrow mono-

nuclear cells isolated from healthy individuals ***(Figure 8B-D)***. In Maganti *et al.* 2018, MTF2 knockdown in lineage depleted UBCs resulted in increased proliferation.[62] Similarly, MTF2 rescue in THP-1 cells resulted in decrease proliferation further validating the tumour suppressive role of MTF2 in the hematopoietic system ***(Figure 8E)***. Achieving a sustained MTF2-rescue of at least 2-fold compared to empty vector transduced cells was extremely challenging and likely the result of CMV promoter silencing.[121, 122] Alternatively, the competition among the polyclonal population following transduction with the MTF2-rescue lentiviral vector could have led to cells with a smaller increase in MTF2 expression out-proliferating cells with a more profound change. Finally, both MTF2-deficient and rescued cohorts were over 95% positive for Cas9 endonuclease compared to untransduced controls which was likely the result of prolonged exposure to blasticidin where transcription of both Cas9 and $Blast^R$ mRNA was under the control of an EFS bicistronic promotor ***(Figure 8F)***.

4.2 Genome-scale CRISPR Knock-out

4.2.1 Pilot GeCKO quality control

To test the GeCKO screening platform prior to generating matched MTF2-deficient and rescued stable Cas9 expressing THP-1 cells, 205 million untransduced stable Cas9 expressing THP-1 cells were infected with sufficient GeCKOv2 lentiviral sgRNA library to achieve 30% transduction efficiency. Following puromycin selection for enrichment of successfully transduced cells, 60 million cells (487X) were lysed and LentiGuide-Puro genomic integrations were PCR amplified and sequenced to establish baseline representation. To identify depleted or enriched sgRNA sequences, this was repeated in remaining cells following 14 days of culture allowing Cas9 and sgRNAs to achieve full knock-out ***(Figure 9A)***. MAGeCK-RRA analysis determined the median sgRNA representation to be approximately 500 for both the baseline and

endpoint which is reflection of both the GeCKOv2 library coverage used (487X) as well as the sequencing depth achieved on the Illumina HiSeq 2500 platform (minimum: 60 million read counts). The increase in IQR in the endpoint compared to the baseline as well as the widening of the read count distribution is indicative of both depletion and enrichment of subsets of sgRNA sequences in the library from the baseline through to the endpoint ***(Figure 9B-C)***. Interestingly, representation of the most depleted sets of redundant sgRNA sequences always dramatically decreased from the baseline through to the endpoint whereas the most enriched sets tended to be highly variable which is likely the result of variable targeting efficiencies. (***Figure 9D-E)***.

Using an FDR cut-off of 0.05, 628 genes were identified as having highly depleted redundant sets of sgRNA sequences while only 358 genes had highly enriched sets. The increased number of negatively selected sets is consistent with what was observed by Li *et al.* 2014 and is likely the result of a few positively selected sgRNAs dominating the total sequencing reads.[107] Tzelepis *et al*. 2016 performed Genome-scale CRISPR knock-out in 5 AML cell-lines and 2 non-AML cell lines to identify 5 *pan-essential AML genes*; IREB2, CEBPA, MYB, FPGS and CDS2 while further studying a selected gene, KAT2A. In THP-1 cells, 4 out of the 5 *pan-essential AML genes* were depleted in THP-1 cells with sgRNA sequences targeting CDS2 and KAT6A being neither depleted nor enriched.[104] Using the same list of 628 genes, among the Hart *et al.* 2015 daisy model derived list of 1580 core fitness genes, only 435 genes were conserved while the Cell Reports publication identified 1145 independent targets leaving 193 targets independent to THP-1 cells.[101] While the data generated from pilot GeCKO in THP-1 cells is highly consistent with the former study, it is highly inconsistent with the latter which was carried out in exclusively non-AML or hematopoietic cancer cell-lines. Finally, all top 10 most depleted genes from the pilot GeCKO in THP-1 cells were also depleted in the RNAi knock-down subset

identified in Chan *et al.* 2015.[118] Altogether, this data not only validates the GeCKO platform in THP-1 cells, it also suggests that there are differences in core-fitness and essential gene sets among cancer cell-lines deriving from diverse tissue types.

4.2.2 Matched MTF2-deficient and rescued GeCKO quality control

Following validation of the GeCKO platform in stable Cas9 expressing THP-1 cells, matched MTF2-deficient and rescued cohorts were generated by lentiviral transduction with the pLenti-GIII-CMV-GFP-2A-Zeo and corresponding empty vector. MTF2-matched GeCKO experiments were carried out exactly as in the pilot GeCKO except for the addition of 0.25 μM cytarabine to half of cells following puromycin selection and cryopreservation of 60 million baseline cells from each cohort. Following deep sequencing of PCR amplified LentiGuide-Puro genomic integrations, total read counts were highly variable between samples ranging between 81.9 million reads (663X) for the empty vector baseline to as low as 50.4 million reads (408X) for the MTF2-rescue baseline ***(Figure 10A)***. As a result, the MAGeCK generated median read-count for all samples was normalized to 408X ($10^{2.61}$) coverage of the GeCKOv2 library which is slightly below the target value of 500 yet sufficient for precise identification of MTF2-specific synthetic lethal interactions especially since the mean quality score for all samples was 34.4 corresponding to an average base miscalling of approximately 1/2750 ***(Figure 10B-C)***. Despite lower than expected GeCKOv2 library coverage, read count IQR values increased for all endpoints compared to their respective baselines indicating both depletion and enrichment of subsets of sgRNA sequences. Furthermore, both zero-counts and Gini indexes increased for all endpoints relative to respective baselines indicating both drop-out of specific sgRNA sequences from datasets as well as increased sgRNA sequence biases respectively ***(Figure 10D-E)***.

4.2.3 MTF2-specific synthetic lethal interactions

Using MAGeCK-Flute, 1358 genes were identified as synthetic lethal with MTF2 in THP-1 cells while 1484 were further identified upon addition of cytarabine to maintenance conditions ***(Figure 11A)***. KEGG analysis of the former list was used to identify many highly enriched groups including Spliceosome, Ribosome, Transcriptional miss-regulation in cancer and RNA transport. Such pathways correspond to gene ontology groupings previously identified as upregulated upon MTF2 knock-down in lineage depleted UBCs described in Maganti *et al.* 2018, particularly cell cycle and RNA processing.[62] Furthermore, upon addition of cytarabine, the same top pathways were identified along with the addition of proteasome, ribosome biogenesis and thermogenesis suggesting that upon addition of cytarabine, MTF2-deficient cells rely on additional processes to achieve continued proliferation despite accumulation of DNA damage ***(Figure 11B)***.

After applying an FDR cut off of 0.05, 100 highly significant MTF2-specific synthetic lethal interactions remained; 168 when cytarabine was present. Since screening was only performed in a single cell line, many of the identified targets may be highly specific to THP-1 cells. To isolate targets that would both broadly target hematopoietic tissue while inducing low toxicity in other tissues, all 1580 core-fitness genes identified using the daisy model from Hart *et al.* 2015 were removed leaving 48 remaining targets in the absence of cytarabine and 74 in its presence.[101] A total of 18 of targets were conserved between both conditions and listed in ***Figure 11C***. Among the many ribosomal genes in this list, CEPBA, a gene highly implicated in AML holding widely accepted prognostic value was consistently the highest ranked MTF2-specific synthetic lethal interaction. Validating this interaction in primary samples is therefore an important next step as it could explain why patients with biallelic CEBPA mutations experience

a favourable outcome.[123] MPL, which codes for the thrombopoietin receptor CD110, is another gene that has been highly implicated in myeloid malignancies. Recently, an antagonist has been developed however, it is not yet commercially available.[124] Needless to say, the benefit of genome-wide screening is the identification of several targets previously not implicated in AML. Of these, 4 genes (RPS7, NUF2, RPL27 and ARHGAP11A) were previously identified as up-regulated upon MTF2 shRNA knock-down in lineage depleted UBCs while the majority are newly identified.[62] Therefore, this unbiased approach enabled the identification of targets that have not been identified through traditional forward or reverse genetics strategies.

Genome-scale genetic screens can also identify 10-fold more targets than drug screens because less than 10% of genes are enzymatic and can be targeted using small molecule inhibitors. Consistent with this estimation, to isolate so-called druggable targets, a less strict FDR cut-off of 0.2 was applied isolating 7 targets of intermediate significance, 4 of which have been previously validated by RNAseq as having been upregulated upon MTF2 knock-down in lineage depleted UBCs ***(Figure 11D)***. Although these targets do not meet as high of a statistical significance threshold, they can be exploited to more easily develop a robust validation strategy.

4.2.4 Cytarabine-specific synthetic lethal interactions

The highest tolerable cytarabine concentration for both MTF2-deficient and rescued THP-1 cells for a duration of 2 weeks was 0.25 μM. Since the absence or presence of cytarabine had a smaller effect on proliferation than the level of MTF2 expression did, the distribution of beta scores between conditions was tighter and as a result, fewer sgRNA sequences were highly depleted in one condition compared to the other ***(Figure 12A)***. An FDR cut-off of 0.2 was used to identify 9 cytarabine-specific synthetic lethal targets in empty vector cells, 5 entirely non-overlapping targets in MTF2-rescue cells and SAMHD1 as the only target to be conserved

between both cohorts ***(Figure 12B)***. This is consistent with the role of SAMHD1 as a mammalian dNTP hydrolase which is known to convert the active antileukemic form of cytarabine, Ara-C-triphosphate to the inactive pro-drug, Ara-C facilitating cytarabine resistance.[125] Furthermore, it was recently demonstrated that mice injected with stable luciferase-expressing, SAMHD1 knock-out THP-1 cells had greater survival following cytarabine treatment compared to control luciferase-expressing THP-1 cells.[126] The only target to have been previously validated by RNAseq as upregulated upon MTF2 knock-down in lineage depleted UBCs is STYX, a pseudophosphatase that has been shown to exert oncogenic effects in colorectal cancer despite having no enzymatic activity.[127] Curiously, ablation of EED, a core structural member of the PRC2 complex conferred cytarabine resistance upon knock-out only when MTF2 was rescued. This is intuitive since not only does loss of MTF2 mirror loss of the entire PRC2 complex and act as a core member in hematopoietic tissues, the enzymatic component EZH2 can be compensated through EZH1 activity. However, if EED is acting through a canonical PRC2 mechanism, it would be anticipated that SUZ12 should also be a highly significant target since it also confers structural integrity to the complex while its loss results in loss of both genome-wide H3K27me3 deposition as well as expression of other PRC2 complex members.

4.3 Validation of druggable targets

To validate the druggable targets identified from GeCKO screening, matched MTF2-deficient and rescued THP-1 cells were generated by lentiviral transduction with the pLenti-GIII-RFP-2A-Puro and corresponding empty vector followed by FACS ***(Figure 13A)***. For all validation experiments, 3 replicates were performed where a mean MTF2 mRNA rescue of approximately 2-fold was observed compared to empty vector transduced cells ***(Figure 13B)***.

When cultured in defined media with DMSO for 48 hours, over 95% viability was observed for both cohorts suggesting little to no toxicity associated with the culturing method or vehicle control used. Upon addition of 2 μM cytarabine to maintenance conditions for the same duration, empty vector transduced cells maintained greater than 90% viability whereas MTF2-rescue THP-1 cells were dramatically sensitized achieving an average viability of 39.5% albeit with a high degree of variability ***(Figure 13C-D)***. This result suggests that MTF2-deficiency could lead to cytarabine resistance in pathways that are analogous to MDM2-mediated p53 degradation, which is contrary to the findings of Liang *et al.* 2018 which demonstrated that in breast cancer, MTF2-deficiency has little to no predictive capacity in the absence of detectable p53 activity.[61] It is also possible that the cytarabine sensitizing effect of MTF2-rescue in this p53-mutant background is the result of decades of acclimation to highly specific cell culture conditions. In the future, analysis of survival data from both MTF2-deficient and basal, p53-mutant patients will serve to validate whether MTF2-deficiency is predictive of resistance to standard therapy upon loss of p53. Furthermore, TP53 genetic knock-out and rescue experiments in patient derived bone-marrow blasts should be conducted to better validate this discrepancy especially since incidence is high in relapsed patients.

Identical experiments were performed in the presence of small molecule inhibitors targeting genes listed in ***Figure 11D*** at determined concentrations pre-titrated to achieve approximately 90% cell death in untransduced THP-1 cells in both the absence and presence of 2μM cytarabine. Since the selected inhibitor concentrations were titrated to achieve 90% early or late apoptosis in MTF2-deficient THP-1 cells, drugs targeting true MTF2-specific synthetic lethal genes should induce significantly less toxicity in MTF2-rescued THP-1 cells. Only in the case of dual POLA/RRM1 inhibition through clofarabine or fludarabine treatment in the absence of

cytarabine was a significant sensitivity observed exclusively in MTF2-deficient cells where in each case, between 40-50% early or late apoptosis was observed on average ***(Figure 14)***. This result is consistent with RNA sequencing data from Maganti *et al.* 2018 which show that upon MTF2 knock-down following lentiviral delivery of shRNAs in lineage depleted UBCs, upregulation of both POLA and RRM1 is observed whereas the molecular target of cytarabine, POLB is not. Although, the benefit of using a single small molecule inhibitor concentration is that it easily facilitates drug cytotoxicity validation as the list of potential small molecule inhibitors is far greater then tested in this study, this strategy can also increase observation of false negatives. It is therefore imperative that at least one lower concentration is tested for each small molecule before ruling out potential therapeutic options. Most of the small molecule inhibitors tested in this study have more than one accepted target. It is therefore unclear outside of genetic perturbation whether POLA or RRM1 inhibition is facilitating synthetic lethality or whether there is a combinatorial effect. Interestingly, dual inhibition of RRM1 and RRM2 facilitated by gemcitabine was unsuccessful while the same is true for POLA inhibition alone through Nelarabine suggesting that RRM1 inhibition is causing the observed effect. Additionally, as predicted from GeCKO screening, RRM1 inhibition should induce cell death exclusively to MTF2-deficient THP-1 cells regardless of the absence or presence of cytarabine. To address these inconsistencies, the previously mentioned strategies including genetic perturbation as well as further testing of multiple drug concentrations will be performed. Needless to say, both clofarabine and fludarabine are candidate therapeutic strategies that require further testing in patient derived bone-marrow blasts from patients that are p53 mutant under both deficient and basal MTF2 expression. Such experiments will serve to test whether observed trends are THP-1 specific or whether they apply to a broader cohort of poor-prognosis AML

patients. Furthermore, in contrast to the monoclonal nature of leukemia cell lines, patient derived samples are representative of the true hierarchical and polyclonal characteristics of acute myeloid leukemia.

It was not necessary to apply sophisticated genome-scale CRISPR screening techniques to identify clofarabine and fludarabine as potential therapeutic strategies for treating pediatric AML. This is especially true given that these options along with hematopoietic stem cell transplantation and RHEB inactivating farnesyl-transferase inhibition are already applied as common regimens for treating juvenile myelomonocytic leukemia (JMML).[128] The true strength of the GeCKO platform along with the development of an Annexin V/SYTOX Green validation workflow is the identification of a plethora of non-druggable genes. However, the fact that two small molecule inhibitors indicated for the treatment of refractory JMML proved efficacious validates the proposed high-content validation approach for druggable targets. Furthermore, it will be interesting to explore the possibility of whether or not such inhibitors truly induce selective toxicity to MTF2-deficient cells as well as if MTF2-deficiency can serve as a robust prognostic indicator in JMML as it is in adult *de novo* AML. A major future direction of this study includes testing the therapeutic potential of targeting all non-druggable MTF2 and cytarabine-synthetic lethal interactions potentially exploiting lipid nano-particles to deliver Anti-sense Oligonucleotides (ASO) in both matched MTF2-deficient and rescued THP-1 cells as well as patient derived bone-marrow derived AML cells. Eventually, *in vitro* validated therapeutic strategies must be validated under *in vivo* conditions using a patient derived xenograft (PDX) preclinical animal model of AML using immunocompromised NOD *scid* gamma (NSG) mice.

Conclusion

Acute myeloid leukemia (AML) is a disease characterized by expansion of abnormally differentiated, hyper-proliferative myeloid cells known as blasts in bone-marrow and blood. AML is the most common form of adult leukemia in Canada with a disappointing five-year overall survival rate below 40%. Dismal outlook among patients is the result of vast heterogeneity in the molecular etiology of AML; including abnormal cytogenetics, gain and loss of function mutations, and altered epigenetic landscapes rendering a single treatment regimen unlikely to suit all those affected. Despite recent advances in risk stratification systems including the European Leukemia Net (ELN) 2017 stratification of AML to better manage the disease, robust biomarkers identifying patients who would benefit from novel therapeutic options are still lacking. Our laboratory has previously demonstrated that loss of epigenetic repression by the polycomb repressive complex 2 (PRC2), which is mediated by complex member metal response element binding transcription factor 2 (MTF2), drives chemo-resistance resulting in refractory AML. Our systems biology analyses revealed that MDM2, a negative regulator of p53, is a direct target of MTF2/PRC2. Hence, decreased MTF2 levels result in increased MDM2 levels and decreased p53 levels. Thus, cells are unable to undergo p53-mediated apoptosis in response to induction drugs. Furthermore, we demonstrated both *in vitro* as well as *in viv*o that MTF2-deficient refractory AML cells treated with a MDM2 inhibitor in combination with standard induction drugs were able to undergo p53-mediated apoptosis. Since approximately 8% of AML patients express mutant p53, it is unlikely that this treatment strategy will work for all chemoresistant patients. In this study, to identify alternative therapeutic options, a genome-scale CRISPR Knock-out (GeCKO) synthetic lethal screen was performed in matched MTF2-deficient

and rescued THP-1 cells in both the absence and presence of the standard induction chemotherapeutic cytarabine.

Careful analysis of screening data has resulted in the identification of 104 highly significant (FDR>0.05) putative MTF2-specific synthetic lethal interactions, 18 of which did not depend on the presence of cytarabine in maintenance conditions. Reducing the stringency to an FDR cut off of 0.2 resulted in the identification of seven additional MTF2-specific synthetic lethal interactions that could be targeted by commercially available small molecule inhibitors. An additional 15 cytarabine-specific synthetic lethal interactions were also identified with only SAMHD1 being conserved among both MTF2-deficient and rescued THP-1 cells. To begin developing a validation strategy, commercially available small molecule inhibitors were tested using a standard apoptosis assay in matched MTF2-deficient and rescued THP-1 cells both in the absence and presence of cytarabine. Among eight small molecule inhibitors tested, only Clofarabine and Fludarabine were effective.

This body of work not only provided greater evidence of the strength of the GeCKO strategy for identifying genotype-specific cancer liabilities related to loss of tumour suppressor function, it also generated several potential avenues for the development of novel therapeutics for treating poor-prognosis AML. Furthermore, the establishment of a first-pass validation strategy based on an Annexin V/DNA dye flow cytometric apoptosis assay serves as a starting point for the continued interrogation of the many remaining potential candidate drug targets. One of the major benefits of whole-genome genetic screening compared to drug screening is the identification of non-druggable synthetic lethal interactions which make up the vast majority of the results. In the near future, validation of these many targets will involve the use of lentiviral delivery of shRNAs targeting top synthetic lethal genes and pathways. In the more distant future,

positive hits will be further validated in patient-derived bone-marrow aspirates which are more representative of the true clonal and hierarchical nature of AML. Eventually, *in vitro* validated targets will be validated under *in vivo* conditions using a patient derived xenograft (PDX) preclinical animal model of AML using immunocompromised NOD *scid* gamma (NSG) mice.

Works Cited

1. Till, J.E., McCulloch E.A. *et al.* (1964). "A stochastic model of stem cell proliferation, based on the growth of spleen colony-forming cells." PNAS 51: 29-36.

2. Notta, F., Zandi, S. *et al*. (2016). "Distinct routes of lineage development reshape the human blood hierarchy across ontogeny." Science 351(6269): aab2116 1-9.

3. Orkin, S.H. (2000). "Diversification of haematopoietic stem cells to specific lineages." Nature Reviews Genetics 1: 57-64.

4. Dykstra, B. Kent, D. *et al.* (2007). "Long-term propagation of distinct heamatopoietic differentiation programs *in-vivo*." Cell Stem Cell 1: 218-229.

5. Benveniste, P., Frelin, C. *et al.* (2010). "Intermediate-term hematopoietic stem cells with extended but time-limited reconstitution potential." Cell Stem Cell 6: 48-58.

6. Orkin, S.H., Zon, L.I. (2008). "Hematopoiesis: an evolving paradigm for stem cell biology." Cell 132: 631-644.

7. Challen, G.A., Boles, N.C. *et al.* (2010). "Distinct hematopoietic stem cell subtypes are differentially regulated by TGF-β1." Cell Stem Cell 6: 265-278.

8. Dohner, H., Weisdorf, D.J. *et al.* (2015). "Acute myeloid leukemia." The New England Journal of Medicine 373(12): 1136-1152.

9. Harada, Y., Nagata, Y. *et al.* (2018). "Prognostic analysis according to the 2017 ELN risk stratification by genetics in adult acute myeloid leukemia patients treated in the Japan Adult Leukemia Study Group (JALSG) AML201 study." Leukemia Research 66(2018) 20-27.

10. The Cancer Genome Atlas Research Network (2013). "Genomic and epigenomic landscapes of adult de novo acute myeloid leukemia." The New England Journal of Medicine 368(22): 2059-2074.

11. Papaemmanuil, E., Gerstung, M. *et al.* (2016). "Genomic classification and prognosis in acute myeloid leukemia." The New England Journal of Medicine 374(23): 2209-2221.

12. Egger, G., Liang, G. *et al.* (2004). "Epigenetics in human disease and prospects for epigenetic therapy." Nature 429: 457-463.

13. Wouters, B.J., Delwel, R. (2016). "Epigenetics and approaches to targeted therapy in acute myeloid leukemia." Blood 127(1): 42-52.

14. Cabezas-Wallscheid, N., Klimmeck, D. *et al.* (2014). "Identification of regulatory networks in HSCs and their immediate progeny via integrated proteome, transcriptome and DNA methylome analysis." Cell Stem Cell 15(4): 507-522.

15. Abdel-Wahab, O., Levine, R.L. (2013). "Mutations in epigenetic modifiers in the pathogenesis and therapy of acute myeloid leukemia." Blood 121(18): 3563-3572.

16. Fong, C.Y., Morison, J. *et al.* (2014). "Epigenetics in the hematological malignancies." Haematologica 99(12):1772-1783.

17. Greenblatt, S.M., Nimer, S.D. (2014). "Chromatin modifiers and the promise of epigenetic therapy in acute myeloid leukemia." Leukemia 28: 1396-1406.

18. Figueroa, M.E., Lugthart, S. *et al.* (2010). "DNA methylation signatures identify biologically distinct subtypes in acute myeloid leukemia." Cancer Cell 17(1):13-27.

19. Jaiswal, S., Fontanillas, P. *et al.* (2014). "Age-related clonal hematopoiesis associated with adverse outcomes." New England Journal of Medicine 371(26): 2488-2498.

20. Lewis, E.B. (1978). "A gene complex controlling segmentation in *Drosophila*." Nature 276: 565-570.

21. Ingham, P.W., Pinchin, K.R. *et al.* (1985). "Genetic analysis of the hairy locus in *Drosophila melanogaster*." Genetics 111:463-486.

22. Kennison, J.A., Tamkin, J.W. (1988). "Dosage-dependant modifiers of polycomb and antennapedia mutations in *Drosophila*." PNAS 85: 8136-8140.

23. Steffen, A., Ringrose, L. (2014). "What are memories made of? How polycomb and trithorax proteins mediate epigenetic memory." Nature Reviews 15: 340-356.

24. Kuzmichev, A., Nishioka, K. *et al.* (2002). "Histone methyltransferase activity associated with a human multiprotein complex containing the enhancer of zeste protein." Genes and Development 16: 2893-2905.

25. Levine, S.S., King, I.F.G. *et al.* (2004). "Division of Labour in Polycomb group repression." Trends in Biochemical Sciences 29(9): 478-485.

26. Lund, A.H., van Lohuizen, M. (2004). "Polycomb complexes and silencing mechanisms." Current Opinion in Cell Biology 16: 239-246.

27. Satjin, D.P.E., Otte, A.P. (1999). "RING1 Interacts with multiple polycomb-group proteins and displays tumorigenic activity." Molecular and Cellular Biology 19(1): 57-68.

28. Wang, H., Wang, L. *et al.* (2004). "Role of histone H2A ubiquitination in polycomb silencing." Nature 431: 837-878.

29. Tavares, L., Dimitrova, E. *et al.* (2012). "RYBP-PRC1 complexes mediate H2A ubiquitination at polycomb target sites independently of PRC2 and H3K27me3." Cell 148: 664-678.

30. Blackledge, N.P., Farcas, A.M. *et al.* (2014). "Variant PRC1 complex-dependant H2A ubiquitination drives PRC2 recruitment and polycomb domain formation." Cell 157: 1445-1459.

31. Zhang, Z., Jones, A. *et al.* (2011). "PRC2 complexes with Jarid2, MTF2, and esPRC2p48 in ES cells to modulate ES cell pluripotency and somatic cell reprogramming." Stem Cells 29: 229-240.

32. Cao, R., Wang, L. *et al.* (2002). "Role of histone H3 lysine 27 methylation in polycomb-group silencing." Science 298: 1039-1043.

33. Cao, R., Zhang, Y. (2004). "SUZ12 is required for both the histone methyltransferase activity and the silencing function of the EED-EZH2 complex." Molecular Cell 15: 57-67.

34. Faust, C., Schumacher, A. *et al.* (1995). "The eed mutation disrupts anterior mesoderm production in mice." Development 121: 273-285.

35. Kim, H., Kang, K. *et al.* (2009). "AEBP2 as a potential targeting protein for polycomb repressive complex PRC2." Nucleic Acids Research 37(9): 2940-2950.

36. Sun, A., Li, F. *et al.* (2018). "Structural and biochemical insights into human zinc finger protein AEBP2 reveals interaction with RBBP4." Protein Cell 9(8): 738-742.

37. Pavlopoulos, E., Jones, S. *et al.* (2013). "Molecular mechanisms for age-related memory loss: the histone binding protein RbAp48." Science Translational Medicine 5(200): 200-228.

38. Takeuchi, T., Kojima, M. *et al.* (1999). "*Jumonji* gene is essential for the neurulation and cardiac development of mouse embryos with a C2H/He background." Mechanisms of Development 86: 29-38.

39. Peng, J.C., Valouev, A. *et al.* (2009). "Jarid2/Jumonji coordinates control of PRC2 enzymatic activity and target gene occupancy in pluripotent cells." Cell 139: 1290-1302.

40. Landeira, D., Sauer, S. *et al.* (2010). "Jarid2 is a PRC2 component in embryonic stem cells required for multi-lineage differentiation and recruitment of PRC1 and RNA Polymerase II to developmental regulators." Nature Cell Biology 12: 618-625.

41. Mejetta, S., Morey, L. *et al.* (2011). "Jarid2 regulates mouse epidermal stem cell activation and differentiation." The EMBO Journal 30(17): 3635-3646.

42. Klose, R.J., Kallin, E.M. *et al.* (2006). "JmjC-domain-containing proteins and histone demethylation." Nature Reviews Genetics 7: 715-727.

43. Pasini, D., Cloos, P.A.C. *et al.* (2010). "JARID2 regulates binding of the polycomb repressive complex 2 to target genes in ES cells." Nature 464: 306-311.

44. Margueron, R., Reinberg, D. (2011). "The polycomb complex PRC2 and its mark in life." Nature 469: 343-349.

45. Duncan, I.M. (1982). "Polycomblike: A gene that appears to be required for the normal expression of the bithorax and antennapedia gene complexes of *Drosophila melanogaster*." Genetics 102: 49-70.

46. Salva, U., Benes, J. *et al.* (2008). "Recruitment of *Drosophila* Polycomb-group proteins by polycomblike, a component of a novel protein complex in larvae." Development 135: 813-817.

47. Nekrasov, M., Klymenko, T. *et al.* (2007). "Pcl-PRC2 is needed to generate high levels of H3-K27 trimethylation at polycomb target genes." The EMBO Journal 26(18): 4078-4088.

48. Casanova M., Preissner *et al.* (2011). "Polycomblike 2 facilitates the recruitment of PRC2 polycomb group complexes to the inactive X chromosome and to target loci in embryonic stem cells. Development 138: 1471-1482.

49. Brien, G.L., Healy, E. *et al.* (2015). "A chromatin-independent role of polycomb-like 1 to stabilize p53 and promote cellular quiescence." Genes and Development 29: 2231-2243.

50. Cao, R., Wang, H. *et al.* (2008). "Role of hPHF1 in H3K27 methylation and hox gene silencing." Molecular and Cellular Biology 28(5): 1862-1872.

51. Sauvageau, M., Sauvageau, G. (2010). "Polycomb group proteins: Multi-faceted regulators of somatic stem cells and cancer." Cell Stem Cell 7: 299-313.

52. Wang, S., Robertson, G.P. *et al.* (2004). "A novel human homologue of *Drosophila* polycomblike gene is up-regulated in multiple cancers." Gene 343: 69-78.

53. Brien, G.L., Gambero, G. *et al.* (2012). "Polycomb PHF19 binds H3K36me3 and recruits. PRC2 and demethylase NO66 to embryonic stem cell genes during differentiation." Nature Structural and Molecular Biology 19(12): 1273-1283.

54. Cai, L., Rothbart, S.B., *et al.* (2013). "An H3K36 methylation-engaging tudor motif of polycomb-like proteins mediates PRC2 complex targeting." Molecular Cell 49: 571-582.

55. Coulson, M., Robert, S. *et al.* (1998). "The identification of a human gene with sequence similarity to polycomblike of *Drosophila melanogaster*." Genomics 48: 381-383.

56. Kawakami, S., Mitsunaga, K. *et al.* (1998). "Tctex3, related to *Drosophila* Polycomblike, is expressed in male germ cells and mapped to the mouse t-complex." Mammalian Genome 9: 874-880.

57. Wang, S., He, F. *et al.* (2007). "Polycomblike-2-deficient mice exhibit normal left-right asymmetry." Developmental Dynamics 236: 853-861.

58. Wang, S., Yu, X. *et al.* (2004). "Chick Pcl2 regulates the left-right asymmetry by repressing Shh expression in Henson's node." Development and Disease 131: 4381-4391.

59. Walker, E., Chang, W.Y. *et al.* (2010). Polycomb-like 2 associates with PRC2 and regulates networks during mouse embryonic stem cell self-renewal and differentiation." Cell Stem Cell 6: 153-166.

60. Rothberg, J.L.M., Maganti, H.B. *et al.* (2018). "Mtf2-PRC2 control of canonical Wnt signaling is required for definitive erythropoiesis." Cell Discovery 4(21): 1-16.

61. Liang, Y., Yang, Y. *et al.* (2018). "PCL2 regulates p53 stability and functions as a tumour suppressor in breast cancer." Science Bulletin 63: 629-639.

62. Maganti, H.B., Jrade, H. *et al.* (2018). "Targeting the MTF2-MDM2 axis sensitizes refractory acute myeloid leukemia to chemotherapy." Cancer Discovery 8(11): 1376-1389.

63. Ernst, T., Chase, A.J. *et al.* (2010). "Inactivating mutations of the histone methyltransferase gene EZH2 in myeloid disorders." Nature Genetics 42(8): 722-727.

64. Nikoloski, G., Langemeijer, S.M. *et al.* (2010). "Somatic mutations of the histone methyltransferase gene EZH2 in myelodysplastic syndromes." Nature Genetics 42(8): 665-666.

65. Gollner, S., Oellerich, T. *et al.* (2016). "Loss of the histone methyltransferase EZH2 induces resistance to multiple drugs in acute myeloid leukemia." Nature Medicine 23(1): 69-82.

66. Morin, R.D., Johnson, N.A. *et al.* (2010). "Somatic Mutations altering EZH2 (Tyr641) in follicular and diffuse large B-cell lymphomas of germinal-centre origin." Nature Genetics 42(2): 181-187.

67. Schlesinger, Y., Straussman, R. *et al.* (2007). "Polycomb-mediated methylation on Lys27 of histone H3 pre-marks genes for *de novo* methylation in cancer." Nature Genetics 39(2): 232-236.

68. Sterkers, Y., Preudhomme, C. *et al.* (1998). "Acute myeloid leukemia and myelodysplastic syndromes following essential thrombocytopenia treated with hydroxyurea: High proportion of cases with 17p deletion." Blood 91(2): 616-622.

69. Epstein, R.J. (2013). “The unpluggable in pursuit of the undruggable: tackling the dark matter of the cancer therapeutics universe.” Frontiers in Oncology 3(304): 1-7.

70. O’Neil, N.J., Bailey, M.L. *et al.* (2017) “Synthetic lethality and cancer.” Nature Reviews Genetics 18: 613-628.

71. Bridges, C.B. (1922). “The origin of variations in sexual and sex-limited characters.” The American Naturalist 56(642): 51-63.

72. Farmer, H., McCabe, N. *et al.* (2005). “Targeting the DNA repair defect in BRCA mutant cells as a therapeutic strategy.” Nature 434: 917-921.

73. Vyse, S., Howitt, A. *et al.* (2017). Exploiting synthetic lethality and network biology to overcome EGFR inhibitor resistance in lung cancer.” Journal of Molecular Biology 429: 1767-1786.

74. Pan, R., Ruvolo, V., *et al.* (2017). “Synthetic lethality of combined Bcl-2 inhibition and p53 activation in AML: Mechanisms and superior antileukemia efficacy.” Cancer Cell 32: 748-760.

75. Bender, A., Pringle, J.R. (1991). “Use of a screen for synthetic lethal and multicopy suppressee mutants to identify two new genes involved in morphogenesis in *saccharomyces cerevisiae*.” Molecular and Cellular Biology 11(3): 1295-1305.

76. Reid, R.J.D., Du X. *et al.* (2016). “A synthetic dosage lethal genetic interaction between CKS1B and PLK1 is conserved in yeast and human cancer cells.” Genetics 204: 807-819.

77. Duffy, S., Fam, H.K. *et al.* (2016). “Overexpression screens identify conserved dosage chromosome instability genes in yeast and human cancer.” PNAS 113(36): 9967-9976.

78. Lucchesi, J.C. (1968). “Synthetic lethality and semi-lethality among functionally related mutants of *Drosophila melanogaster*. Genetics 59: 37-54.

79. Hartin, S.N., Hudson, M.L. *et al.* (2015). A synthetic lethal screen identifies a role for Lin-44/Wnt in *C. elegans* embryogenesis. PLOS One 10(5): 1-22

80. Barrangou, R., Marraffini, L.A. (2014). “CRISPR-Cas systems: Prokaryotes upgrade to adaptive immunity.” Molecular Cell 54: 234-244.

81. Grissa, I., Vergnaud, G. *et al.* (2007). “The CRISPRdb database and tools to display CRISPRs and to generate dictionaries of spacers and repeats.” BMC Bioinformatics 8(172): 1-10.

82. Ishino, Y., Shinagawa, H. *et al.* (1987). “Nucleotide sequence of the *iap* gene, responsible for alkaline phosphatase isozyme conversion in *Escherichia coli*, and identification of the gene product.” Journal of Bacteriology, 169(12): 5429-5433.

83. Jansen, R., van Emben, J.D.A. *et al.* (2002). "Identification of genes that are associated with DNA repeats in prokaryotes." Molecular Microbiology 43(6): 1565-1575.

84. Bolotin, A., Quinquis, B. *et al.* (2005). "Clustered regularly interspaced short palindrome repeats (CRISPRs) have spacers of extrachromosomal origin." Microbiology 151: 2551-2561.

85. Mojica, F.J.M., Diez-Villasenor, C. *et al.* (2005). "Intervening sequences of regularly spaced prokaryotic repeats derive from foreign genetic elements." Journal of Molecular Evolution 60: 174-182.

86. Pourcel, C., Salvignol, G. *et al.* (2005). "CRISPR elements in *Yersinia pestis* acquire new repeats by preferential uptake of bacteriophage DNA, and provide additional tools for evolutionary studies." Microbiology 151" 653-663.

87. Barrangou, R., Fremaux, C. *et al.* (2007). "CRISPR provides acquired resistance against viruses in prokaryotes." Science 315: 1709-1712.

88. Garneau, J.E., Dupuis, M. *et al.* (2010). "The CRISPR/Cas bacterial immune system cleaves bacteriophage and plasmid DNA." Nature 468: 67-72.

89. Makarova, K.S., Aravind, L. *et al.* (2011). "Unification of Cas protein families and a simple scenario for the origin and evolution of CRISPR-Cas systems." Biology Direct 6(38): 1-27.

90. Chylinski, K., Makarova, K.S. *et al.* (2014). "Classification and evolution of type II CRISPR-Cas systems." Nucleic Acids Research 42(10): 6091-6105.

91. Hsu, P.D., Lander, E.S. *et al.* (2014). "Development and applications of CRISPR-Cas9 for genome engineering." Cell 157(6): 1262-1278.

92. Jinek, M., Chylinski, K. *et al.* (2012). "A programmable dual-RNA-guided DNA endonuclease in adaptive bacterial immunity." Science 337: 816-821.

93. Cong, L., Ran, A. *et al.* (2013). "Multicomplex genome engineering using CRISPR/Cas systems." Science 339: 819-823.

94. Lagutina, I.V., Valentine, V. *et al.* (2015). "Modelling of the human alveolar rhabdomyosarcoma *Pax3-Foxo1* chromosome translocation in mouse myoblasts using CRISPR-Cas9 nuclease." PLOS Genetics 11(2): 1-24.

95. Freedman, B.S., Brooks, C.R. *et al.* (2015). "Modelling kidney disease with CRISPR-mutant kidney organoids derived from human pluripotent epiblast spheroids." Nature Communications 6(8715): 1-13

96. Flynn, R., Grundmann, A. *et al.* (2015). "CRISPR-mediated genotypic and phenotypic correction of a chronic granulomatous disease mutation in human iPS cells." Experimental Hematology 43: 838-848.

97. Long, C., Amoasii, L. *et al.* (2016). "Postnatal genome editing partially restores dystrophin expression in a mouse model of muscular dystrophy." Science 351(6271): 400-403.

98. Veres, A., Gosis, B.S. *et al.* (2014). "Low incidence of off-target mutations in individual CRISPR-Cas9 and TALEN targeted human stem cell clones detected by whole-genome sequencing." Cell Stem Cell 15: 27-30.

99. Shalem, O., Sanjana, N.E. *et al.* (2014). "Genome-scale CRISPR-Cas9 knock-out screening in human cells." Science 343(6166): 84-87

100. Wang, T., Wei, J.J. *et al.* (2014). "Genetic screens in human cells using the CRISPR-Cas9 system." Science 343(6166). 80-84.

101. Hart, T., Chandrashekhar, M. *et al.* (2015). "High-resolution CRISPR screens reveal fitness genes and genotype-specific cancer liabilities." Cell 163: 1515-1526.

102. Parnas, O., Jovanovic, M. *et al.* (2015). "A Genome-wide CRISPR screen in primary immune cells to dissect regulatory networks." Cell 162: 675-686.

103. Toledo, C.M., Ding, Y. *et al.* (2015). "Genome-wide CRISPR-Cas9 screens reveal loss of redundancy between PKMYT1 and WEE1 in glioblastoma stem-like cells." Cell Reports 13: 2425-2439.

104. Tzelepis, K., Koike-Yusa, H. *et al.* (2016). "A CRISPR dropout screen identifies genetic vulnerabilities and therapeutic targets in acute myeloid leukemia." Cell Reports 17:1193-1205.

105. Fei, T., Chen, Y. *et al.* (2017). Genome-wide CRISPR screen identifies HNRNPL as a prostate cancer dependency regulating RNA splicing." PNAS 114(26): E5207-E5215.

106. Sanjana, N., Shalem, O. *et al.* (2014). "Improved vectors and genome-wide libraries for CRISPR screening." Nature Methods 11(8): 783-784.

107. Li, W., Xiao, T. *et al.* (2014). "MAGeCK enables robust identification of essential genes from genome-scale CRISPR/Cas9 knockout screens." Genome Biology 15(554): 1-12.

108. Robinson, M.D., McCarthy, D.J. *et al.* (2009). "edgeR: a Bioconductor package for differential expression analysis of digital gene expression data." Bioinformatics 26:139-140.

109. Anders, S., Huber, W. (2010). "Differential expression analysis for sequence count data." Genome Biology 11: R106.

110. Hardcastle, T.J., Kelly, K.A. (2010). "baySeq: empirical Bayesian methods for identifying differential expression in sequence count data." BMC Bioinformatics 11: 422.

111. Konig, R., Chiang, C.Y. *et al.* (2007). "A probability-based approach for the analysis of large-scale RNAi screens." Nature Methods 4: 847-849.

112. Luo, B., Cheung, H.W. *et al.* (2008). "Highly parallel identification of essential genes in cancer cells." PNAS 105: 20380-20385.

113. Li, W., Koster, J. *et al.* (2015). "Quality control, modeling, and visualization of CRISPR screens with MAGeCK-VISPR." Genome Biology 16(281): 1-13.

114. Tsuchiya, S., Yamabe, M. *et al.* (1980). "Establishment and characterization of a human acute myeloid leukemia cell line (THP-1)." International Journal of Cancer 26:171-176.

115. Sugimoto, K., Toyoshima, H. *et al.* (1992). "Frequent mutations in the p53 gene in human myeloid leukemia cell lines." Blood 79(9): 2378-2383.

116. Gallagher, R., Collins, S. *et al.* (1979). "Characterization of the continuous, differentiating myeloid cell-line (HL-60) from a patient with acute myeloid leukemia." Blood 54: 713.

117. Koeffler, H.P., Golde, D.W. (1978). "Acute myelogenous leukemia: A human cell-line responsive to colony-stimulating activity." Science 200(4346): 1153-1154.

118. Chan, S.M., Thomas, D. *et al.* (2015). "Isocitrate dehydrogenase 1 and 2 mutations induce BCL-2 dependence in acute myeloid leukemia." Nature Medicine 21(2): 178-187.

119. Sander, J.D., Joung, J.K. *et al.* (2014). "CRISPR-Cas systems for editing, regulating and targeting genomes." Nature Biotechnology 32(4): 347-355.

120. Gorter de Vries, A.R., Couwenberg, L.G.F. *et al.* (2019). "Allele-specific genome editing using CRISPR-Cas9 is associated with loss of heterozygosity in diploid yeast." Nucleic Acids Research 47(3): 1362-1372.

121. Grassi, G., Maccaroni, P. *et al.* (2003). "Inhibitors of DNA methylation and histone deacetylation activate cytomegalovirus promotor-controlled reporter gene expression in human glioblastoma cell line U87." Carcinogenesis 24(10): 1625-1635.

122. Hsu, C., Li, H. *et al.* (2010). "Targeted methylation of *CMV* and *E1A* viral promotors." Biochemical and Biophysical Research Communications 402: 228-234.

123. Leroy, H., Roumier, C. *et al.* (2005). "CEBPA point mutations in hematological malignancies." Leukemia 19: 329-334.

124. Wang, X., Haylock, D. *et al.* (2016). "A thrombopoietin receptor antagonist is capable of depleting myelofibrosis hematopoietic stem and progenitor cells." Blood 127(26): 3398-3409.

125. Schneider, C., Oellerich, T. *et al.* (2017). "SAMHD1 is a biomarker for cytarabine response and a therapeutic target in acute myeloid leukemia." Nature Medicine 23(2): 250-255.

126. Kodigepalli, K.M., Li, M. *et al.* (2018). "SAMHD1 inhibits epithelial cell transformation *in vitro* and affects leukemia development in xenograft mice." Cell Cycle 17(23): 2564-2576.

127. He, D., Ma, Z. *et al.* (2019). "Pseudophosphatase STYX promotes growth and metastasis by inhibiting FBXW7 function in colorectal cancer." Cancer Letters 454: 53-65.

128. Corey, S.J., Elopre, M. *et al.* (2005). "Complete remission following clofarabine treatment is refractory juvenile myelomonocytic leukemia." Journal of Pediatric Hematology Oncology 27(3): 166-168.

Appendix

Table 1 – RT-qPCR Primers

Primer Name	5' – 3' Sequence
MTF2 Forward	TGCAGGTAGAATAGCATGTGGCGA
MTF2 Reverse	GTTGCTCCTTCCCATTCCACAAGA
GAPDH Forward	AGGTCGGTGTGAACGGATTTG
GAPDH Reverse	TGTAGACCATGTAGTTGAGGTCA

Table 2 – RT-qPCR Settings

Step	Temperature (°C)	Time (s)	Number of Cycles
Pre-incubation	95	300	1
Denaturation	95	10	
Annealing	60	10	45
Elongation	72	10	
Melting	95	continuous	1

Table 3 – Fluorochrome Summary

Fluorochrome	Laser wavelength (nm)	Filter (nm/nm)
Annexin V – BUV395	355	379/28
Green Fluorescent Protein	488	530/40
Alexafluor488	488	530/40
SYTOX Green	488	530/40
7-AAD	488	620/29
Red Fluorescent Protein	561	580/30
Alexafluor647	640	670/30

Table 4 – GeCKO Screening Primers (Demultiplexing Barcodes – Red)

Primer Name	5' – 3' Sequence
PCR1 Forward	AATGGACTATCATATGCTTACCGTAACTTGAAAGTATTTCG
PCR1 Reverse	TCTACTATTCTTTCCCCTGACTGTTGTGGGCGATGTGCGCTCTG
PCR2 Forward	AATGATACGGCGACCACCGAGATCTACACTCTTTCCCTACACGACG CTCTTCCGATCTNNNNNNNNNTCTTGTGGAAAGGACGAAACACCG
PCR2 Reverse – EV Baseline	CAAGCAGAAGACGGCATACGAGATAAGTAGAGGTGACTGGAGTTC AGACGTGTGCTCTTCCGATCTTTCTACTATTCTTTCCCCTGCACTGT
PCR2 Reverse – EV Day 14	CAAGCAGAAGACGGCATACGAGATACACGATCGTGACTGGAGTTCA GACGTGTGCTCTTCCGATCTATTCTACTATTCTTTCCCCTGCACTGT
PCR2 Reverse – EV Day 14 + AraC	CAAGCAGAAGACGGCATACGAGATCGCGCGGTGTGACTGGAGTTCA GACGTGTGCTCTTCCGATCTGATTCTACTATTCTTTCCCCTGCACTGT
PCR2 Reverse – MTF2 OE Baseline	CAAGCAGAAGACGGCATACGAGATCATGATCGGTGACTGGAGTTCAG ACGTGTGCTCTTCCGATCTCGATTCTACTATTCTTTCCCCTGCACTGT
PCR2 Reverse – MTF2 OE Day 14	CAAGCAGAAGACGGCATACGAGATCGTTACCAGTGACTGGAGTTCAG ACGTGTGCTCTTCCGATCTTCGATTCTACTATTCTTTCCCCTGCACTGT
PCR2 Reverse – MTF2 OE Day 14 + AraC	CAAGCAGAAGACGGCATACGAGATTCCTTGGTGTGACTGGAGTTCAGA CGTGTGCTCTTCCGATCTATCGATTCTACTATTCTTTCCCCTGCACTGT

Table 5 – GeCKO PCR Step 1 Settings

Step	Temperature (°C)	Time (s)	Number of Cycles
Pre-incubation	98	30	1
Denaturation	98	10	12
Annealing and Elongation	65	75	
Final Elongation	65	300	1

Table 6 – GeCKO PCR Step 2 Settings

Step	Temperature (°C)	Time (s)	Number of Cycles
Pre-incubation	98	30	1
Denaturation	98	11	
Annealing	70	5	12
Elongation	72	35	
Melting	72	60	1

Table 7 – Small Molecule Inhibitor Accepted Targets

Inhibitor name	Concentration used	Accepted target(s)
Cytarabine	2 µM	POLB
Clofarabine	1 µg/mL	POLA/RRM1
Fludarabine	3 µg/mL	POLA/RRM1
Nelarabine	500 µg/mL	POLA
Pemetrexed	15 µg/mL	TYMS/GART
Raltitrexed	15 µg/mL	TYMS
Gemcitabine	1 µg/mL	RRM1/RRM2
Abemaciclib	100 µg/mL	CDK4/CDK6
Palbociclib	100 µg/mL	CDK4/CDK6

Lentivector Maps

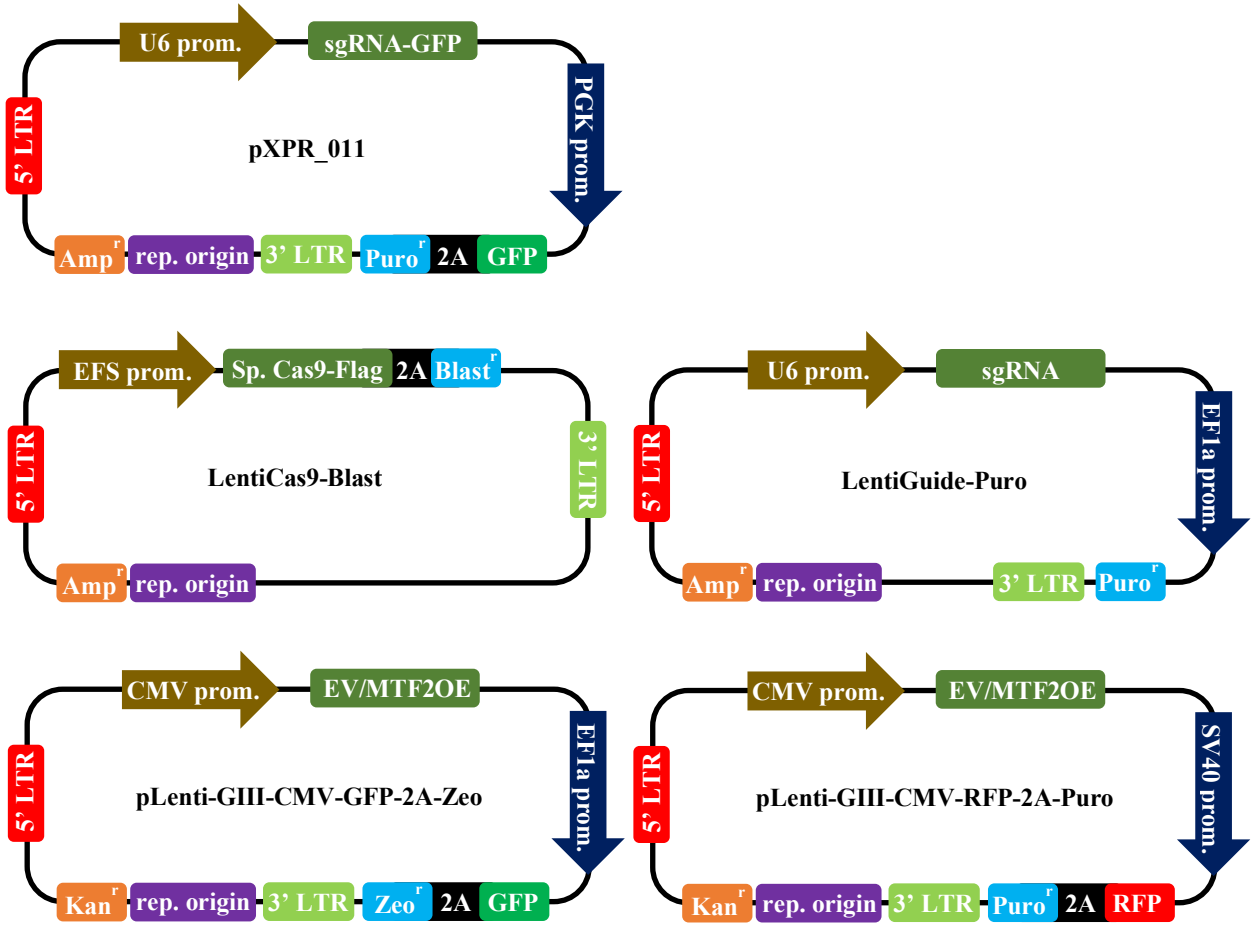

CURRICULUM VITAE

CHRISTOPHER G. P. CAFARIELLO

PROFESSIONAL MEMBERSHIP:

1. The Sprott Center for Stem Cell Research, Regenerative Medicine Program, Ottawa Hospital Research Institute, Ottawa, Ontario, Canada
2. Ottawa Institute of Systems Biology, Ottawa, Ontario, Canada
3. Let's Talk Science, Ottawa Chapter

EDUCATION:

Master of Science, Cellular & Molecular Medicine - 2019

Faculty of Medicine, University of Ottawa

Supervisors: William L. Stanford, PhD & Caryn Ito, PhD

Thesis: The identification of synthetic lethal interactions in acute myeloid leukemia using CRISPR

Bachelor of Science, Honours Specialization in Biochemistry - 2016

Faculty of Science, Department of Chemistry, University of Ottawa

RELEVANT WORK EXPERIENCE:

Graduate Student – 2016-2019

Ottawa Hospital Research Institute, The Ottawa Hospital

Ottawa, Ontario, Canada

Supervisors: William L. Stanford, PhD & Caryn Ito, PhD

- Used creativity to develop and execute a CRISPR-based whole-genome synthetic lethal screen for the identification of synthetic lethal interactions in acute myeloid leukemia
- Developed and optimized a workflow for the validation of novel therapeutic strategies identified by our lab
- Contributed to the development of a novel flow cytometry based diagnostic assay to prospectively identify acute myeloid leukemia patients who will not respond to frontline induction chemotherapy
- Contributed to the development and revision of several technical or scientific reports, two independent manuscripts, 3 conference abstracts and posters and 1 patent application
- Presented data to senior management (principal investigators and physicians) at the Ottawa Hospital for the purpose of informing the future directions of research aims, clinical trials and operating procedures
- Leveraged effective interpersonal skills to gather intelligence and developed collaborations and relationships with principal investigators from different institutes
- Respectfully coordinated and mentored a diverse team of 9 new hires in laboratory techniques and acted as most responsible person (MRP) for various biotechnological instruments including the BD LSR Fortessa flow cytometer

ACQUIRED TECHNICAL LABORATORY EXPERTISE:

- Advanced cloning and techniques such as recombinant DNA preparation and purification, plasmid prep, PCR, RT-PCR, q-RTPCR, oligonucleotide design, gel electrophoresis & ChIP
- Lentivirus preparation and titration
- Transformations, transfections and lentiviral transductions
- Advanced flow cytometry, imaging flow cytometry, panel design and cell sorting
- Stem cell & tissue culture of both adherent and suspension cell-lines and primary immune cells
- Hematopoietic assays such as CFU-C, LTC-IC, LDA and competitive repopulation assay, processing cord blood and primary leukemia samples
- Stem cell enrichment and lineage depletion of primary hematopoietic samples and immune cells
- Significant experience with PDX animal models of disease, mouse genetics, animal handling, injections and drug testing (blood drawing + organ harvesting included)
- Fluorescence and light microscopy
- DNA and RNA sequencing, DNA alignment, plasmid sequencing and ChIP sequencing included
- CRISPR and high throughput genetic screening using CRISPR (GeCKO)
- Techniques in microbiology and bacteriology including quantification and enumeration
- Experience with biosafety level 2 containment facilities and PHAC standard operating procedures for laboratory work

- Proficiency with downloading, installing and executing opensource computer software including programming in R and Python

CONFERENCES ATTENDED:

1. 2018 Till and McCulloch Meetings – Ottawa, Ontario
2. 2017 University of British Columbia Flow Course – Vancouver, British Columbia
3. 2017 Till and McCulloch Meetings – Montreal, Quebec

PUBLICATIONS:

1. Harinad B. Maganti*, Hani Jrade*, **Christopher Cafariello**, Janet L. Manias Rothberg, Christopher J. Porter, Julien Yockell-Lelièvre, Hannah L. Battaion, Safwat T. Khan, Theodore J. Perkins, Mitchell Sabloff, Yuefeng Li, Adrian Grzybowski, Alexander Ruthenburg, Jeff Dilworth, Joel Howard, Elham Sabri, Caryn Ito & William L. Stanford. Targeting the MTF2-MDM2 axis sensitizes refractory acute myeloid leukemia to chemotherapy. Cancer Discovery. 2018. 8: 1376-1389. (Impact Factor: 26.4)
2. Janet L. Manias Rothberg*, Harinad B. Maganti*, Hani Jrade, Christopher J. Porter, Gareth A. Palidwor, **Christopher Cafariello**, Hannah L. Battaion, Safwat T. Khan, Theodore J. Perkins, Robert F. Paulson, Caryn Ito & William L. Stanford. Mtf2-PRC2 control of canonical Wnt signalling is required for definitive erythropoiesis. Cell Discovery. 2018. 4;21: 1-16. (Impact Factor: 4.6)

SPECIAL TRAINING:

- OHRI: WHMIS (2019)
- OHRI: Emergency Codes (2019)
- OHRI: Privacy and Information Security (2019)
- OHRI: Emergency Procedures (2019)
- OHRI: Respectful Behaviour in the Workplace (2019)
- OHRI: Lab Safety Refresher (2019)
- OHRI: Radiation Safety (2019)
- OHRI: Accessibility in a Healthcare Environment (2019)
- OHRI: Violence and Harassment Prevention (2019)
- Ministry of Labour: Safety Awareness - Workers (2019)
- University of British Columbia: UBC Flow Course (2017)

VOLUNTEER EXPERIENCE:

- Judge - Ottawa Regional Science Fair (2019)
- Let's Talk Science - Stem Cell Talks (2018-2019)
- Youth Soccer Coach - Kinsmen Minor Soccer (2012-2015)
- Triage Assistant, Children's Hospital of Eastern Ontario (2014)
- Canvasser for The Heart & Stroke Foundation (2013)

LANGUAGE SKILLS:

	Speaking	***Reading***	***Writing***
English:	Fluent	Fluent	Fluent
French:	Beginner	Intermediate	Intermediate
Italian:	Intermediate	Intermediate	Intermediate

SPECIAL AWARDS AND DISTINCTIONS:

- Recipient of 2017 UBC Flow Course Travel Bursary
- Recipient of 2017 Stem Cell Network TMM Travel Bursary
- Recipient of University of Ottawa Undergraduate Internal Scholarship (Level 4)
- Recipient of The Dr. Arthur and Anna Battista Scholarship